UNIVERSITY OF OULU

FACULTY OF INFORMATION TECHNOLOGY AND ELECTRICAL ENGINEERING

Salla Hiltunen

C-TREND PARAMETERS AND POSSIBILITIES OF FEDERATED LEARNING

Master's Thesis
Degree Programme in Biomedical Engineering
August 2023

Hiltunen S. (2023) C-Trend Parameters and Possibilities of Federated Learning. University of Oulu, Degree Programme in Biomedical Engineering. Master's Thesis, 80 p.

ABSTRACT

In this observational study, federated learning, a cutting-edge approach to machine learning, was applied to one of the parameters provided by C-Trend Technology developed by Cerenion Oy. The aim was to compare the performance of federated learning to that of conventional machine learning. Additionally, the potential of federated learning for resolving the privacy concerns that prevent machine learning from realizing its full potential in the medical field was explored.

Federated learning was applied to burst-suppression ratio's machine learning and it was compared to the conventional machine learning of burst-suppression ratio calculated on the same dataset. A suitable aggregation method was developed and used in the updating of the global model. The performance metrics were compared and a descriptive analysis including box plots and histograms was conducted.

As anticipated, towards the end of the training, federated learning's performance was able to approach that of conventional machine learning. The strategy can be regarded to be valid because the performance metric values remained below the set test criterion levels. With this strategy, we will potentially be able to make use of data that would normally be kept confidential and, as we gain access to more data, eventually develop machine learning models that perform better.

Federated learning has some great advantages and utilizing it in the context of qEEGs' machine learning could potentially lead to models, which reach better performance by receiving data from multiple institutions without the difficulties of privacy restrictions. Some possible future directions include an implementation on heterogeneous data and on larger data volume.

Keywords: EEG, C-Trend, burst suppression ratio, amplitude integrated EEG, alpha-to-delta ratio, C-Trend Index, qEEG, machine learning, federated learning, ICU, anesthesia, GDPR, AI Act

Hiltunen S. (2023) C-Trend-teknologian parametrit ja federoidun oppimisen mahdollisuudet. Oulun yliopisto, Lääketieteen tekniikan tutkinto-ohjelma. Diplomityö, 80 s.

TIIVISTELMÄ

Tässä havainnointitutkimuksessa federoitua oppimista, koneoppimisen huippuluokan lähestymistapaa, sovellettiin yhteen Cerenion Oy:n kehittämään C-Trend-teknologian tarjoamaan parametriin. Tavoitteena oli verrata federoidun oppimisen suorituskykyä perinteisen koneoppimisen suorituskykyyn. Lisäksi tutkittiin federoidun oppimisen mahdollisuuksia ratkaista yksityisyyden suojaan liittyviä rajoitteita, jotka estävät koneoppimista hyödyntämästä täyttä potentiaaliaan lääketieteen alalla.

Federoitua oppimista sovellettiin purskevaimentumasuhteen koneoppimiseen ja sitä verrattiin purskevaimentumasuhteen laskemiseen, johon käytettiin perinteistä koneoppimista. Kummankin laskentaan käytettiin samaa dataa. Sopiva aggregointimenetelmä kehitettiin, jota käytettiin globaalin mallin päivittämisessä. Suorituskykymittareiden tuloksia verrattiin keskenään ja tehtiin kuvaileva analyysi, johon sisältyi laatikkokuvioita ja histogrammeja.

Odotetusti opetuksen loppupuolella federoidun oppimisen suorituskyky pystyi lähestymään perinteisen koneoppimisen suorituskykyä. Menetelmää voidaan pitää pätevänä, koska suorituskykymittarin arvot pysyivät alle asetettujen testikriteerien tasojen. Tämän menetelmän avulla voimme ehkä hyödyntää dataa, joka normaalisti pidettäisiin salassa, ja kun saamme lisää dataa käyttöömme, voimme lopulta kehittää koneoppimismalleja, jotka saavuttavat paremman suorituskyvyn.

Federoidulla oppimisella on joitakin suuria etuja, ja sen hyödyntäminen qEEG:n koneoppimisen yhteydessä voisi mahdollisesti johtaa malleihin, jotka saavuttavat paremman suorituskyvyn saamalla tietoja useista eri lähteistä ilman yksityisyyden suojaan liittyviä rajoituksia. Joitakin mahdollisia tulevia suuntauksia ovat muun muassa heterogeenisen datan ja suurempien tietomäärien käyttö.

Avainsanat: EEG, C-Trend, purskevaimentumasuhde, amplitudi-integroitu EEG, alfa-delta-suhde, C-Trend-indeksi, qEEG, koneoppiminen, federoitu oppiminen, teho-osasto, anestesia, GDPR, tekoälylaki

TABLE OF CONTENTS

FOREWORD

This paper serves as my master's thesis for Biomedical Engineering master's degree for which I have been studying in the University of Oulu during the academic years of 2021-2023. The amount of skills and knowledge gained during these years and the writing process of this thesis is enormous – shall this learning remain never ending.

I will always be grateful for the chance to conduct the research on such an engaging subject under the supervision of Cerenion company. I owe a big thank you to my supervisors, Jukka Kortelainen and Tapio Seppänen. I also want to express my gratitude to Eero Väyrynen for his innovative ideas, technical oversight and steady guiding throughout the process's difficult moments. The process has also been greatly aided by Miikka Salminen, and I want to thank him for all of that. Additionally, all of my Cerenion coworkers have been a tremendous help and inspiration to me.

Oulu, 11.08.2023

Salla Hiltunen

LIST OF ABBREVIATIONS AND SYMBOLS

ACNS	American Clinical Neurophysiology Society
ADC	Analog-to-Digital Conversion
ADR	Alpha-to-Delta Ratio
aEEG	Amplitude-integrated EEG
AIA	Artificial Intelligence Act
AP	Action Potential
ASA	American Society of Anesthesiologists
BSR	Burst-Suppression Ratio
BSS	Blind Source Separation
CC0	Creative Commons Zero license
CRR	Common Recording Reference electrode
CT	Computed Tomography
DOC	Disorder of Consciousness
ECG	Electrocardiogram
EEG	Electroencephalogram
EOG	Electrooculography
EPSP	Excitatory Post-Synaptic Potentials
FDA	Food and Drug Administration
GABA	Gamma-Aminobutyric Acid
GDPR	General Data Protection Regulation
HADO	High Amplitude Delta Oscillations
HIE	Hypoxic Ischemic Encephalopathy
ICA	Independent Component Analysis
ICU	Intensive Care Unit

iEEG	Intracranial EEG
IPSP	Inhibitory Post-Synaptic Potentials
MEG	Magnetoencephalogram
MPE	Mean Percentage Error
MRI	Magnetic Resonance Imaging
MSE	Mean Squared Error
NCT	Narcotrend
NICU	Neonatal Intensive Care Unit
NREM	Non-Rapid Eye Movement
OR	Operating Room
PD	Periodic Discharge
RPP	Rhythmic and Periodic Pattern
PSP	Post-Synaptic Potentials
qEEG	Quantitative parameters of EEG
STD	Error Standard Deviation
TTM	Targeted Temperature Management
WHO	The World Health Organization

1. INTRODUCTION

In the core of the study's topic is the brain, a complex and mysterious structure that we are still trying to completely figure out. When we are attempting to understand the brain, we are actually attempting to comprehend individuals. There are no two minds and two brains alike and that is what makes everything so fascinating – and very complicated.

Electroencephalogram (EEG) measurements are one way to explain and analyze how our brains work. It is a unique and intricate biological electricity transmission that expresses our brain's and our mental health's functional status. We can gather crucial data from EEG to diagnose patients, track their health, and recognize various neurological conditions. EEG is a low-cost instrument that is used for a variety of therapeutic and diagnostic purposes, including determining the depth of anesthesia, identifying, and categorizing encephalopathies, and identifying patients who are experiencing non-convulsive epileptic seizures.

EEG is a complicated signal, and there has been a great interest in processing and analyzing it. Machine learning has been a major factor in the emergence of new computing techniques. Cerenion C-Trend® technology, which also makes use of machine learning, provides four straightforward parameters, one of which is the C-Trend Index, to make the study of EEG simpler. The C-Trend Index and other qualitative metrics can be helpful in evaluation of the brain function during the anesthesia as well as the condition of the brain.

This works aims for exploring the technical aspects and the clinical environment (including anesthesia and different patient groups) of different parameters that C-Trend Software provides (C-Trend Index, burst-suppression ratio (BSR), amplitude-integrated EEG parameter (aEEG) and alpha-to-delta ratio (ADR)). One of the parameters, BSR is discussed in more depth as it is used in the implementation of federated learning system. BSR was chosen for the implementation due to its algorithmic simplicity, but in the future, federated learning could be implemented as well on the other C-Trend parameters.

An essential problem in the machine learning of qEEG parameters is being addressed by the use of federated learning. Machine learning models need large amounts of data to perform well, but for now privacy concerns are limiting the use of a lot of health data. In order to solve the concerns of data governance and privacy brought on by the requirements of GDPR and the AI Act in the medical device industry, the study seeks to incorporate federated learning approaches in the calculation process of BSR.

In order to improve the machine learning parameters of medical devices and to comply with GDPR and AI Act regulations, including data governance and privacy, federated learning sought to apply parameter computation in edge devices. If federated learning was utilized instead of sending patient data, the use of medical data would be more widely approved by the end users in terms of general legislation, hospital processes and standards, and patient data security. Federated learning was evaluated and compared to the conventional technique as a potential machine learning solution for the BSR algorithm.

EEG data from cardiac arrest patients receiving propofol-induced anesthesia are being used in the study. So, the study starts with a survey of the literature on the EEG from the perspectives of history, brain origin, technology, and signal. The use of EEG for diagnosis in intensive care unit and operating room settings, as well as concepts of anesthesia, are covered after that. The last step is the incorporation of the qualitative parameters offered by C-Trend Technology as well as background data on federated

learning and privacy concerns. The federated learning system is introduced at the conclusion of the study and there is a broad discussion on data privacy and data governance as well as complying with the AI Act and GDPR requirements.

2. EEG AND ANESTHESIA

2.1. EEG introduction

Electroencephalography (EEG) is measuring brain's electric fields and the result is a complex, non-stationary, non-linear, and often noisy EEG signal. EEG records the electrical activity generated by the cerebral neurons as potential differences between the used electrodes. These electrodes are either positioned over the scalp or they are placed directly on the surface of the brain to record the electrical activity from the cerebral cortex. The former and noninvasive option is more commonly used, and we will be focusing on these types of electrodes in this study. EEG can only record a portion of all the electrical activity going on in the brain. It often also includes a lot of noise meaning for example other kinds of physiologic electrical activity like ocular or muscular activity in the body and environmental noise such as power lines. [1]

Millions of spatially aligned cortical neurons exhibit synchronized activity, which is captured by EEG as a temporal summation [2]. EEG measurement is commonly considered to have a great temporal resolution but a poor spatial resolution [3]. EEG offers several benefits as a brain monitor, including the ability to capture changes milliseconds after they occur and the ability to represent both normal and abnormal aggregated electrical activity of various brain regions [4].

2.2. History of EEG

Measuring EEG is not a brand-new invention as the first human EEG was recorded in 1924 and several recordings of animals were performed before that. The first human recording was done by very familiar to all in the field of EEG, German psychiatrist, Hans Berger. Before that, an English scientist, Richard Caton, recorded electrical activity from the brains of animals using a galvanometer and electrodes, and thus he is credited with discovering the electrical activities of the brain. [5] The spontaneous electrical rhythms of the mammalian brain were also investigated by other researchers at that time like Napoleon Cybulski, Adolf Beck and Fleischl von Marxow [6]. Soon after also the effects of certain drugs like scopolamine, barbiturates, morphine, and ether on EEG were noted [7].

Caton was able to record electrical activity from the exposed brains of rabbits, monkeys, and cats and for that he used a mirror galvanometer. His work was first reported in the years 1875 and 1877. He observed variations associated with sleep and wakefulness, anesthesia, and death. His setup consisted of William Thomson’s reflecting galvanometer and Du Bois-Reymond’s non-polarizable electrodes. The electrodes were of high-quality in these days and this instrument had a very limited frequency response range from 0 Hz to 6 Hz. To visualize the weak signals, he amplified the waveform optically by shining an oxyhydrogen lamp on the mirror and having it reflected onto a large scale placed on the wall. [8]

William Einthoven created the string galvanometer in 1901 and it was more sensitive than earlier galvanometers, which had lower temporal resolution and inadequate amplification. The oscillating brain activity that those earlier galvanometers recorded could not be captured and stored by them. The string galvanometer recorded the shadows created by electrically induced deflections of a string on photographic paper. It was initially created and applied to the recording of electrocardiograms of the heart, but Vladimir

Neminsky in 1913 also used it to analyze the frequencies of EEG cycles. After this, galvanometers developed further. [9]

Later Berger started to research the brain's electrical activity and record brainwaves. He tried different methods like injecting Novocaine into the scalp and placing the electrode in the periosteum. He developed a recording technique later where he connected the electrode to the scalp as it is done nowadays and thus, he was the first person to record the electrical activity of the human brain as non-invasive recording. He recorded the first EEG in 1924 and in 1929 he published his first paper on EEG called *Über das Elektrenkephalogramm des Menschen.* In the paper he already used the terms alpha and beta waves, and because of this, alpha waves are also known as Berger waves. Berger found out in his studies that brainwaves change during mental activities and during sleep and that there are different electrical waves around tumors. [10]

Berger used a string galvanometer from the year 1910, first with the Einthoven type and later with the smaller Edelmann model. After 1924 he used the string galvanometer with the larger Edelmann model. In 1926 he started to use the more powerful Siemens double coil galvanometer. With the Siemens instrument he recorded the human EEG tracings shown in his paper of 1929. The records were on photographic paper with recordings from 1 to 3 minutes duration. He used a dipolar recording technique with fronto-occipital leads for his one-channel EEG recordings. Also, electrocardiogram (ECG) was recorded simultaneously and there was a time marker. [11]

In his most recent configuration, he employed platinum needle electrodes that were connected to a double-coil Siemen's galvanometer on one end and to the scalp of his 15-year-old son on the other. The frontal and occipital poles of the head were where the electrodes were positioned, effectively capturing non-local voltage changes covering almost the entire brain. He observed the alpha rhythm at the frequency of 8-12 Hz while his son sat passively, eyes closed and observed how it suppressed when the subject opened his eyes. Then the alpha rhythm was replaced with a lower amplitude, higher frequency, 14-30 Hz rhythm. This area was named a beta rhythm. [9]

Berger's contribution has been the greatest in the history of the EEG. He was a diligent scientist in his EEG work, but he also had very unscientific ideas about the nature of EEG. His driving force was the search for nature of the all-powerful force of mental energy. He had early personal experiences convincing him that such a mental energy – even capable of transmitting thoughts and emotions from person to person – does exist. [11]

In 1934 Adrian and Matthews published the paper which verified the concept of "human brain waves" and identified regular oscillations around 10-12Hz which they termed "alpha rhythm" [12]. EEG became commonly accepted as a method of analysis of brain functions in health and disease after Adrian and Matthew's demonstrations that the alpha rhythm was likely generated in the occipital lobes in man and was not artefactual. The neuronal sources of the alpha rhythm remained undefined until the 1970s, when it was demonstrated that the alpha rhythm is generated by a dipole layer catered at layers IV and V of the visual cortex [13].

2.3. EEG brain origin

The brain is a sophisticated organ made up of nerve tissue that controls a variety of our activities, including task-evoked reactions, movement, emotions, language, communication, thinking, and memory. Together with spinal cord the brain comprises the central nervous system. The central nervous system sends and receives messages from

other parts of the body through the peripheral nervous system. The brain has three main parts: cerebrum, cerebellum, and brainstem. Left and right cerebral hemispheres make up the cerebrum, which also controls feelings, intelligence, memory, and motor and sensory information as well as conscious and unconscious activities. The cerebrum has an outer layer called cortex and an inner layer. The cortex is mainly gray matter, and the inner layer is white matter. There are four lobes in the cortex: the frontal lobe, parietal lobe, temporal lobe, and occipital lobe. The cerebellum coordinates voluntary movement, perfects motor action, and supports some cognitive processes. The brainstem has centers for autonomic processes like breathing, temperature, respiration, and heart rate among many others. It also connects the cerebrum and cerebellum to the spinal cord. [14]

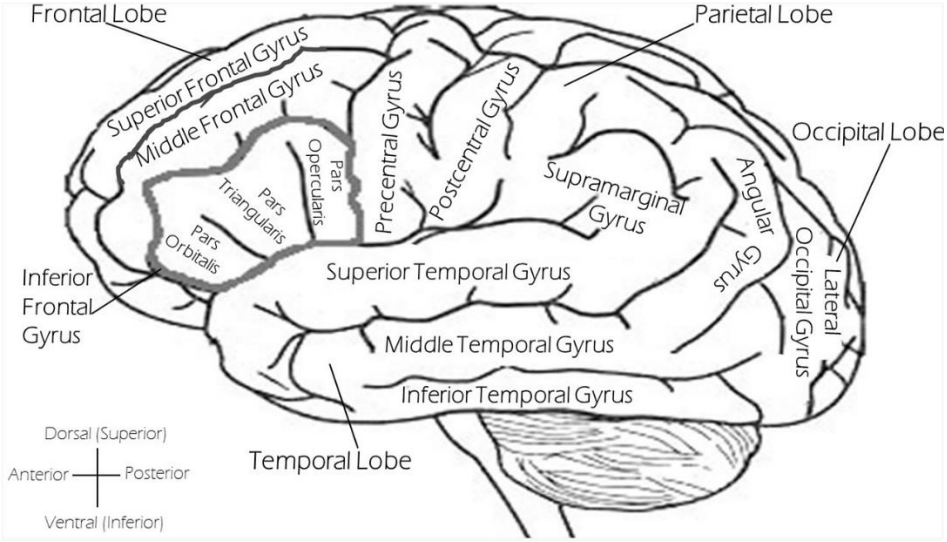

Figure 1. Left lateral of the brain. Cortex, lobes, spinal cord, and cerebellum are visible. By OpenClipart-Vectors via Pixabay, CC0 license.

The lobes of the cerebrum are responsible for different tasks. The frontal lobe of the cerebrum is the largest one and it has several significant functions. In this area prospective memory, speech and language, personality, and movement control take place. Broca's area is located in the frontal lobe, and it is involved in speech production. The primary and secondary sensory cortex, as well as the somatosensory association cortex, are located in the parietal lobe. In that area integration of, for example visual and auditory inputs to form higher-order complex functions happens. The primary and secondary auditory cortex, which translate, and process sounds and tones, are located in the temporal lobe. It also houses Wernicke's region, which was once thought to play a significant part in speech perception and understanding but which, according to recent research, is really dispersed throughout the entire brain. The representation of phonological information is thought to be the area's main purpose. The occipital lobe is the smallest lobe in the cerebrum cortex. It has a role in visual processing and interpretation and the visual cortex is located there. [15]

Altogether we have about 10^{10} nerve cells (also called neurons) in our brain. The activity of these neurons produces electrical and magnetic fields. EEG measures electrical activity and for measuring the magnetic fields there is a magnetoencephalography (MEG) developed. One single neuron generates only a small amount of electrical activity, and it alone cannot be picked up by electrodes because there is also a lot of activity going on in

neighboring neurons. The electrodes can pick up the electrical activity when a large group of neurons are simultaneously activated, and the EEG is generated. [16]

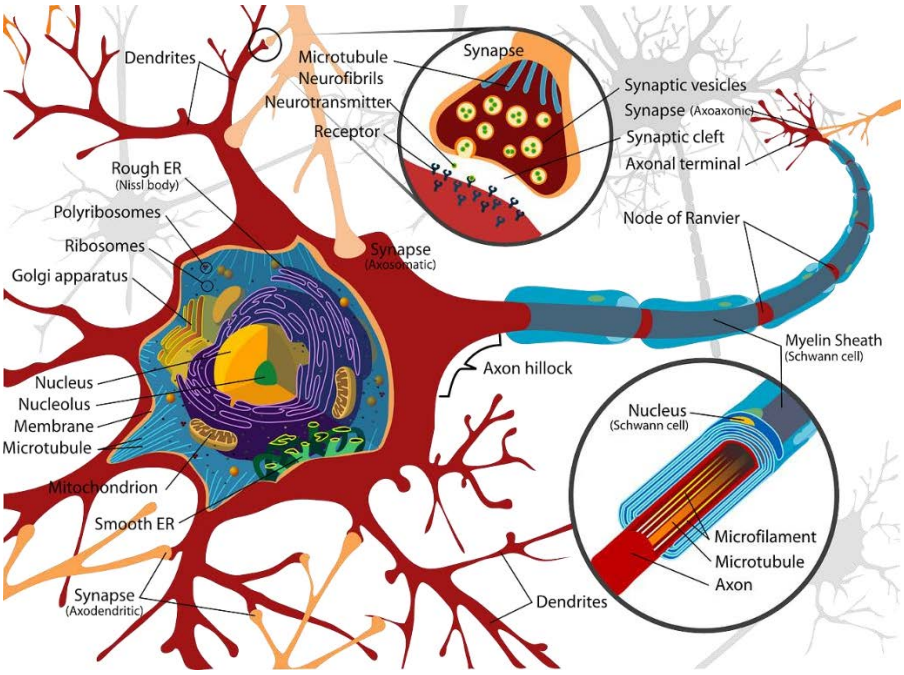

Figure 2. Neuron structure consisting of cell body, nucleus, dendrites, axon, Schwann cell, myelin sheath, node of Ranvier and axon terminal. Also, a synapse is visible. Synapse is a small gap between two communicating neurons. In synapse the message is transferred in a chemical form, when elsewhere it is electrical. Action potential (AP) arrives from the presynaptic neuron via axon terminal and from the synapse it continues to the postsynaptic neuron's dendrite. [17] By Clker-Free-Vector-Images via Pixabay, CC0 license.

Neurons have a unique ability to receive and transmit information. They employ both electrical and chemical components in this transmission. There are various varieties of neurons, and they are distinguished primarily by the quantity and configuration of their axons and dendrites. Synapses are the connections between neurons, while neuroeffector junctions are the connections between neurons and the effector tissues or cells. Soma contains the nucleus and other organelles crucial for neuronal function. Dendrites receive afferent signals and axons carry efferent signals. At the end of the axon there is typically an axon terminal at which neurotransmitters, neuromodulators, or neurohormones are released. Here previously an electrical signal transforms into a chemical signal. [17]

There are two types of neuronal activation distinguishable; the fast depolarization of the neuronal membranes (action potentials) and the slower changes in membrane potential (synaptic activation mediated by neurotransmitters). Action potentials consist of fast change in membrane potential, and it also rapidly returns to the resting state. [13] Action potentials induce a very fast (10 ms or less) local current in the axon with a very limited potential field and because of this, they are a very unlikely candidate for the source of the EEG. Post-synaptic potentials (PSPs) are longer (50-200 ms) and they have a much larger field and this is why they are more likely to be the primary generators of the EEG. [18]

The slower changes or PSPs can be divided into the excitatory (EPSPs) and the inhibitory (IPSPs) potentials, which depend on the neurotransmitter, receptors, and their interactions with ionic channels and/or intracellular second messengers. The summation of IPSPs and EPSPs creates electrical currents that are flowing in and around the cells. The

flow of current creates a field that spreads out from the origin of an electrical event (like a spike or slow wave). These potential fields are usually oval and may be quite restricted or very widespread. As the distance from the source increases, the field's effect diminishes. As a result, events that produce a high voltage on one electrode will also affect its neighbors, albeit to a lower amount. [13]

According to [19], cortical neurons must meet several conditions in order to be able to generate electrical fields that can be measured at the scalp and some of which are:

- These neurons are close to the scalp in distance.
- The quantity of these neurons should be large enough.
- The neurons must be synchronously activated and with a certain geometric configuration.

The neurons that mainly contribute to the EEG are those that form open fields according to the classic description of Lorente de Nó. He developed the concept of 'open' and 'closed' field configurations meaning that the cells with the dendrites along the longitudinal axis are said to have 'open-field' configurations because the electrical fields from these cells extend over long distances. These cells are typically pyramidal cells, and they may produce signals detectable on the scalp with EEG. Cells which have radially symmetric dendrites like aspiny stellate cells are said to have closed-field configurations as their electrical fields are confined within the volume of the cells. Cells with this configuration are not expected to produce EEG signals at large distances. When the pyramidal neurons are activated with a certain degree of synchrony, they generate coherent electric/magnetic fields. This is how neurons act like current dipoles, the activity which can be detected by electrodes. [13, 20]

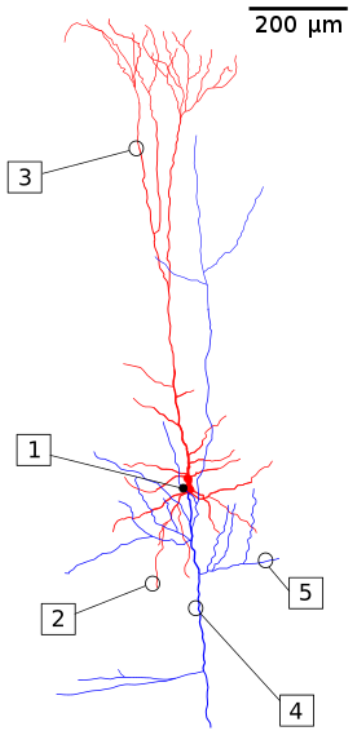

Figure 3. Structure of a pyramidal neuron. Soma (1), basal dendrite (2), apical dendrite (3), axon (4), and collateral axon (5). by Fabuio via Wikimedia Commons, CC0 license.

The transmission of the electric potential from pyramidal neurons to the detecting surface is described by a mathematical law known as the Poisson equation. Pyramidal cells act like dipole sources and generate dipolar fields, as was already mentioned. These dipolar fields are the sum of the separate potential fields produced by each source and are the result of a linear combination. There must be a considerable number of depolarized neurons working together in order to generate external potential. Since less than 5% of pyramidal cells can account for more than 90% of the energy of the EEG signal, this phenomenon is known as local synchronization, and it is crucial in the creation of EEG rhythms. [20]

2.4. EEG technology

The technology we need for recording the EEG consists of a combination of electrodes composed of conductive materials, operational amplifiers, computer and usually also a monitor. As electrocortical activity from the brain is measured in microvolts, it must be amplified by a factor of 1,000,000 to be displayed on a computer screen. [18]

The most common electrode type in EEG is a scalp electrode which can be either wet, semi-dry or dry electrode. These scalp electrodes have electrolytic paste-filled contact surfaces with a maximum diameter of 10 mm. They are constructed of non-polarized materials such as platinum, gold, or silver-silver chloride. The electrical resistance of the skin and the degree of skin-to-electrolyte contact determine the electrode impedance. Although they must be balanced and may produce noise distortions, in EEG caps and cup electrodes, which are wet electrodes, electrode impedance can reach 10,000 Ohms. It is recommended that the electrode impedance should be at least 100 Ohms in this case. [21]

A type of semi-dry electrode, adhesive electrodes—also known as sticker electrodes—often have a wider impedance range than cup electrodes and EEG caps. Adhesive electrodes are made up of a conductive substance, such as metal or carbon, that is encased in an adhesive coating. [22] As an illustration, Bittium BrainStatus electrodes are considered to be in short circuit if their impedance is less than 1 kOhm, and they are considered to have good impedance if it is greater than that but less than 50 kOhm. Lower than 100 kOhms is considered average, while higher than 190 kOhms indicates that the electrode is likely detached. [23]

In order to improve resistive contact while using wet electrodes, certain electrolytic gels or salts are typically placed between the electrode and the skin. Better signal quality is obtained as a result of the conductive gel's contribution to increased electrical conductivity between the electrode and the scalp. Dry electrodes, which have just lately been developed in addition to wet and semi-dry electrodes, are used to decrease the requirement for participant scalp preparation and to speed up setup. They don't need conductive liquid or gel, and they don't have an adhesive layer, but they frequently use specialized materials or designs that encourage good electrical contact and reduce resistance. [1] Dry electrodes can be more prone to electrical noise or motion abnormalities because of their increased impedance. The dry electrode typically has an electrode-scalp impedance of several hundred kOhms or much greater. [24]

Another type of EEG recording is intracranial EEG (iEEG), which is captured with electrodes placed directly on the surface of the brain to record the activity of the brain from the cerebral cortex. Capturing the signal from the surface of the brain is quite risky and it requires lots of expertise and thus it is not so commonly used. [25]

In a standard recording, electrodes are placed on the scalp at standard positions according to the International 10-20 classification system and it typically uses 21 electrodes. With this system the electrodes are spaced at 10% or 20% of the total distances between them and it ensures that each electrode is relatively positioned to all the others, and it makes every EEG study consistent despite peoples' different head shapes and sizes. Electrode positions have been named in a standardized way. The names consist of two symbols; the first symbol is a letter abbreviation of the underlying brain region and the second one is a number that indicates its more precise location in this region.
The letter abbreviations are the following: [26]

- Fp, frontal-polar
- F, frontal
- C, central sulcus
- P, parietal
- O, occipital
- T, temporal
- A, auricular

The number appears after the letter abbreviation, and electrodes with even numbers are placed on the right side of the head and electrodes with odd numbers on the left. Higher number electrodes are further from the midline than lower number electrodes, and vice versa. [21]

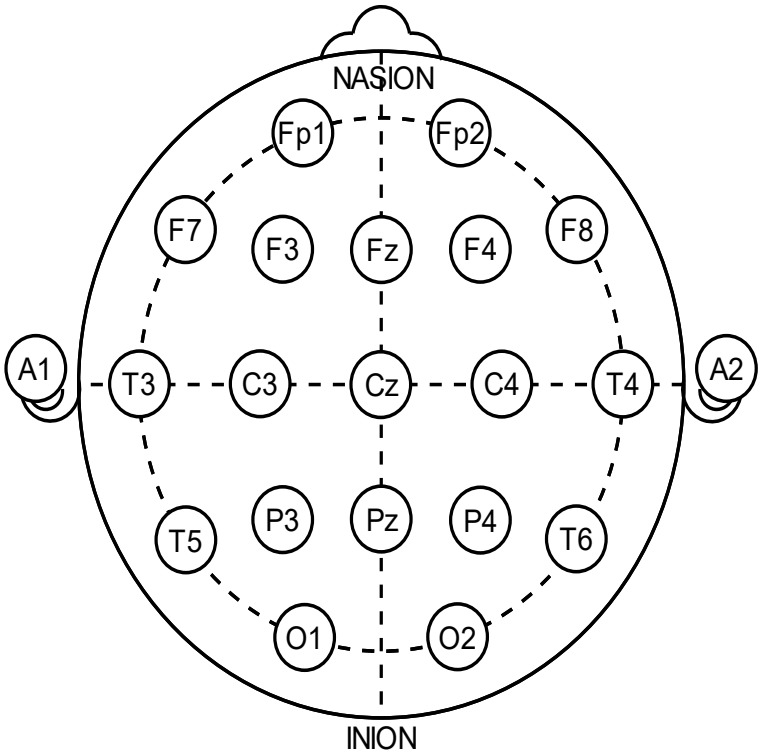

Figure 4. The International 10-20 electrode placement system is shown in a single-plane projection. The outer circle is at the level of the nasion and inion. The inner circle is the temporal line of electrodes. by Asanagi via Wikimedia Commons, CC0 license.

Midline or sagittal electrodes are identified by the letter "z" rather than a number. The "z" stands for zero, and because these electrodes are positioned above the corpus callosum, they are insufficient to effectively represent either of the two hemispheres. Corpus callosum connects the two hemispheres and permits communication between them. “z” electrodes are usually used as ground electrodes. The purpose of ground electrodes is to prevent power line noise from interfering with the small biopotential signals that we are interested in.

A1 and A2 electrodes are usually used for referential montages and if they are both used, it can be called “summed ears”. Those electrodes are placed on the auricle of the ear. All the measured electrical potentials come from the comparison of active electrodes and these reference electrodes or electrode which will be discussed in more depth below.

There are also additional electrodes called T1 and T2 which are sub temporal electrodes and used to provide more information about the anterolateral temporal region. Those electrodes are basically part of a newer system, the 10-10 system, but are commonly added onto the 20-10 montages for evaluation of seizure activity. The location of the T1 and T2 is close to F7 and F8 and in the temporal region. [27]

The input from the electrodes must be amplified to make them compatible with devices like displays. Each active electrode on the scalp has its own channel in the amplifier. To make sure that the current is only flowing from the patient to the machine and not the other way around, there is a protection circuit or isolation transformer. There could be electric shocks originating from the EEG apparatus and thus this is protecting the patient from that. [21]

In a simple amplifier input from a single active electrode is conducted to the amplifier and compared with ground which is earth. The output is the potential difference between the active electrode and ground. In differential amplification, signals from two active electrodes are conducted to the amplifier and the potential difference between these two is measured. There is in-phase cancellation in differential amplification if there is any signal affecting both inputs identically as there is no potential difference. [18] The high-amplitude signals coming from other regions of the body are influencing the brain signal because the brain impulses have extremely low amplitudes. EEG channels can reflect voltage coming from the underlying brain thanks to in-phase cancellation. [21]

Electrodes detect individual discharges and by connecting them all, we get a rich set of data across the entire span of the scalp. This is done with montages. Montages are different logical arrangements of EEG channels, and they work in displaying activity over the entire head and allow lateralization and localization of information. Lateralization means the comparison of the activity on the two sides of the brain. Most often, bipolar, and referential montages are used for EEG recordings. There are also other montages like common average and Laplacian, which use computed values as a reference. [28] The electric potential difference between the active and reference electrodes is represented by the voltage that the EEG system records in each channel. A common recording reference electrode (CRR), which is typically positioned somewhere between Cz and Pz, is used by digital EEG devices to record voltages. [21]

Dipolar montages electronically link following electrodes as a chain or line. The voltage at one electrode is compared with the voltage affecting adjacent electrodes. In this montage, each amplifier has two inputs, I and II. If input I is negative with respect to input II, there is an upward deflection. And if the input II is negative with respect to input I, there is a downward deflection. As seen, the convention in neurophysiology is that upward deflection is negative, and a downward deflection is positive. One example of this, where we have electrode pairs F8-T8 and T8-P8: [18]

$$Channel\ 1: F8 - T8 = -20\mu V - (-100\mu V) = 80\mu V\ (downward\ deflection)$$
$$Channel\ 2: T8 - P8 = (-100\mu V) - (-20\mu V) = -80\mu V\ (upward\ deflection)$$

Equation 1. The first one being channel 1 and the second one being channel 2, in channel 1 T8 is in input II and in channel 2 it is in input I.

There are two types of dipolar montages: longitudinal and transversal. As one begins with an anterior electrode (Fp1/Fp2) as the active electrode and links it to the next posteriorly placed electrode (F3/F4) as the reference electrode, the longitudinal dipolar montage is also known as the "double banana" montage. The prior reference electrode (F3/F4) that was acting as the active electrode in the subsequent channel is changed to the reference electrode (C3/C4). In the transverse variant, channel one moves the electrode pairs to the right starting from the left. [28]

Signals from each electrode in referential recording are conducted to input I of the associated amplifier, while signals from the reference are conducted to input II. In referential recording, we are recording the potential difference between a particular electrode and a referential electrode. No note, reference montages produce a higher amplitude EEG recording because of the longer interelectrode distances.

In referential montage, each electrode can be referred to as the same electrode and this is usually located at Cz or over an earlobe such as A1 or A2 or as those connected. In the old analogue EEG machines, montages meant physically connecting the input electrodes to the amplifier channel inputs. But for digital EEG, the channels can be calculated from the values of the voltage measured at the electrodes.

In referential montages, the reference electrode should preferably be inactive such that the channel only reflects the potential at the active electrode. The voltage depends equally on the active and reference electrodes. On the other hand, there is nowhere on the scalp that is electrically neutral or inactive. When the reference electrode is contaminated with large, recorded potentials for example during sleep, all the channels are also contaminated when that electrode is used as a reference. The reference can also be placed outside the head but in that case ECG artifact will be present on all channels. [29] Also, if the reference is at too distant location, it will be contaminated with ambient electrical noise at 50 Hz or 60 Hz. Ears are usually relatively free from these two artifacts, but they do pick up cerebral activity and ECG sometimes. One example, where A1 is a contralateral ear reference: [18]

$$Channel\ 1: Fp2 - A1 = (-50\mu V) - (-20\mu V) = -30\mu V\ (small\ upward\ deflection)$$
$$Channel\ 2: F8 - A1 = (-100\mu V) - (-20\mu V) = -80\mu V\ (big\ upward\ deflection)$$
$$Channel\ 3: T8 - A1 = (-50\mu V) - (-20\mu V) = -30\mu V\ (small\ upward\ deflection)$$
$$Channel\ 4: P8 - A1 = (-20\mu V) - (-20\mu V) = 0\mu V\ (no\ deflection)$$

Equation 2.

The Laplacian montage involves the weighted average of voltages from surrounding electrodes of a particular electrode as a local reference. Computation of the Laplacian is relatively complicated and depends on the electrode involved in the montage. The usage of the Laplacian is useful in displaying relatively focal discharges with minimal field. Common average montage uses the averaged potential of all the electrodes as the referential electrode. [29]

Montages in signal processing involve creating linear combinations of electrode measurements with respect to a reference electrode. The reference electrode can be located anywhere since its value can be subtracted from other electrodes. For instance, in a referential montage using a reference electrode (Ref):

$$(Fp1 - Ref) - (F3 - Ref) = Fp1 - F3 + (Ref - Ref) \rightarrow Fp1 - F3$$

Equation 3.

It is important to note that montages are primarily a method of visualizing and projecting signals on a screen, and they don't inherently provide new information mathematically. From a machine learning perspective, using a specific montage is unnecessary, although classifiers can learn linear combinations directly from the input structure.

In an analog-to-digital conversion (ADC), the obtained electric and analogue signals are digitally processed, which in a computer translates them into numbers or virtual signals. Each channel's voltage is measured for a very brief period of time, and the resulting value is saved in the computer as a digital signal. Each EEG channel displays the voltage's change over time, and the length of the time frame determines the channel's temporal resolution. Considering that the EEG is a rhythmic signal with cycles that show a change in positive and negative polarity, we require at least two measurements throughout each cycle, ideally at each polarity. For a signal having a frequency of 40 Hz and 40 polarity shifts each second, the voltage must be measured at least 80 times per second, or twice as many cycles. Because the sampling frequency must be at least twice as high as the highest frequency required to be recorded, the minimum criterion for EEG sampling frequency is 128 samples/second. Most contemporary EEG devices are capable of recording at 256 Hz and even higher. [21]

2.5. EEG signal

EEG signals are non-stationary, non-linear, and noisy. Analyzing and interpreting the EEG has been said to be both an art and science, since the normal EEG is extremely diverse and has a wide range of physiological variability. EEG waveforms may be characterized based on their location, amplitude, morphology, symmetry etc., but the most frequently used method to classify EEG waveforms is by frequency. A single normal EEG recording does not rule out the possibility of pathology or abnormalities because electrographic events are frequently fleeting, which is important to keep in mind when performing the EEG analysis. [2]

The American Clinical Neurophysiology Society (ACNS) [30] has been publishing standardized terminology of periodic and rhythmic EEG patterns in the critically ill to aid in future research involving such patterns since the year 2005 by publishing the initial proposed terminology. The standardized terminology has led to several investigations into the clinical significance of rhythmic and periodic patterns (RPPs) in critically ill patients, for example. This chapter will follow the terminology defined by ACNS when discussing related topics.

2.5.1. Frequency

Frequency means the number of waves passing by a specific point per second (when expressed in Hertz). Different EEG frequency ranges have been named by using Greek numerals. In Figure 6, a recorded EEG and the most studied waveforms can be seen in the order from the lowest to the highest frequency. The frequency bands are the following: [30]

- Delta δ 0.5 – 4 Hz
- Theta θ 4 – 8 Hz
- Alpha α 8 – 13 Hz
- Beta β 13 – 30 Hz

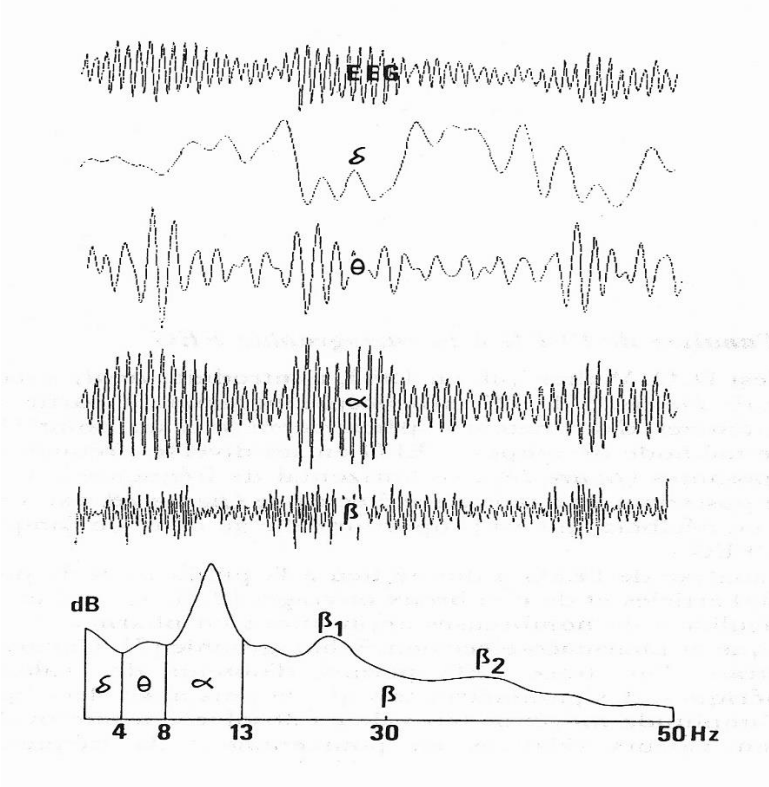

Figure 5. Spectral analysis of an EEG recording. The EEG is decomposed to different frequency bands and there is a power spectrum showing the power of different bands. by Pierre Raymond Esteve via Wikimedia Commons, CC0 license.

In addition to the most frequently studied frequency bands, there are:

- Infra slow oscillations (ISO) less than 0.5 Hz
- Slow waves less than 1 Hz
- Sigma waves or spindles 12 Hz – 16 Hz
- High-frequency oscillations (HFOs) greater than 30 Hz
    - Gamma γ 30 Hz – 80 Hz
    - Ripples 80 Hz – 200 Hz
    - Fast Ripples 200 Hz – 500 Hz

Figure 6. An example of HFO burst recorded in neurophysiological in vivo experiment. by Wsredniawa via Wikimedia Commons, CC0 license.

These are outside the conventional bandwidth of clinical EEG but are of clinical importance in digital signal processing. [2] Frequency bands are often defined individually for each subject, but it must be emphasized that EEG frequencies vary between different recording sites. For example, the frequency of alpha waves is faster at posterior and slower at anterior recording sites. [31]

The Fast Fourier Transformation (FFT) algorithm is a key technique when considering the frequency bands. FFT is used for transforming a signal from the time domain to frequency domain. When used in EEG signals, it can extract information about different frequency bands by providing a power spectrum showing the amount of power at each frequency band. [32]

FFT breaks down a complex EEG into sine waves with varying amplitudes or frequencies. The signal power (energy against time) at a certain frequency is then plotted on a graph to create the power spectrum. It has two domains: frequency and time. It is possible to define the frequency domain as the relative distribution of the component waveforms at various frequencies. The frequency pattern's evolution through time can be seen in the time domain. [33]

$$X(f_i) = \sum_{t_i} x(t_i) e^{-i2\pi f_i t_i}$$

Equation 4. Fourier Transform. In the equation, $x(t_i)$ is a set of signal values sampled at time moments t_i which Fourier transform can transform into a set of an equal number of complex values $X(f_i)$ corresponding to a set of frequencies f_i. Basically, $X(f_i)$ is a frequency spectrum, which is a histogram of amplitudes or phase angles as a function of the frequency of signal $x(t_i)$. [34]

FFT was invented in 1965 and it deserves much of the credit for early progress in the field as it made it simpler to compute the spectral coefficients and perform the spectral analysis of EEG. [35] Before the publication of the FFT methods, computer programs were using hundreds of hours of computer time with procedures requiring a lot of operations to compute Fourier Transforms of data points [36]. Fourier Transform power spectrum is an important method for obtaining the power spectrum including the contribution of sine waves with different frequencies. The spectrum is continuous, but the brain state of an individual may make certain frequencies more dominant. [12]

The power spectrum can provide us with information about the state of a patient and changes in it can reflect changes in brain activity. Adults have a prominent alpha rhythm in the posterior head regions during calm wakefulness, which responds to eye opening and closing. With faster beta-range frequency waveforms over the frontal regions

and slower waveforms over the posterior regions, there is an anterior-to-posterior gradient. While awake, there is no delta activity and only a little amount of theta activity. Theta activity increases primarily in the central or parasagittal areas when a person becomes more sleepy. Delta activity is primarily seen during non-rapid eye movement (NREM) sleep, which is divided into rapid eye movement (REM) and non-rapid eye movement (NREM) phases. [37]

Despite the fact that the delta rhythm is not the slowest EEG rhythm, most EEG processing pipelines high-pass filter EEG to remove oscillations that are slower than the filter cutoff. The cutoff frequency is typically set between 0.1 and 0.5 Hz. In general, the delta band has more strength than other EEG frequency bands in all the distinct brain states. This is due to the inverse relationship between power and frequency, or what is known as a 1/f distribution, in the EEG power spectrum. [38]

Delta waves, a type of high voltage slow wave, can usually be seen in a waking state. While posterior activity is frequently below 1 Hz, anterior delta activity has a frequency range of 1.5 to 2 Hz and is more sinusoidal in shape. Delta therefore displays polymorphic patterns. In varying degrees, delta is present during various stages of sleep. The duration of earlier wakefulness may have an impact on how much delta power is present during sleep, which is why it is thought to be a sign of the homeostatic process. The role of slow wave sleep in downscaling synaptic potentials generated during waking has also been suggested and delta plays a role in learning processes. [39]

Delta oscillations during wakefulness have been associated with an absence of consciousness since the early days of EEG research. Commonly the presence of high amplitude delta oscillations (HADOs), a large variety of delta activity, is often seen to be observed during states of unconsciousness or diminished consciousness such as slow wave sleep, anesthesia, and disorders of consciousness (DOC), which includes coma and vegetative state. [40]

Theta waves are a specific form of EEG brain wave with a frequency range of 4–8 Hz and are frequently linked to creativity, meditation, and states of deep relaxation. Theta waves have no defined amplitude range, and they have a maximum over the central and temporal cortex. [39] They frequently appear during moments of light sleep, daydreaming, and intense concentration. Theta waves have been linked to learning and memory consolidation, according to studies. Theta waves have also been connected to a number of mental health issues, including anxiety and depression. [41]

Alpha is the best-known and the most extensively studied rhythm of the brain. Alpha oscillations are present in healthy adult brain when relaxed and eyes closed, and it is the dominant frequency in the human scalp EEG. Alpha oscillations are manifested as a peak in spectral analysis, and they are reflecting rhythmic alpha waves. [42] Alpha has maximum occurrence over the occipital lobe, and it attenuates strongly by eye opening and mental operations like mental imagination. In most cases, the amplitude of alpha rhythm ranges between 10 and 50 μV. [39]

Beta is a high frequency EEG activity which Berger first observed in the waking state in 1937 and he hypothesized that such activity must be a “material concomitant of mental processes”. Beta and gamma activities have been associated with attention, perception and more generally, cognitive function in humans. [42] Beta rhythms may be present bifrontally and attenuated with eye opening, alerting, and movement. [43]

Slow waves are EEG activity of frequency below 1 Hz. Slow waves occur in the state of anesthetic-induced coma and in slow-wave sleep. These slow waves are seen to be important for memory consolidation during natural sleep. Tracking the emergence of slow waves during transition to unconsciousness may be helpful in identifying drug-induced alterations and provide insight into the mechanisms of general anesthesia. [44]

The frequency of EEG activity can have different properties and it can be either rhythmic, arrhythmic, or dysrhythmic. Rhythmic means EEG activity consisting in waves of approximately constant frequency. In arrhythmic EEG there are no stable rhythms present. Dysrhythmic EEG can point to the underlying morphological and functional brain abnormalities. [45]

2.5.2. Amplitude

In EEG, frequency and amplitude are inversely related. When the frequency of the EEG decreases, the amplitude commonly increases. Amplitude means the distance from the center line or the still position to the maximum displacement of the wave. It is the strength of the EEG pattern in terms of microvolts of electrical energy. Amplitude of EEG signals measured on the scalp usually ranges from 10 to 100 μV, which is about 100 times lower than the amplitude of ECG signals. [12]

Pathologies like a tumor or hydrocephalus can impede signals or affect conductivity, resulting in a reduction of the EEG voltage. If the amplitude is less than 20 μV, it is defined as low amplitude EEG. In low amplitude EEG, it is hard to detect clinically relevant EEG abnormalities. [46]

EEG signals can be classified into four categories according to their amplitude: [30]

- High: most or all activity ≥ 150 mV
- Normal
- Low: most or all activity < 20 mV
- Suppressed: all activity < 10 mV

2.5.3. Rhythmicity

Rhythmicity is observed in certain EEG patterns despite the complex and seemingly random nature of neural electrical activity. These patterns exhibit rhythmic characteristics and can be observed during both sleep and wakefulness. Two key processes contribute to the mechanisms underlying this phenomenon: the interaction between the cortex and thalamus, and the intrinsic potential for rhythmicity in large neural networks within the cortex.

The interaction between the cortex and thalamus, along with the functional characteristics of neural networks, give rise to distinguishable EEG patterns that vary across different regions of the neocortex. These patterns help us understand the intricate world of brain waves. EEG waves can be categorized into monomorphic and polymorphic waves, with monomorphic waves being rhythmic and showing uniform frequency and amplitude. [18]

The ACNS has defined four terms to categorize rhythmic EEG patterns based on their spatial characteristics: [30]

- Generalized (G)
    - This term encompasses any bilateral, bisynchronous, and symmetric pattern. It can include patterns with a restricted field, such as bifrontal patterns. These patterns involve synchronous activity spread across both hemispheres.

- Lateralized (L)
    - Lateralized patterns encompass both unilateral and bilateral synchronous but asymmetric patterns. They involve activity that is predominantly concentrated on one side of the brain or exhibits asymmetry in terms of amplitude or distribution.
- Bilateral Independent (BI)
    - This term describes the presence of two independent lateralized patterns, each occurring in a different hemisphere. These patterns are asynchronous, occurring independently of each other. Each hemisphere can have its own lateralized activity.
- Multifocal (Mf)
    - Multifocal patterns indicate the presence of at least three independent lateralized patterns, with a minimum of one pattern in each hemisphere. These patterns are distinct and localized in different regions of the brain, representing multiple independent sources of rhythmic activity.

2.5.4. Symmetry

The balance or resemblance in electrical activity between homologous regions of the left and right hemispheres of the brain is referred to as symmetry in EEG. A certain amount of symmetry between the hemispheres is anticipated in a typical EEG. This means that the frequency, amplitude, and waveform shape of the electrical activity patterns recorded from the corresponding electrodes on either side should be similar.

Different clinical circumstances, such as brain lesions, strokes, or neurodegenerative diseases, can cause symmetry in the EEG to be disturbed. Asymmetrical electrical activity patterns in the brain may result from these diseases, revealing abnormalities or functional problems within particular regions or networks. Significant asymmetries or departures from symmetrical patterns might offer important diagnostic clues about the underlying neurological illness, but evaluating and interpreting them requires expertise. Symmetry of EEG can be categorized with the following three labels: [30]

- Symmetric
    - Similar or nearly identical electrical activity on both sides.
- Mild asymmetry
    - Minor deviation from perfect symmetry.
    - 0.5 – 1 Hz difference between sides.
- Marked asymmetry
    - Significant difference between sides.
    - Higher than 50% voltage difference between sides.

2.5.5. Morphology

Morphology is one way to interpret the EEG and it describes the overall shape of a waveform or set of waves. Commonly, each part of a wave in an individual waveform is considered a phase. Monophasic wave begins on one side of the baseline, and it has two parts, up slope, and down slope. An example of a monophasic wave is a simple spike. A biphasic wave starts on one side of the baseline with an up slope and a down slope going through the baseline and crossing it again during the up slope. The classic epileptiform spike and slow wave discharge are examples of a biphasic wave. Polyphasic waves cross the baseline multiple times. [47]

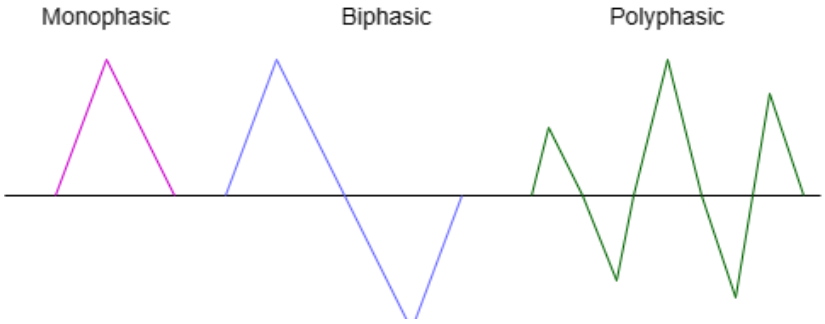

Figure 7. Monophasic, biphasic and polyphasic waves visualized. created with draw.io.

Both epileptiform and non-epileptiform aberrant waveforms can be noticed in an EEG recording. The reader should have a basic awareness of the normal EEG patterns in various physiological states in children and adults in order to recognize distinct aberrant waveforms in EEG. [48]

Waveforms or complexes in the EEG that are isolated and distinct from background activity are called transients. It is important to distinguish between benign EEG transients, which are common in healthy people, and pathogenic transients. These waveforms are transients that are not epileptiform but look to be epileptiform; yet they are unrelated to epileptic seizures. The ability to recognize these waveforms as non-epileptic requires training and experience. [2]

Wicket waves or wicket spikes are the most encountered benign pattern. The pattern has medium to high voltage and is a normal variant EEG pattern consisting of bursts or trains of sharply contoured 6 to 11Hz monophasic arciform waves. This pattern's maximum is in the middle temporal regions but can also occur as fragmented single sporadic spikes. [43] They can also occur in the anterior areas, and they have a negative polarity, and they usually evolve as arcuate-shaped, brief rhythmic discharges. These spikes are mostly seen in adults over 30 years old during drowsiness or light sleep or in individuals who have sharply contoured waveforms in the background activity. [49]

In awake states, lambda waves are positive acute transients that primarily develop during visual investigations and frequently vanish when closing the eyes. They occur in the occipital head area. [2]

Most healthy people have positive sharp transients similar to lambda waves during NREM sleep, known as positive occipital sharp transients of sleep (POSTS). [2]

Phantom spikes and waves are low amplitude, difficult to see spikes that occur in a complex of recurring spikes and slow waves. These are frequently observed in young adults and teenagers. Ctenoids have a widespread distribution of arciform morphology and

are unilateral, bi-synchronous, or asynchronous repetitions. They are typically observed during light sleep and sleepiness. [2]

Vertex Sharp Transients (VSTs) are surface negative sharp waves with phase reversal at or around the vertex. They can be mono or diphasic, and frequently triphasic, waves. This happens during NREM sleep and sleepiness. [2]

Small Sharp Spikes (SSS), Bening Sporadic Sleep Spikes (BSSS), or Bening Epileptiform Transients of Sleep (BETS) are low-amplitude, sharply counterbalanced monophasic or diphasic transients that are most common in N1 and N2 sleep. [2]

Rhythmic Mid-temporal Theta of Drowsiness (RMTDs) are theta activity trains seen during sleep-wake transition. They feature a monomorphic design with curves that are sharp or serrated. [2]

A rare benign EEG pattern called Subclinical Rhythmic Electroencephalographic Discharges of Adults (SREDA) is sometimes identified as an epileptiform pattern despite having no evident clinical significance. The rhythm may change from a slower delta to a faster theta rhythm abruptly or widely. [2]

The spectral peaks in the alpha and beta frequency bands that define mu rhythms might be referred to as mu-alpha and mu-beta. A sensory source close to the locations of two basal ganglia loops involved in motor control is the usual feature of mu rhythms. Therefore, the basal ganglia and sensorimotor activity have an impact on this rhythm. Both jobs requiring movement and those requiring thought are sensitive to power in mu. [50] Mu is sometimes more evident during drowsiness and when the eyes are open. Mu tends to attenuate when there is movement in the opposite upper limb or even thinking about such an action. Mu is a normal finding in the EEG pattern and that is where its importance mainly lies. [18]

K-complexes have a long duration and low amplitude. It has been described as a bi-triphasic EEG complex with a first rapid negative component and a second slow wave that is occasionally fused with a third rapid component (sleep spindles). It can be challenging to recognize these K-complexes. Because K-complexes can be induced by both internal and external stimuli, many people think they are an arousal reaction that can happen on its own. Frequently, a noticeable arousal or even wakefulness occurs after it. According to some, K-complexes limit cortical arousal while indicating information processing occurs during sleep. It is common knowledge that this pattern is related to autonomous activation. [39]

Sleep spindles appear during sleep, and they are a burst-like pattern consisting of 11-16 Hz sinusoidal cycles. Sleep spindles are generated in thalamic circuits and the thalamic reticular nucleus (TRN) of the thalamus serves as the pacemaker for the generation of sleep spindles. Spindles are present all over the human scalp but the majority of them appear in central regions. These spindles are used as an EEG hallmark of the N2 stage of non-rapid-eye-movement sleep and there are some expectations that this pattern may tell us about the development, efficacy, and plasticity of the forebrain circuits that make us intelligent individuals. [39] [51]

In intensive care, frequently encountered patterns in the EEG include slow wave activity, frontal intermittent rhythmic delta activity (FIRDA), triphasic waves, epileptiform patterns, and periodic discharges (PDs), suppression and burst suppression. Interpretation of these patterns and different waveforms usually happens by visual inspection, but it can also be performed by quantitative analysis of the frequency, amplitude, topographical distribution, cross correlation, and reactivity. [52]

Periodic Discharges (PDs) are regular and repetitive waveforms often displaying consistent frequency, morphology, and temporal features. PDs can occur in various clinical conditions and are typically indicative of underlying brain dysfunction. The periodicity of the discharges may vary, ranging from very frequent (every few seconds) to less frequent

(every few minutes). Discharges are waveforms lasting less than 0.5 seconds having no more than three phases. Bursts, on the other hand, are waveforms that last at least 0.5 seconds and have at least four phases. Both bursts and discharges must conspicuously stand out from the background activity. [30]

Rhythmic Delta Activity (RDA) is a rhythmic pattern of slow wave activity in the delta frequency range. It is characterized by repetitive, regular, and sustained delta waves occurring at a consistent frequency and duration. The patterns is associated with deep sleep and certain pathological conditions. It can be said rhythmic activity in the frequency range of 0.5 to 4 Hz. The duration of the rhythmic pattern should vary by less than 50% from the duration of the subsequent cycle for most cycle pairs to qualify as rhythmic. Sinusoidal waveform but also a pattern sharp at the top and/or bottom of the waveform are some examples of a rhythmic pattern. [30]

Spike-and-wave or Sharp-and-wave (SW) consists of a spike, polyspike, or sharp wave consistently followed by a slow wave in a regularly repeating and alternating pattern with a consistent relationship between the spike component and the slow wave for at least six consecutive cycles. There should not be an interval between one spike-wave complex and the next. These complexes are typically observed in patients with epilepsy or other related seizure disorders. They are especially associated with petit mal seizures. [30]

2.5.6. EEG signal analysis

In the intensive care unit and operating room settings, filters should be applied in the same way for standard EEG. We are mostly interested in frequencies between 1 and 50 Hz, but depending on the proposed study, we may also consider frequencies between 0.3 and 70 Hz. Band-pass filtering, which consists of low-pass and high-pass filters, can be used for this. If necessary, electricity lines should also have a notch filter (also called band-stop filter) that operates at either 50Hz or 60Hz, depending on the country. When electrodes make loose contact with the scalp, a noticeable notch artifact is often visible. [53] Applying filters is recommended as the first step of preprocessing and especially before segmenting the EEG into epochs. If this is not done, there will be filtering artifacts at epoch boundaries if the segmented EEG is being filtered.

Low-pass, high-pass, band-pass, band-stop filters are the most common filters. Low-pass filter removes the signals which are higher than a selected cutoff and passes signals which are below that. High-pass filter does the opposite. Band-pass filter passes signals which are in a specified range and attenuates the ones outside it. Band-stop filter or notch filter attenuates only the signals in a specified range. [54]

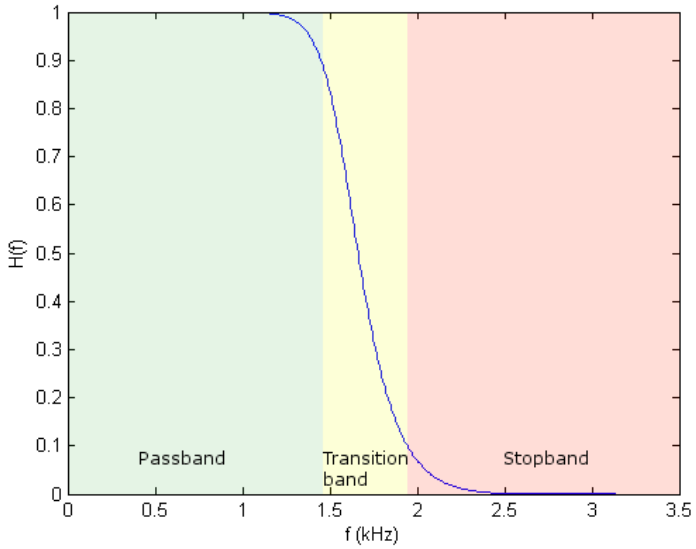

Figure 8. An example of a Butterworth lowpass filter's transfer function. The filter has a cutoff frequency of 2 kHz. Butterworth filter's key characteristic is the flat passband and the flat stopband also visible in the figure. by Runverzagt via Wikimedia Commons, CC4 International license.

The human subject and measuring environment constantly introduce a variety of artifacts into the raw EEG. Extrinsic artifacts include environmental artifacts and experimental errors caused by outside forces. Intrinsic artifacts are those caused by the body itself, such as physiological artifacts. Intrinsic artifacts can be for example eye blinking, muscle activity and heartbeat. [55] To correctly interpret the data, it is important to remove artifacts as part of preprocessing of the signal. In the case of EEG, preprocessing can be said to refer to removing noise to get closer to the true neural signals. [56]

Due to the fact that artifacts can skew the visual interpretation and diagnosis and interfere with brain signals or imitate cognitive or pathogenic activities, artifact identification and removal can be considered to be the most crucial step in the preprocessing in clinical diagnosis or practical applications. [55]

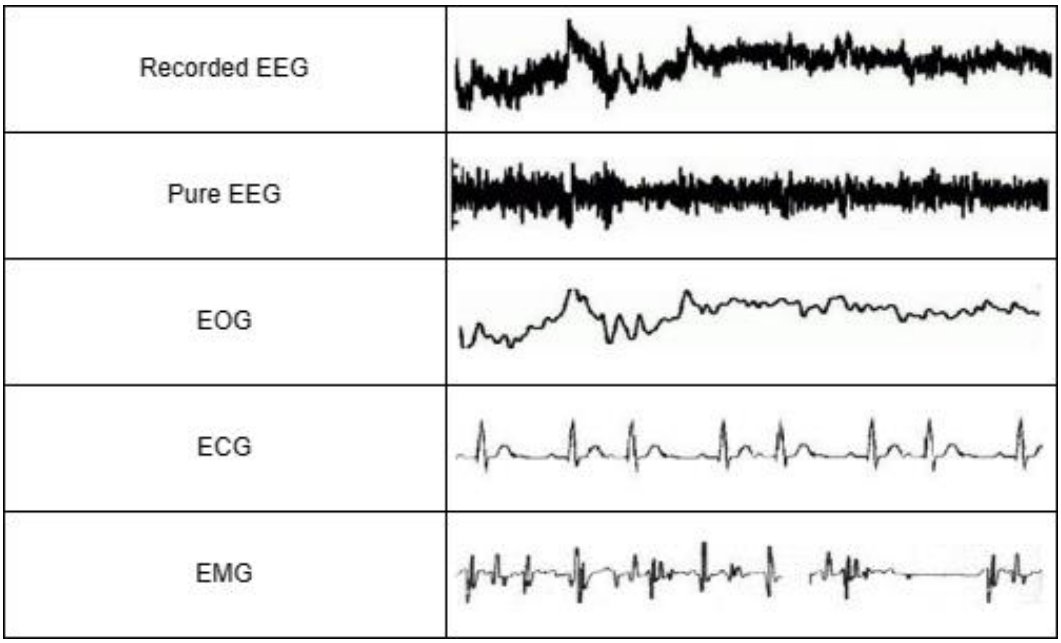

Figure 9. Examples of different physiological artifacts that are possibly present in the recorded EEG. created with draw.io.

Eye movements and blinks are a significant source of electro-oculography (EOG) aberrations, which are a typical problem in the processing of EEG recordings. EOG artifacts frequently emerge bilaterally and synchronously, are anteriorly located, have a higher amplitude, and have a lower or equal frequency to EEG signals. Ocular artifacts do not destroy the EEG but linearly sum on top of it. There are several methods developed for attenuating the EOG artifacts like decomposition-based and regression-based techniques. [57] [54]

Electrocardiogram (ECG) artifacts have been shown to significantly degrade the quality of quantitative EEG measures which can be used as a support in analysis of EEG in addition to visually observing the raw EEG. [58] ECG artifacts are electric potentials generated by the pulsating human heart. The ECG normally has a frequency range of 0.05-100 Hz. It is characterized by five peaks and valleys labelled by the letters P, Q, R, S and T. QRS complex together with the T-wave represent the excitation of the ventricles or the lower chamber of the heart. Detection of this QRS complex is the most important task when automatically analyzing ECG signal. [59] There is also another type of cardiac artifact called pulse artifact or vasopressor artifact. The expansion and contraction of the heart create pulse artifacts, which are detected in the electrode that is positioned on or close to a blood artery. ECG has a regular pattern, and it can be easily removed using a reference waveform measured from the heart. [55] Cardiac interference recorded by EEG is often spiky, quasi-periodic signals and it can seriously affect EEG basic rhythm waves (0-30Hz). Using traditional filters may result in the loss of EEG components as the ECG artifacts have a spectral overlap with EEG. Usually, referential montage is used to attenuate ECG artifacts. [58]

Electromyography (EMG) artifacts are common in the EEG nowadays as the measurements are not only done in well-controlled clinical settings but also in ambulatory care and especially in long-term EEG monitoring EMG artifacts are impossible to avoid. EMG artifacts are caused by muscle movements and contraction on the head surface. It has

non-stationary characteristics, and the activity has a wide frequency range overlapping all classic EEG rhythms. EOG and ECG artifacts can be suppressed by using adaptive filters and BSS techniques but eliminating EMG artifacts is challenging. We can't use classical filters in case of EMG in EEG as the frequency bands of the noise and the signal of interest are often overlapping. Adaptive filtering with a reference muscle signal and Kalman filtering can be used for example, but many other methods have been developed also. [60]

For the removal of artifacts, many methods have been developed, particularly for physiological artifacts. These methods fall into one of two categories: either decomposing the EEG signal into several domains or estimating the artifactual signals using a reference channel. Regression, Blind Source Separation (BSS), Empirical-mode Decomposition (EMD), Wavelet Transform algorithm, and their hybrid methods are just a few examples of techniques. According to [55], the most popular algorithms are BSS-based ones and, in particular, ICA. Many prefer to employ a hybrid approach to improve the effectiveness of techniques. It is important to highlight that there is still disagreement over the best solution for various kinds of artifacts.

Artifacts have traditionally been removed from EEG with regression methods. These presumptively represent each channel as the total of pure EEG data plus a certain amount of artifact. It defines the amplitude relation between reference channel and EEG channel by transmission factors and then subtracts the estimated artifacts from EEG. The algorithm requires exogenous reference channels like EOG or ECG to omit different artifacts. In case of EOG artifacts:

$$EEG_{cor} = EEG_{raw} - \gamma F(HEOG) - \delta F(VEOG)$$

Equation 5. Here γ and δ depend on the transmission coefficient between EOG and EEG, and EEG_{cor} and EEG_{raw} are corrected EEG data and raw EEG data. HEOG and VEOG are recordings from horizontal and vertical EOG channels. [55]

In the BSS method, multiple unsupervised learning methods without prior knowledge and additional reference channels are included. BSS typically functions as follows:

$$X = AS$$

Equation 6. Observed scalp electrode signals are denoted by the symbol X, whereas source signals, including original signals and artifacts, are denoted by S. An unidentified matrix A linearly combines these source signals.

The BSS algorithm is a reversed version for the signals that were observed:

$$U = WX$$

Equation 7. Where W is the reverse mixing of X and U is the estimation of sources. Following the removal of the artifact components, the remaining components reconstitute EEG data. [55]

Independent Component Analysis (ICA) is a BSS technique, and it is often used in the preprocessing phase for filtering out artifacts from the signal. ICA has been shown to work best with multichannel recordings. ICA searches for a linear transformation which minimizes the statistical dependence between the components that are involved in the signal. [61] ICA assumes that signal sources are instantaneously linear mixtures of cerebral and artifactual sources and it decomposes the signal into independent components (ICs).

After ICs are removed from the original signals, the clean signal is rebuilt by removing ICs that contain artifacts. [55]

Feature extraction is meant for calculating the features or information that are the most important for the analysis. By the feature we mean a distinctive or characteristic measurement, transform or structural component that is being extracted from a segment of a pattern. Feature extraction minimizes the loss of important information in the signal and simplifies the number of resources needed to describe a large set of data accurately. It is important to minimize the complexity of implementation, to reduce costs of the processing and to cancel the need to compress the information. Classification is the final stage of EEG signal processing, and it can be solved by linear analysis, non-linear analysis, adaptive algorithms, clustering and fuzzy techniques and neural networks for example. [62]

2.6. EEG in diagnosis in Intensive Care and Operating Room

EEG is being used in the Intensive Care Units (ICUs) and Operating rooms (ORs) both as a diagnostic and as a prognostic tool. Monitoring the depth of anesthesia with EEG is well established in the OR but less studied in the ICU. EEG has some great advantages compared to other brain imaging techniques and thus, its usage has increased over the years. EEG is used for diagnosis of epilepsy, and it is especially useful in detecting non-convulsive seizures. It is useful also with patients with encephalopathies and it can be used for the prediction of prognosis after cardiac arrest or stroke.

The biggest advantage of EEG is its speed. It only takes fractions of a second to record complex patterns of neural activity after a stimulus has been administered. EEG does not provide as good spatial resolution as MRI and PET do, and thus EEG images are often combined with MRI scans. [12] MEG, fMRI, and PET are expensive, non-portable, partially invasive and there is usually high stress due to noise, space confinement, and the need to be motionless. Also, fMRI and PET scans have poor temporal resolution. EEG is a cheap, fast and portable technique measuring neuronal activity directly and non-invasively.

The measurements used for the C-Trend analysis in the study are performed in the environment of OR. In ORs, EEG is mainly used for depth of anesthesia assessment, and it has been widely used clinically for this purpose since the 1990s. [63] In ORs, postoperative delirium is a common complication after surgery of which prevention processed EEG monitors of anesthetic depth during anesthesia is recommended to be used. The World Health Organization (WHO) stated in 2018 that a depth of anesthesia monitor is suggested (but not universally used) to be used in cases at risk of awareness under general anesthesia or postoperative delirium. [64]

The measurements used for the federated learning in this study are performed in the ICU. Intensive care is needed when the patient is seriously ill and requires close monitoring and intensive treatment. There are many different situations in which the patient needs intensive care. Most people in intensive care have problems with one or more organs and, for example, may be unable to breathe on their own. Also, after surgery intensive care may be needed for recovery. An ICU is an integral part of the health care system. Most of the ICUs in the World are in high-income countries but they are also becoming a feature of health care systems in low- and middle-income countries. An ICU has been defined to be an organized system for organizing the care for critically ill patients who need intensive and specialized medical and nursing care. The ICU has enhanced monitoring capacity and several modalities of physiological organ support to sustain life during a time of life-threatening organ system insufficiency. [65]

In the ICU, patients with unexplained consciousness disorders typically undergo blood testing, blood gas analysis, and head computed tomography (CT) or magnetic resonance imaging (MRI). These only offer data at the time the examination is conducted, but because the brain experiences dynamic and ongoing changes, continuous EEG is a crucial technique for determining consciousness. [66] Intensive care units have many electrical and artifact resources and EEG that is being measured there is prone to different artifacts. For example, in ICU there are mechanical ventilation, medication pumps, and other electrical devices and environmental noises which must be considered when working with the EEG signals. [53]

There are guidelines provided for the indications of EEG in the ICU by several different critical care and neurophysiology societies. The main recommendations include seizure detection for:

1) Patients who have convulsive status epilepticus and have not recovered their baseline.
2) Comatose patients without a clear explanation of their mental state, whether they have brain damage or not.
3) Patients with unresponsive hypoxic ischemic brain injury who are hypothermic and who are rewarmed within 24 hours.
4) Also, detection of delayed cerebral ischemia in subarachnoid hemorrhage patients, prognostication after coma and monitoring of continuous sedation. [67]

All types of acute illness and trauma patients also in the ICU can be assessed using the widely used Glasgow Coma Scale (GCS) to determine how severely their consciousness has been affected. GCS has been the gold standard for assessment of the level of consciousness in patients with significant brain injury. It is simple and practically useful. Using GCS is not a useful choice in case the patient is sedated as they are not responsive. The scale does the assessment based on three aspects of responsiveness: eye-opening, motor, and verbal responses. Each of these is separately reported, and it provides a clear picture of the patient's state. Each of these has maximum points of 5 and altogether 15 points 15 being normal. Comas are generally classified in the following way: [68]

Severe (GCS $\leq$ 8)
Moderate (GCS 9 - 12)
Minor (GCS $\geq$ 13)

Another simple scale with 4 components is the "FOUR Score," where "4" represents the maximum possible score for each item. The brainstem pupil, cornea, and cough reflexes, as well as the respiration (breathing rhythm and respiratory drive in ventilated patients), are the elements. The ocular responses include eye opening and eye tracking. The FOUR Score is a step forward from earlier scales and is more accurate in identifying and communicating impaired consciousness. [69]

Lastly, Cerebral Performance Category (CPC) score is a commonly used and a simple measure for assessing the neurological condition during the ICU stay and recovery after that for example 6 months after leaving the ICU. It is commonly used for describing the outcome after cardiac arrest as approximately half of the survivors of that have cognitive impairments due to hypoxic brain injury. The CPC consists of a 5-point scale (Figure 10), where scores 1 and 2 are mostly considered as good outcomes and 3,4 and 5 as poor outcomes. There is no standardized method for determining the CPC score and as a result the procedure of it varies greatly. [70]

The CPC score assessed 3-6 months after leaving the ICU is commonly used in the annotation of EEG data for machine learning. Patients' data is categorized into good and poor outcome groups based on the CPC score. This is also utilized in the C-Trend technology. Below, the definitions of different groups can be seen.

Grading	Neurofunctional manifestations	Clinical manifestations
CPC 1	Good cerebral performance:	Conscious, alert, able to work, might have mild neurologic or psychologic deficit.
CPC 2	Moderate cerebral disability	Conscious, sufficient cerebral function for independent activities of daily life. Able to work in sheltered environment.
CPC 3	Severe cerebral disability	Conscious, dependent on others for daily support because of impaired brain function. Ranges from ambulatory state to severe demaletia or paralysis.
CPC 4	Coma or vegetative state	Any degree of coma without the presence of all brain death criteria. Unawareness, even if appears awake (vegetative state) without interaction with environment; may have spontaneous eye opening and sleep/awake cycles. Cerebral unresponsiveness.
CPC 5	Brain death	Apnea, areflexia, EEG silence, etc.

Figure 10. CPC score scales and their neurofunctional and clinical manifestations. Scientific figure on ResearchGate, available from: www.researchgate.net/figure/Cerebral-performance-category-CPC-score-scale-1_tbl1_345403226, CC4 International license.

2.6.1. Important patient groups

This chapter discusses epileptic seizures, encephalopathies, cardiac arrest, stroke, coronary artery bypass graft, and carotid endarterectomy, all of which can have tremendous effects of the wellbeing of the patient and for which EEG can be useful in a way or another.

An epileptic seizure happens when there is an abnormal excessive and synchronous neuronal activity in the brain. There are many different types of seizures, and they can, for example, be divided into partial and generalized seizures. Epilepsy can be said to be a condition of recurrent unprovoked seizures. Status epilepticus is a prolonged epileptic condition. [71]

In the ICU, there are cases of non-convulsive status epilepticus (NCSE), which refers to an epileptic seizure lasting more than five minutes without such dramatic convulsions that are seen in generalized tonic-clonic status epilepticus. If the duration of subtle status epilepticus is more than 60 minutes, mortality associated with it exceeds 30%. [72]

In the ICU, non-convulsive status epilepticus occurs especially during acute brain damage, recent convulsive status epilepticus, tumor postoperative care, subdural

hematomas, subarachnoid hemorrhages, poisoning and metabolic and electrolytic alterations. [73] Epilepsy affects more than 2% of the people worldwide and developed countries are being affected the most. Epilepsy significantly reduces productivity and quality of life. When a seizure occurs, it can hurt a patient or put them in danger if they're doing something dangerous, like operating machinery or driving. [25]

Seizure periods are difficult, and time consuming to locate and detect, as EEG recordings can be tens or even hundreds of hours long. Therefore, automatic seizure detection methods are needed. Epilepsy seizures are classified mainly as generalized or local, and partial seizures or focal. Generalized seizures are produced by electrical impulses throughout the brain and are classified as Grand Mal, Absence, Myoclonic, Clonic, Tonic, and Atonic. Partial seizures occur in a small part of the brain and are classified as simple and complex. In seizure signal, there are four states identified:

- Pre-ictal
- Ictal
- Inter-ictal
- Post-ictal

Pre-ictal and post-ictal are portions of the signal before the first seizure and after the last one. Ictal and inter-ictal are the intervals of seizures and between seizures. Seizure detection methods are many different kinds, but they can be categorized into five domains: time domain, frequency domain, wavelet domain (time-frequency), empirical mode decomposition (EMD), and rational transform domain. The performance of different seizure detection algorithms depends primarily on the following: transformation technique, feature selection, classifier used, window size, type of window or mother wavelet, the levels of decomposition of the original signal, and optimization algorithm, for example. [25]

Encephalopathy is a typical complication in critically ill patients and means some damage or disease affecting the brain resulting in altered attention, cognition, or consciousness, and it can have many causes. The cause can be, for example, metabolic problems, infections, drugs, toxins, physiological changes, etc. [52] Encephalopathies can have two forms: acute and chronic. The acute form can range from mild confusion and delirium to coma. In the more chronic one, slowly progressive or static conditions of encephalopathy there may be just a loss of cognitive capacity at first. Encephalopathies can be associated with poor prognosis and even death. [37]

EEG is being used in evaluating patients with acute and chronic encephalopathies. Mainly the focus is in differentiating the conditions associated with seizures. EEG patterns in encephalopathies are sensitive but rarely specific to a particular etiology but it can provide a good measure of cerebral dysfunction and give information of the severity of the encephalopathy. There is usually some slowing of cerebral activity and diffuse slow waveforms in the background. [37] Slowing or missing alpha rhythm is one of the early signs of encephalopathy [52].

Some EEG patterns are found in encephalopathy. Diffuse slowing, triphasic waves (TWs), generalized rhythmic delta activity (GRDA), lateralized periodic discharges (LPDs) or periodic lateralized epileptiform discharges (PLED), generalized periodic epileptiform discharges (GPEDs), bilateral independent periodic epileptiform discharges (BiPEDs), alpha coma and spindle coma, burst suppression and electrocerebral inactivity (ECI) or silence (ECS) can occur. [37]

Cardiac arrest is a sudden ending of cardiac activity, and it makes the patient unresponsive, without normal breathing and signs of circulation. Cardiac arrest is usually

reversed by cardiopulmonary resuscitation (CPR), defibrillation, cardioversion, or cardiac pacing and with fast medical care survival is possible. The cause of cardiac arrest is generally an underlying cardiac disease, and approximately 70% of cardiac arrest cases are believed to be due to ischemic coronary disease. In addition to this, there are other structural and non-structural causes of cardiac arrest. [74]

Hypoxic ischemic encephalopathy (HIE) is the largest contributor to disability and mortality after cardiac arrest. HIE causes brain injury and neuronal cell death as blood circulation to the brain is blocked. EEG is a widely used tool for neurological prognostication in cardiac arrest and HIE. For example, epileptiform patterns or presence of burst-suppression patterns have been shown to predict poor neurological function. Also, EEG background reactivity (EBR) has been seen as a powerful predictive factor. [75] EBR has been defined as a reproducible change in cerebral EEG activity meaning amplitude or frequency, including attenuation. It basically means any change in background rhythm. [76]

There are three types of strokes: ischemic, hemorrhagic, and subarachnoid, of which ischemic and hemorrhagic are the most common types. Stroke is one of the most common causes of death. Approximately 10% of the patients who experienced a stroke leave the hospital alive and most of them neurologically impaired. [77]

Ischemic stroke is the most common type of stroke and occurs because of a clot in a blood vessel that is in the brain or leads in the brain. There are two types of ischemic stroke: cerebral thrombosis and cerebral embolism. In the thrombotic stroke, there is a clot in the brain and in the embolic stroke, there is a clot elsewhere in the circulatory system blocking the blood flow to the brain. [77]

A hemorrhagic stroke occurs when there is a weak vessel that ruptures and bleeds in the brain. There are two types of hemorrhagic strokes: intracerebral hemorrhage (ICH) and subarachnoid hemorrhage (SAH). These two differ in the space they are bleeding into. ICH bleeds into the brain parenchyma and SAH bleeds into the subarachnoid space. It is important to diagnose this early as it may expand and cause deterioration of consciousness and neurological dysfunction. [78]

Coronary artery bypass graft (GABG) is the most performed major surgical procedure and is a treatment option if the patient has a blocked artery to the heart. The operation is being performed under general anesthesia and after it the patient needs ICU care. In coronary artery bypass graft a healthy blood vessel is being connected to the blocked arteries to redirect the blood flow. CAGB has some complications like stroke, wound infection, graft failure, renal failure, postoperative atrial fibrillation and even death. [79]

Carotid endarterectomy (CEA) is a surgery which is being performed to remove plaque buildup in the common carotid and internal carotid arteries. The operation is being done to reduce the risk of stroke and there is neurological impairment during the operation. When the plaque builds up in the artery, it can lead to atherosclerosis and stenosis of the artery. This kind of artery disease increases patient's risk for cerebrovascular disease and stroke. [80]

2.7. Fundamentals of anesthesia

Anesthesia – medically induced, controlled sleep-like state to prevent sensation of pain during medical procedures is a cornerstone of modern medicine. Anesthesia is a result of several inhibitor processes which interact to lead to the four components of anesthesia: loss of consciousness, amnesia, immobility, and analgesia. [81]

Anesthesia and analgesia (loss of sensation of pain) can be thought to have existed as long as mankind itself has. In 1846, William T.G Morton got credit for being the first one to perform surgical procedure with anesthesia together with J. C. Warren. They used inhalable ether and suggested that in the proper dose it provides safe and effective anesthesia. Morton became credited with discovering the procedure, but Crawford Long was the true pioneer of this medical advancement as he used ether to painlessly remove a tumor from neck of a patient already in 1847. [82] [83]

The first significant anesthetics were ether and nitrous oxide. Ether was first known as "sweet vitriol" and that time it was described as follows: "It quiets all suffering without harm and relieves all pain". In 1730 it was named ether. Nitrous oxide was discovered in 1772 but its anesthetic and analgesic qualities were not recognized until 1799. [83]

Before Morton and Crawford, many dentists and doctors used nitrous oxide for anesthetic purposes. [82] Nitrous oxide is seen as the oldest of all anesthetics and these days it is the least potent inhalational anesthetic. It cannot be a sole anesthetic agent and thus it is usually used with a more potent and volatile anesthetic. [84] The use of ether in anesthesia was opposed by some surgeons but its use spread rapidly around the world after the year 1846. In 1847, James Y. Simpson proposed chloroform as an alternative to ether. John Snow, who is considered by many to be the first anesthesiologist, popularized chloroform. [85]

The anesthetic agents used these days can be divided into two main classes: intravenous and volatile agents used for anesthesia induction and maintenance. By modern anesthetic techniques typically a hypnotic drug is co-administered with an analgesic drug and a muscle relaxant. [86]

Intravenous anesthetics induce anesthesia rapidly as they achieve high concentrations in the central nervous system rather quickly. Commonly used intravenous agents are thiopental, propofol, ketamine and benzodiazepines. [87] [88] Intravenous anesthetic agents can be broadly classified into the following classes: sedative-hypnotics, muscle relaxants, and opioids. Opioids and relaxants are commonly used together with sedatives to provide analgesia, supplement sedation and to relax the patient, so that the operation is easier to perform. As all patients are individuals and there is variability between them, it is impossible to precisely anticipate the effect of intravenous anesthetic. It requires the anesthesiologist to carefully titrate the anesthetics according to each patient's individual response. [89]

Opioids are being used during almost every phase of surgeries. The most used opioids in anesthesia include fentanyl, morphine, hydromorphone, sufentanil, remifentanil and alfentanil. Fentanyl has been the favored intraoperative agent for years as it has a rapid onset, it is very potent, and it is simple for anesthesiologists to dose. [90]

These days, volatile anesthetics include sevoflurane, desflurane, and isoflurane. Volatiles are liquid substances that must be vaporized before inhalation. To administer these volatiles, routine bedside gas monitoring is required. The cerebral concentration can be monitored in real time with the use of the expired end-tidal concentration, which also helps with titration and reduces the risk of overdose. Patient waking and extubation periods may be shortened due to volatile anesthetics. [88]

There are different types of anesthesia and which one the patient is receiving depends on factors like the procedure and patient's health. General anesthesia is commonly used for major operations, and it is induced with anesthetics inhaled or intravenous. When the anesthesia starts working, the patient will be unconscious and many of the body's functions will slow down. When the procedure is completed, the medication will be reversed, and the effects of anesthetics will gradually vanish. [91]

The anesthetic agents may induce unconsciousness, amnesia, analgesia, skeletal muscle relaxation, and the loss of autonomic system reflexes. The patient is not responsive to verbal, tactile, or painful cues when under general anesthesia. To maintain the patency of the upper airway, a laryngeal mask airway or endotracheal tube may be required. Additionally, a patient's spontaneous breathing is frequently insufficient, necessitating mechanical support and positive pressure ventilation. The patient's cardiovascular system may also deteriorate. [92]

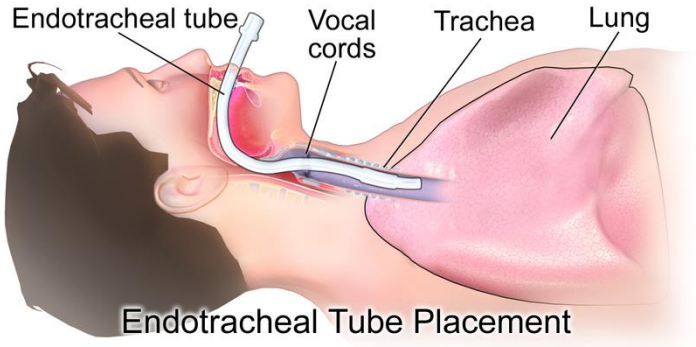

Figure 11. An example of endotracheal intubation that may be needed during anesthesia. by BruceBlaus via Wikimedia Commons, CC4 International license.

During the surgery or procedure, the patient's heart rate, blood pressure, breathing and other vital signs are monitored. [91] The cardiovascular system is monitored using invasive and noninvasive methods and the respiratory system is being observed by arterial blood samples and ventilator curves. Also, the function of renal system is analyzed by checking urine output and creatine levels. [64]

We do know that anesthetics predominantly target the GABA receptor, the NMDA receptor, and the two-pore-domain K+ channels, even though the precise mechanism of anesthesia is still unknown. Other receptors and ion channels are additionally impacted in distinct ways. [78] General anesthetics primarily alter glutamatergic and GABAergic synapses to reduce excitatory and/or increase inhibitory synaptic transmission. Affected mechanisms include dendritic spine dynamics, postsynaptic receptor signaling, and presynaptic neurotransmitter release. Long-term synaptic disruption after anesthesia may have unfavorable neurocognitive effects because synaptic structure and plasticity mediate higher-order activities including learning and memory. [93]

Anesthetics reduce consciousness by impairing brain feedback transmission, while basic neuronal activity and feedforward signaling are mostly unaffected. It is also unknown what causes this selective function. The connection between the thalamo-cortical and cortico-cortical regions, which is thought to be essential for conscious perception, is selectively blocked by anesthesia. [94]

Sedation is a lighter form of anesthesia which is used for pain control in minor surgeries. A medication called analgesic is often combined with sedation and it is used to achieve analgesia meaning pain relief. Sedation and analgesics are often given intravenously. The level of sedation may range from minimal to deep. [95]

Levels of anesthesia from the lightest to the deepest have been defined by American Society of Anesthesiologists (ASA). The levels are: [96]

- Minimal sedation (Anxiolysis)
- Moderate sedation (Conscious sedation)
- Deep sedation

- General anesthesia

During minimal sedation the patient is responsive, ventilation is spontaneous and cardiovascular function is unaffected and the patient can respond to verbal commands and may have some cognitive impairment, but there is no effect on cardiopulmonary status. In moderate sedation, there is a depression of consciousness, but responding to verbal commands is on appropriate level. The airway is maintained independently; ventilation is adequate and cardiovascular function remains unaffected. In deep sedation, the patient can't be aroused easily but may respond to repeated or painful stimulation. Airway support maneuvers and insertion of oral or nasal airways may be needed. At the level of general anesthesia, the patient is not aroused by painful stimuli and there may be impairment of cardiovascular function. It is important to note that individuals have different responses to sedation and different levels of sedation may be needed for the same procedure. [96] [97]

In addition to the levels of anesthesia, there are four stages of anesthesia which are based on Guedel's classification: [92]

Stage 1	Analgesia or disorientation	The anesthetic agent's effects may begin to be felt at this point, but the patient is not yet unconscious. The patient moves from analgesia-free amnesia to analgesia and concurrent amnesia. The loss of consciousness signals the conclusion of the stage.
Stage 2	Excitement or delirium	In the stage the patient may experience disinhibition, delirium, uncontrolled movements, loss of eyelash reflex, hypertension, and tachycardia. Airway reflexes are intact and are often hypersensitive to stimulation. A patient's airway can be compromised due to spastic movements, vomiting and rapid, irregular respirations. Using fast-acting anesthetic agents shortens the time spent in stage 2 and facilitates entry to stage 3.
Stage 3	Surgical anesthesia	Stage 3 is surgical anesthesia meaning the targeted anesthetic level for procedures requiring general anesthesia. The hallmarks of this stage are ceased eye movements and respiratory depression. Manipulation of airway is safe at this point.
Stage 4	Overdose	Stage 4 is overdose and it occurs when too much anesthetic agent is given. Overdose worsens an already severe brain or medullary depression. The stage begins with respiratory cessation and ends with potential death. The patient should not be in this stage and thus, the goal of anesthesiologists is to transition the patient back to stage 3 and keep them there for the duration of the operation.

In addition to Guedel's classification, Brown's study talks about three different periods of anesthesia in which the EEG pattern is different. The periods are: induction, maintenance and emergence. Before the induction, the patient has normal EEG activity with prominent alpha activity. After the induction the patient may enter a state called paradoxical excitation which is similar to being drunk. In this state the patient may experience incoherent speech, euphoria or dysphoria, distorted time perception and depersonalization. The EEG pattern shows an increase in beta activity. This phase ends with LOC. In maintenance phase there can be different EEG patterns depending on the depth of anesthesia. Emergence from anesthesia is a passive process which depends on the amount of drug(s) administered. [34]

When anesthetic agents are being induced, anesthesia deepens, and its effects can be seen in the EEG. The EEG becomes more regular and finally disappears into an isoelectric activity called burst-suppression in a very deep anesthesia. When the anesthesia is at the level of moderate to deep, the EEG is dominated by globally coherent slow wave activity in the delta frequency range (0-4Hz). [98]

Loss of consciousness and return of consciousness are important moments clinically. EEG alterations that occur during the induction and emergence from anesthesia are frequently symmetrical. Patients typically awaken when the amplitude of their EEG begins to decline when analgesia is correctly administered. The return of consciousness is often seen as the time when there is response to verbal command but there are cases when the patient does not respond even if the EEG pattern has returned to normal, wakeful state. [99]

In contrast to the wakeful state, the EEG during NREM sleep and anesthesia exhibits increased power at lower frequencies, particularly delta power in the fronto-medial regions. This occurs during NREM sleep because there are a lot of slow EEG waves. The greatest electrophysiological event of sleep, slow waves, may oversee some of sleep's functional effects. We still don't know how similar slow waves in anesthesia are to slow waves while you sleep. For instance, anesthesia causes rapid frequency rises that are not present during regular sleep, and memory consolidation differs under anesthesia from during sleep. [100]

General anesthesia does not shut down the brain globally and it does not always result in a total absence of consciousness. Depending on the anesthetic agent and its dose, the anesthesia may produce different consciousness states including a complete absence of subjective experience (unconsciousness), a conscious experience without perception of the environment (disconnected consciousness, like during dreaming), or episodes of oriented consciousness with awareness of the environment (connected consciousness). It was believed in the past that anesthesia switches off the brain completely, but nowadays it is clear that the patient may retain many higher-order brain functions until high concentrations of anesthetic agents are attained. [101]

The brain’s origin and function of consciousness is still not fully understood, but it is being studied extensively. There is a lot of debate about what constitutes consciousness on neural level. Since at least 19th century it has been known that cerebral cortex is important for consciousness. Not only one region of the brain is responsible for this phenomenon as several cells and pathways are participating in it. [102]

2.7.1. Propofol induced anesthesia

In this study, propofol was used as an anesthetic agent. It is one of the most popular intravenous anesthetic agents used and thus it is commonly called “milk of anesthesia”. Propofol has many advantages when compared with other anesthetic agents such as rapid effect, short action, and fewer side effects. [100] It has a more rapid onset and termination than thiopental and ketamine and it demonstrates less airway irritability, postoperative sedation and nausea or vomiting. The pain with intravenous injection is one drawback of propofol. [89]

Propofol is an intravenous anesthetic, and it is commonly used for procedural sedation, during monitored anesthesia care or as induction agent for general anesthesia. Propofol induced anesthesia is a state of diminished responsiveness and behaviorally it is

like NREM sleep. Propofol can be administered as a bolus or an infusion or some combination of the two. As with many anesthetic agents, the action mechanism of propofol is poorly understood but commonly it is thought to be related to the effects on GABA-mediated chloride channels in the brain. It may work by decreasing the dissociation of GABA from GABA receptors in the brain and potentiating the inhibitory effects of the neurotransmitter. [103] It has effects in cortex, brainstem, thalamus, and spinal cord [44].

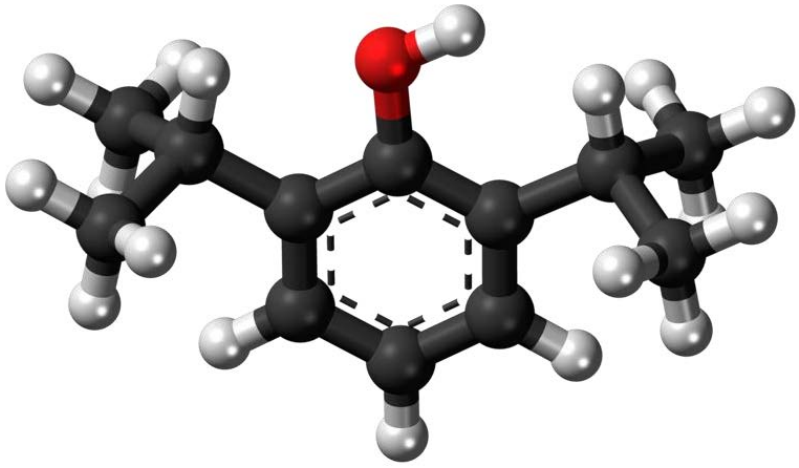

Figure 12. Propofol molecule consisting of Carbon (black), Hydrogen (white), and Oxygen (red). by Jynto via Wikimedia Commons, CC0 license.

Propofol causes effects in the central nervous system, cardiovascular system and in respiration. It causes decreased level of consciousness which is dependent on the dose that is used, and it can be used for moderate sedation to general anesthesia. Propofol is bi-phasic, and it has an initial half-life of around 40 minutes and a terminal half-life of 4 to 7 hours. One induction dose of propofol will affect the patient approximately for 10 minutes and in a longer period under anesthesia is wanted, a prolonged or repeated administration of propofol is needed. [103]

There are a variety of factors affecting the dose of propofol to achieve hypnosis like patient's age, sex, body weight, the rate of infusion, co-administered drugs, and anxiety. These phenomena can be partly explained by their effects on pharmacokinetics which are modulating the concentration of propofol. The propofol concentration can be predicted by using a compartmental pharmacokinetic (PK) model which describes the dynamic linear relationship between drug input and concentration. The concentration can be plasma or effect-site concentration (CeT). Many anesthesiologists are applying the model in clinical settings. [104]

Propofol is commonly titrated by target-controlled-infusion (TCI), but it has been traditionally done manually. TCI systems can improve the accuracy and precision of drug delivery by accounting for its disposition over time and by incorporating complex covariate effects like age and weight which are not possible to incorporate with manual drug administration. [105]

Propofol concentration of 2 – 3μg ml^{-1} is commonly targeted for sedation and 4 - 6μg ml^{-1} for anesthesia. 2 ± 0.9μg ml^{-1} and 1.8 ± 0.7μg ml^{-1} are the concentrations of the loss of consciousness and return of consciousness. [100] Propofol usage is limited up to 4 mg kg^{-1} h^{-1} up to 7 days because of the risk of the propofol infusion syndrome. [106] Propofol infusion syndrome is a rare and potentially fatal condition. It has been reported in adults

who have been receiving a high-dose (>5 mg kg^{-1} h^{-1}) of propofol for more than 48 hours. [107]

Many anesthetics may induce cerebral excitation during administration or withdrawal. For example, propofol can induce clinical seizures and seizure like phenomena (SLP) during induction maintenance or emergence, and it may even be delayed after anesthesia.

Right after the induction of anesthesia there is a marked depression of neuronal activity in the EEG. A spindle-shaped, rhythmic series of waves emerge, to be later joined by typical BS patterns. It is like spindle-waves of sleep and barbiturates, which are generated in the thalamus and distributed to neocortex along thalamo-cortical axons. Propofol burst mainly consists of slow waves which are positive at all electrodes and show the highest amplitude in the frontopolar electrodes and the lowest in the central and parietal electrodes. [108]

2.7.2. Depth of Anesthesia

Anesthetic depth has been defined by Shafer & Stanski as follows:

> *"The probability of non-response to stimulation, calibrated against the strength of the stimulus, the difficulty of suppressing the response, and the drug-induced probability of non-responsiveness at defined effect site concentrations."* [109]

For the purposes of this definition, many stimuli and reactions at different medication doses must be evaluated because anesthesia cannot be sufficiently represented by a single stimulus and response assessment in a clinically or scientifically significant way. In order to reduce the likelihood of response while continuously adjusting the administered dose to achieve the desired anesthetic depth, Shafer and Stanski claim that these observations of stimuli and reactions—such as verbal responses, movement, and tachycardia—are calibrated against the dose and concentration of anesthetic agents used. [109]

The standards for assessing the anesthetic depth include indirect measures of brain state like changes in heart rate, blood pressure, and muscle tone. Also, presumed drug pharmacokinetics, pharmacodynamics, and in case of inhaled anesthetics, the level of exhaled anesthetic gas can be used. [110] Assessment of the depth of anesthesia is important because if the depth of anesthesia is too excessive, there can be hemodynamic changes, delayed emergence, postoperative delirium, and different cognitive issues. If the anesthesia is insufficient, there is a risk of recall or awareness during the anesthesia. Awareness during anesthesia can cause different long-term psychological symptoms, such as anxiety and posttraumatic disorder. [111] [4]

Minimum alveolar concentration (MAC) values for volatile anesthetics have been used to target a predefined level of anesthesia. MAC value is the concentration of an anesthetic gas that suppresses movement in response to a surgical stimulus in 50% of patients. MAC is commonly expressed as volumes percent of alveolar (end-tidal) gas at 1 atm pressure at sea level. This value allows comparison of the effects of inhaled anesthetics at same doses. Also, blood gas analysis and pulse oximeter were used to evaluate the gas exchange and oxygen delivery in the case of volatile anesthetics. [85]

Richmond Agitation-Sedation Scale (RASS) is a 10-point scale (ranging from -5 to +4) that can be rated using 3 clearly defined steps and there are criteria for levels of sedation and agitation. It uses the duration of eye contact following verbal stimulation as the principal means of titrating sedation. Thus, the scale's validation could be linked to both arousal and content of thought – both being components of consciousness. [112]

In the past, a lot of anesthetic overdoses happened because the physical examination was the only way to examine the depth of anesthesia. [92] Traditionally anesthetic drug effects have been measured by the observation of heart rate, blood pressure, breathing pattern, and the absence or presence of different movements. All of these are useful measures, but these cardiopulmonary effects of anesthetics that are observed are only side effects and therefore those measures are not precise enough. Anesthetics are given for sedative and hypnotic reasons and therefore, measurement of anesthetic drug effects on brain should be more useful and accurate. [113] EEG can be used to monitor the depth of anesthesia as it has a high sensitivity to showing sudden changes in neural functioning [5].

Using EEG to determine the depth of anesthesia is based on the characteristic signal changes related to increasing concentrations of anesthetics in the blood and also in the brain. Propofol, for instance, causes several neurophysiological alterations that have an impact on the spectrum characteristics of EEG. The high frequency (>20Hz) activity increases while propofol concentration remains low. The middle-frequency (5-20Hz) activity rises, and the high-frequency activity falls as concentration grows. In the end, activity will move from the mid-range frequencies to the low-frequency range (>5Hz). If the infusion is kept up, the EEG pattern switches to burst-suppression pattern. [114]

Spectral analysis and in particular the analysis of the Relative Power (RP) distribution in various frequency bands is the most studied EEG variable in the general anesthesia environment. It is well known that anesthesia affects EEG by decreasing posterior alpha and increasing fronto-central beta power during the induction phase and increasing frontal power predominance in alpha, theta and delta frequencies in deep sedation. These dynamics are changing during the recovery of consciousness (ROC) and the effects are similar for different sedative and hypnotic agents. [115]

The burst suppression pattern can be used as a marker for the level of anesthesia. This pattern was first described by Derbyshire in 1936 in anesthetized cats. Later it was described occurring in a range of clinical settings during continuous EEG monitoring by Niedermeyer. IF-SECN defines the pattern as “pattern characterized by theta and/or delta waves, at times intermixed with faster waves, and intervening periods of relative quiescence.” In burst suppression that has been induced with anesthetics, duration of bursts and suppressions vary systematically with brain anesthetic concentrations, with higher concentrations there is longer suppressions and eventually there is a continuous EEG suppression. [116]

Most clinicians lack the time and expertise necessary to decipher the intricacy of the raw data and use the information to titrate the delivery of anesthesia, which limits the use of raw EEG in the measurement of depth of anesthesia. Due to this, attempts have been made to simplify the analysis. [33] There are numerous different depth of anesthesia monitors developed for this purpose and those have been available since the 1990s [4]. These monitors aim for providing adequate anesthetic depth and save the amount of anesthetics used and shorten the recovery time. All these monitors analyse the fluctuations of the EEG signals measured from the patient. The analog EEG signal is being amplified and converted to the digital domain and after that different signal processing algorithms are applied. The result is usually one single number and is commonly referred to as an index. Anesthesiologists and hospital personnel can use this number as a reference point when deciding whether the depth of anesthesia is appropriate or not. Then the use of anesthetics can be decreased or increased. [117]

The Bispectral Index Monitor or BIS is the first depth of anesthesia monitor approved by the Food and Drug Administration (FDA), and it was introduced in 1992. BIS monitor is based on EEG signals to obtain a single value that talks about the patient's state of awareness. [117] BIS is calculated by a statistical multivariate model using non-linear

functions of EEG-based sub parameters. It is known that BIS values are calculated from four EEG sub parameters: Burst Suppression-Ratio (BSR), QUAZI Suppression Index, Relative Beta Ratio (RBR), and SyncFastSlow (SFS). In the calculation multiple regression equations are used with different weights according to the depth of anesthesia. BIS calculation method is a proprietary algorithm and the exact method of the QUAZI suppression index, the selection criteria of different regression equations and the weights of sub parameters are not disclosed. [118] Beta Ratio indicates the changes in the log ratio of the 30 to 47Hz and 11 to 20Hz EEG band powers and SyncFastSlow indicates the ratio of the sum of bispectrum peaks in the 0.5 to 47Hz and the 40 to 47Hz range. [119]

The result number of BIS is between 0 and 100, 0 meaning cortical electrical silence and 100 meaning normal awake activity. The number declines with anesthesia-induced unconsciousness. BIS value decreases to levels as low as 30 during normal sleep and sleep is seen as inadequate state for surgery. BIS value encompasses several biological brain states and thus it is not specific for those induced by anesthesia. [33]

Another depth of anesthesia measure is Entropy. Entropy provides a quantitative measurement of depth of anesthesia, and it has two scales, response entropy (RE) and state entropy (SE) scales. RE scale ranges from 0 (no brain activity) to 100 (fully awake) and the SE scale ranges from 0 (no brain activity) to 91 (fully awake). The target range for these values is 40-60, which is clinically relevant, and values close to 40 indicate a low probability of consciousness. The RE is based on both EEG and FEMG (frontal electromyography) signals and provides an indication of the patient's responses to external stimuli and can show signs of early awakening. SE is a stable parameter based on EEG and can be used to assess the hypnotic effect of anesthetic agents on the brain. RE is always higher or equal when compared with SE. [120]

Norcotrend (NCT) is another EEG monitor measuring brain wave activity. It uses spectral analysis in raw EEG data analysis producing a number of parameters. It applies multivariate statistical methods using proprietary pattern recognition algorithms and provides an automatically classified EEG signal based on a visual assessment of the EEG. In the monitor, anesthesia stages range from the awake ‘A’ state to the burst suppression and electrical silence ‘F’ stage, ‘E’ indicating the appropriate depth of anesthesia for surgery. It also includes a unitless index number (NI) ranging from 0 (deeply comatose) to 100 (fully awake). The monitor uses EEG data from three electrodes placed on the forehead. NCT is the only monitor on the market including an age-related algorithm and thus it can also be used for children less than 1 year old. [119,33]

Patient state index (PSI) is an index of the level of hypnosis or awareness. A high-resolution four-channel EEG monitor calculates the PSI by gathering data on brain electric activity frequency and phase in accordance with anterior-posterior relationships in the brain as well as coherence between bilateral brain areas. Independent of anesthetic class, PSI gives a continuous numerical number resulting from systematic examinations of the complex of changes in brain state that were observed to occur reversibly together with loss and return of consciousness. For example, SedLine uses PSI technology. [34]

There are some limitations in using commercial depth of anesthesia monitors. For example, E-Entropy can only be used for patients over the age of 2 years. Also, the BIS index has to be cautiously interpreted in the measurement of depth of anesthesia in children and elderly patients. BIS may not be reliable in patients with known neurological disorders and in case they are taking psychoactive medications. A significant limitation of depth of anesthesia indices is in the neurophysiological basis of them as they assume anesthetics induce slowing of the EEG oscillations with increasing doses of anesthetics. Because of this, slower oscillations should clearly be an indicator of a more profound state of general anesthesia, but not all anesthetics show this EEG pattern. These monitors don’t accurately

distinguish between consciousness and unconsciousness as they use signal analysis rather than consideration of corticocortical connectivity and communication which as a complex entity contribute to consciousness. [34]

2.8. Quantitative parameters of EEG

EEG interpretation has traditionally been done by visual analysis of the raw EEG by certified neurophysiologist. Quantitative parameters of EEG, also called qEEG, have been shown to assist in the interpretation of EEG. In quantitative EEG, one or more numerical values or features are calculated from the EEG using different methods and those can then be used as indicators for the brain state. The digital EEG is first captured, then it is transformed, processed, and evaluated using several sophisticated mathematical methods. With the advent of qEEG, new methods for extracting EEG signal features have been developed, such as signal complexity and frequency band analysis, connectivity analysis, and network analysis. qEEG has a wide range of clinical uses, including the treatment of epilepsy, stroke, dementia, traumatic brain injury, and mental health disorders, among many others. [121]

It is important to emphasize that qEEG tools should not replace careful review of the underlying raw EEG but to be interpreted in conjunction with it. Also, the quality of the signal and the clinical condition of the patient should be considered in the interpretation. In this chapter, four qEEG parameters will be introduced including burst-suppression ratio, amplitude-integrated EEG, alpha-delta ratio, and C-Trend Index.

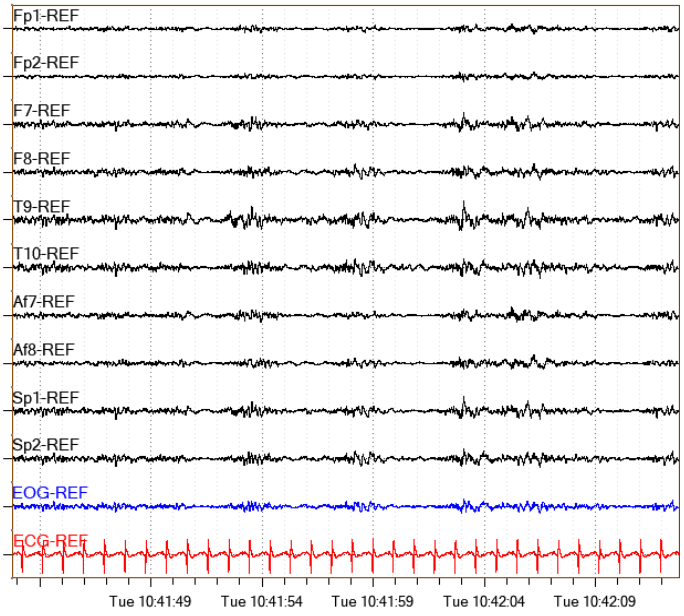

Figure 13. An example image of input EEG signals on C-Trend Software on graphical user interface provided by Bittium. This measurement is done by using Bittium BrainStatus wireless EEG device. In the recording, there is a prominent burst suppression pattern present including periods of higher amplitude bursts and suppressed EEG activity. In the four following figures, the C-Trend parameters are derived from these input signals.

2.8.1. Burst Suppression Ratio

Burst suppression patterns have been identified in hypothermia, coma, early infantile epileptic encephalopathy, and in general anesthesia. Burst suppression consists of periods of suppressed EEG activity and periods of EEG activity with a larger amplitude called bursts. In anesthesia, as it progresses, the ratio of suppressions to burst periods rises. If deepening of the anesthesia continues, eventually the EEG becomes completely isoelectric, resulting in an entirely flat EEG pattern.

Burst-Suppression Ratio (BSR) is meant for aiding in the identification of burst-suppression patterns in the EEG and it can used for example in the treatment of status epilepticus with deep anesthesia. BSR is considered to be a reliable sign of a very profound drug-induced coma when the pattern is induced with anesthetics. BSR is calculated as follows by dividing the entire suppression time in the epoch by the epoch length: [122]

BSR = (total time of suppression / epoch length) x 100%

The percentage of suppression in the input EEG signal is represented by a BSR index from 0 to 100 in C-Trend. The Non-Linear Energy Operator (NLEO) based adaptive tracking technique is the foundation of the machine learning (ML) algorithm that the C-Trend software uses to count the number of suppressions. An adaptive threshold has been introduced to allow for wider operating amplitude ranges for input EEG that is usual in ICU conditions, along with an adaptive filter to decrease the impact of ECG artifacts.

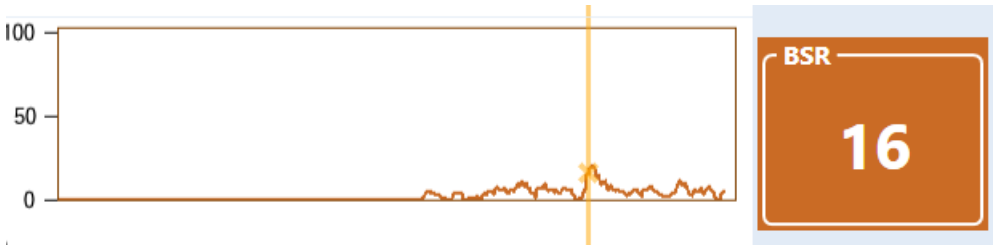

Figure 14. A BSR Index derived from the input signals in Figure 9. An index value of 16 indicates that 16% of the signal in the epoch is suppression.

Although burst suppression can be readily identified in raw EEG, standardizing its measurement is essential to reduce variability. There are various other commercial technologies in addition to C-Trend for calculating burst suppression, including Patient State Index (PSI), Bispectral Index Monitor (BIS) and SedLine. These technologies are using machine learning techniques and although machine learning techniques are simple to understand and correlate with burst suppression, they typically underestimate this phenomenon. Therefore, visual analysis of raw EEG is seen as more accurate but requires training for its assessment. [123] The study [124] proves that machine-generated estimates are underestimating minutes of complete EEG suppression.

In the case of SedLine and BIS monitoring systems BSR stands for the percentage of the previous 63 s epoch of EEG, which is defined as those intervals longer than 0.5s during which the EEG voltage does not exceed 5.0 mV. For an EEG signal with isoelectric periods, the BSR would be 1, while for one without, it would be 0. The patient is at risk for both acute and subacute delirium as well as cognitive impairment if the EEG shows a burst-suppression pattern, which implies a dramatic drop in the brain's neuronal activity and metabolic rate. [124]

2.8.2. Amplitude-integrated EEG

Amplitude-integrated EEG (aEEG) is a commonly used neurophysiology tool used by neurologists and neonatologists, mainly in neonatal intensive care units (NICU). It is displaying the EEG in a way that its changes in amplitude are easy to assess over time. aEEG waveform is meant to help the user to monitor the state of the brain and it can be used in detecting seizure activity. In aEEG's simplest form, it is a processed single-channel EEG that is filtered, and time compressed.

aEEG cannot replace conventional EEG for background monitoring and detection of seizures, but it is a useful tool for completing conventional EEG and is especially used with neonates. The brain of neonates (newborns during the first 4 weeks of their life) is normally monitored with continuous video EEG (cEEG) with electrodes placed according to the international 10-20 system but modified for neonates. This has limitations as the recording and interpretation require special knowledge, it is expensive and there is not always access to the equipment.

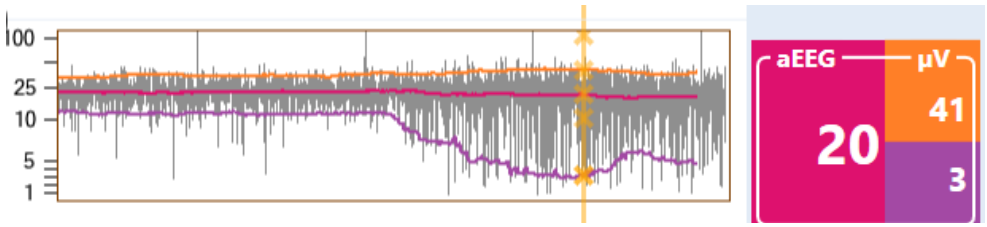

Figure 15. An aEEG Index derived from the input signals in Figure 9. aEEG has the lowest amplitude of 3 and the highest amplitude of 41. aEEG's value then is 20.

aEEG uses a limited number of channels to record the raw EEG signal, which is being filtered, rectified, processed, and then displayed on a semi-logarithmic amplitude and time-compressed scale. [125] aEEG is also helpful for predicting neurodevelopmental outcomes for preterm and term newborns, identifying and treating seizures, and tracking cerebral background activity. [126].

The aEEG usually uses two or four electrodes and the signal from these is passed through a bandpass filter, which enhances frequencies between 2 and 15 Hz. Frequencies outside of this band are attenuated to eliminate artefacts as much as possible. As a further processing, the signal is filtered, rectificated, smoothed, semi-logarithmic amplitude compressed and time compressed. Amplitudes that are smaller than 10 µV are being displayed on a linear scale and amplitudes higher than 10 µV on a logarithmic scale. The lowest amplitude that is detected is shown as the lower border and the highest one as the upper border. This creates a situation where small changes in the lower amplitude are visible but overloading of the display at high amplitudes is avoided. aEEG's visible information is limited to changes of the amplitude. [127]

2.8.3. Alpha-Delta Ratio

Alpha-Delta Ratio or ADR indicates the ratio between signal powers in alpha (8 – 13 Hz) and delta (1 – 4 Hz) ranges and it is meant for helping the user to analyze the EEG waveform and it can be used in detecting brain hypoxia. If there is an increase in ADR, there is a shift of

power from delta frequencies to alpha frequencies, and a decrease means that there is a shift of power from alpha frequencies to delta frequencies.

These changes in the power spectrum of the signal may be a sign of several different conditions. For example, the lack of oxygen in the brain can cause shifts from higher to lower frequencies, and many studies have also shown that the alpha-delta ratio is associated with ischemic brain injury. ADR may also play an important role in the prediction and monitoring of functional rehabilitation outcomes in patients with acquired brain injury. [128] ADR has shown good results also in the detection of delayed cerebral ischemia (DCI) which happens due to vasospasm and is often undetected by clinical exams in patients with subarachnoid hemorrhage (SAH). A decrease in the ADR is related to the detection of DCI. [129]

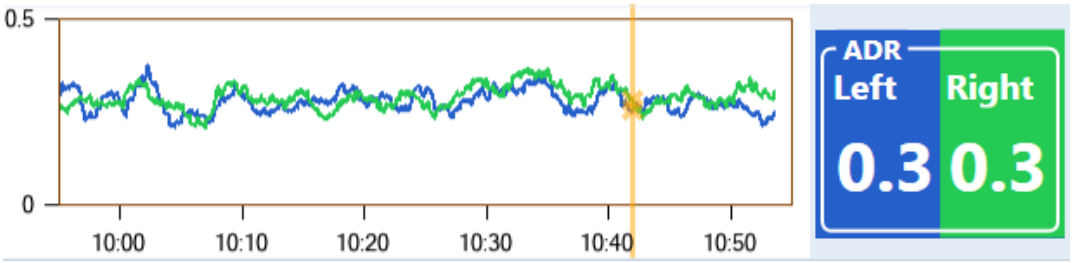

Figure 16. ADR index derived from the input signals in Figure 9. ADR in this case has the same value on both hemispheres.

2.8.4. C-Trend Index

The C-Trend Index is designed to assist in tracking the neurophysiological condition of patients who have been sedated using anesthetic drugs, including those who have experienced comatose cardiac arrest. It is intended to help with neurological outcome prediction, for instance, following cardiac arrest when there is a high risk of developing a hypoxic ischemic encephalopathy. The raw EEG data is processed by the C-Trend software into a single score called the C-Trend Index. The index gives a single number between 0 and 100 to represent the EEG slow-wave activity. Slow-wave activity takes place both during anesthesia and deep sleep, which is necessary for proper brain function. [130]

C-Trend Index values higher than 80 indicate high normal slow wave activity and values between 50 and 80 indicate moderate normal slow wave activity and values lower than 50 indicate abnormal or low slow wave activity. These values are derived from sixty-second long EEG sequences, and it is suggested that the values are read multiple times over a period and not relied on one single number. This is because the occurrence of slow waves can be fleeting.

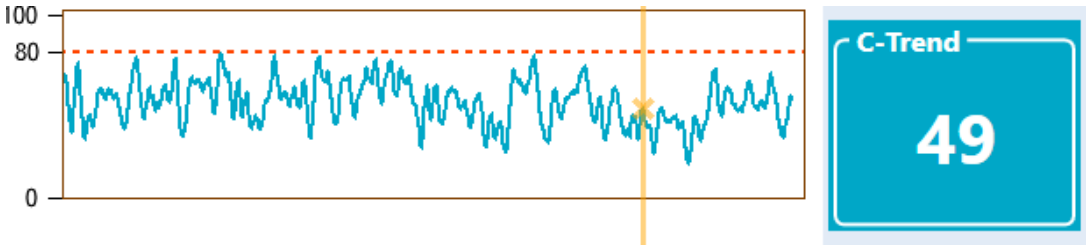

Figure 17. C-Trend Index derived from the input signals in Figure 9. C-Trend Index value below 50 indicates low slow wave activity but C-Trend Index should not be used during burst suppression as an indicator of the brain state as during that it is resulting in lower values than normal. C-Trend Index is the most reliable between loss of consciousness and beginning of burst suppression.

3. PRIVACY AND MACHINE LEARNING

Machine learning (ML) teaches computers to think highly and conduct human-like analysis. ML is frequently defined as a collection of techniques that, when used, enable computers to recognize or learn about significant patterns in data stores with little to no human intervention. Even if it is said to conduct human-like analysis, ML does not learn by reasoning, but rather by different algorithms. [131]

C-Trend Software also utilizes machine learning models. These models commonly require sufficient high-quality data to produce unbiased and generalizable models. State-of-the-art machine learning techniques like deep networks are usually trained using cloud platforms, leveraging the elastic scalability of the cloud. For this kind of processing, data from several sources needs to be transferred to a cloud server. This works well for some application domains, but not for all as there are privacy and network overhead concerns. Health care is one of those domains. There is a lot of medical data being collected by healthcare systems commonly, but it sits in data silos and privacy concerns are restricting access to it. If we can't access sufficient data, machine learning can't reach its full potential, and this is currently a key issue in machine learning development. ML-based technologies require a lot of data, but it is hard to get as health data is highly sensitive and the usage of it is strictly regulated. Data anonymization can bypass some of the limitations, but removing metadata like patient's name or date of birth is not enough to preserve privacy. [132]

There has been the creation of large data repositories like IBM Merge Healthcare but those are challenging to implement and maintain as there are technical and regulatory barriers. Another issue is that locally trained models are required to be validated on data coming from external sources. But sharing sensitive clinical data across different hospitals and research units can be difficult due to concerns with data privacy and data stewardship. Issues like these have led to new approaches for training machine learning models collaboratively and without sharing raw data. Federated learning is one of these methods. It enables people from different institutions to combine efforts by training a model locally on their own data and sharing the parameters of the model with others to generate a central model. Federated learning is a growing field in machine learning and only a few studies on it have been published. [133]

Many EEG investigations employ model-based techniques, which necessitate a substantial quantity of data to construct a reliable model. In those methods, EEG data from several individuals is gathered and sent to a central server for analysis. Because the data reflects brain activity in a variety of ways, its potential misuse could result in serious privacy violations.

The General Data Protection Regulation [134] (GDPR), which the EU adopted in 2016, replaced the 1995 Data Protection Directive, which was passed when the internet was just getting started and the world altered significantly as a result. According to GDPR, health-related data falls under a unique category. The GDPR outlines a number of requirements for preserving user privacy and forbids businesses from sharing users' personal information without their express consent.

The European Parliament is now debating the Artificial Intelligence Act (AIA), which the European Commission proposed in 2021, but it is not yet accepted nor in its final form. The AIA is the first attempt to enact a uniform law to control artificial intelligence. The AIA focuses on companies who offer AI services and either sell them or employ them for their own ends. The AIA determines different rules for different risk levels from artificial intelligence. Many AI systems are posing minimal risk, but they must be assessed. The risk levels and their obligations are the following:

- Unacceptable risk → prohibited AI practices.
- High risk → Regulated high risk AI systems.
- Limited risk → Transparency
- Low and minimal risk → No obligations

Based on the current version of the law (section 6, annex II) Cerenion C-Trend Technology falls under the category of high risk as it is a medical device utilizing artificial intelligence, and the AIA defines all products that fall under the EU health and safety harmonization legislation to be high risk. Cerenion C-Trend Technology is in the device group llb and all the devices in the groups of lla or higher require a verification of a notified body. C-Trend Technology has already passed the EU declaration of conformity assessment and has a CE-mark.

The law (section 10 and 64) also concerns federated learning and brings some challenges for the implementation, as it requires that the manufacturer of the device can deliver the data used for machine learning training to authorities. The law also sets requirements for the data representativeness, completeness, adequacy, and correctness. All of these should be complied with by appropriate means.

3.1.1. Federated learning

By not exchanging the data itself when training the algorithms, the federated learning (FL), also known as collaborative learning, paradigm attempts to address the issues of data governance and privacy. Data privacy refers to a person's right and capacity to manage how their personal information is gathered, processed, kept, and shared. It entails protecting sensitive data and making sure that data is handled in a way that respects people's right to privacy. The framework, processes, policies, and practices known as data governance assure efficient and ethical administration of an organization's data assets. To enhance data quality, integrity, security, and accessibility, it entails developing and enforcing rules for data collection, storage, processing, and consumption.

Federated learning has recently grown in popularity among applications used in healthcare. FL makes it feasible to transfer patient data in the form of a consensus model rather than sending it outside the hospital or other institution where the patient is being treated. Essentially, this means that only model characteristics are sent, and that the ML process happens locally, for instance, at each hospital in the edge. Studies on FL demonstrate that models trained using FL can attain performance levels comparable to those trained on centrally hosted data sets and superior outcomes when compared to models employing isolated data from a single institution. [132]

Federated learning was first introduced by Google in 2016 [135] and it was first called *Federated Optimization*. They first applied it in Google keyboard to collaboratively learn from several android phones. The study suggested a federated optimization algorithm and identified the difficulties federated optimization faces and that must be taken into account. These difficulties stem from federated optimization's massively distributed, non-IID, imbalanced, and sparse characteristics. The term "massively distributed" refers to the storage of data points over a large number of nodes, the number of which may be substantially greater than the typical number of training samples kept on a given node. With the term

“non-IID” they mean that the data that is available locally on some node/client is far from being a representative sample of the overall distribution of the data. And, with “unbalanced” they are pointing out that different nodes may have different amounts of training examples.

One more recent example is a Pandemic AI Engine Without Borders [136] which was a project where researchers and medical professionals from different parts of the world together developed an AI pandemic engine for COVID-19 diagnosis from chest scans by utilizing federated learning. A publicly accessible federated learning architecture was put in place, making it possible for any hospital or institution in the globe to join with the appropriate hardware and information. In exchange for participation, a stakeholder downloads the code and locally trains a new model using the basic model. The participant then gives the framework access to the updated model after it has been trained. The framework then encrypts the model parameters to safeguard patient privacy and sends them back to the main server. After combining the contributions, the server updates the parameters and distributes them once more to all parties involved. Data heterogeneity is another goal of the system. The authors wrote that "Federated learning approaches may provide a means of overcoming a number of obstacles impeding international cooperation in this fight."

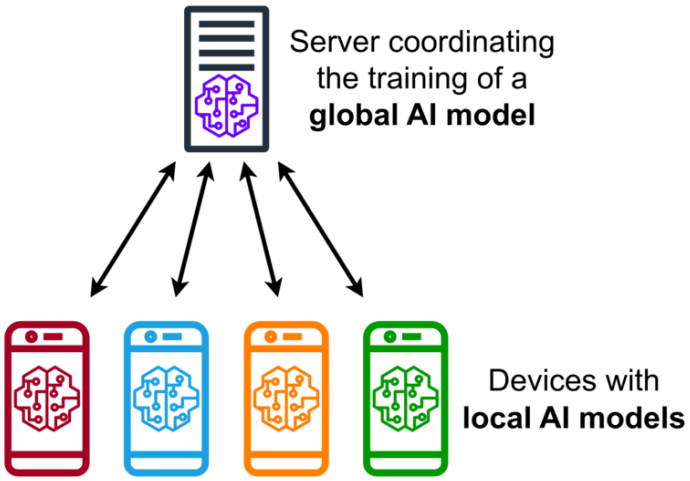

Figure 18. A simple example of a centralized federated learning protocol. A central server orchestrates the various steps of the algorithms in the centralized federated learning setup and coordinates all of the participating nodes throughout the process. by MarcT0K via Wikimedia Commons, CC0 license.

The central server, also called an aggregator, coordinates/supervises the building and training of a joint machine learning algorithm in which multiple parties are collaborating. Federated learning is usually deployed in two scenarios: it can be either *cross-device* or *cross-silo*. In the cross-device scenario, there is a large number of parties (more than 100) present, but all of them may have a small number of data items, constrained computing capability, and limited energy reserve. Cross-silo scenario involves small number of parties (less than 100) but each of them have extensive computing capabilities and large amount of data. [137]

Additionally, federated learning can be horizontal or vertical. Each device in vertical federated learning holds a dataset with unique attributes culled from sample examples. For instance, vertical FL can be used to create a shared ML model between two businesses that have data about the same group of people but distinct feature sets. Each device in horizontal federated learning has a dataset that has the same feature space as the others, but distinct

sample examples. The first use case of FL – Google keyboard uses vertical FL where the participating mobile phones have different training data with same features. [138]

Another variety of federated learning frameworks is federated transfer learning. It is comparable to traditional machine learning, where we wish to add a new feature to a model that has already been trained. As an illustration, let's say we wish to expand vertical federated learning to include more sample cases that aren't present across all participating firms. [138]

Conventional, centralized machine learning techniques often collect the dispersed raw data produced across various hospitals, for instance, to a single server or a cluster with shared data storage. Serious security and data privacy issues could result from this. FL differs from centralized approaches in three ways: FL forbids direct exchange of raw data, FL makes use of distributed computing resources across several areas or organizations, and FL makes use of other defense mechanisms such as encryption to ensure data privacy or security. FL forbids the transfer of training data and only permits the transfer of intermediate data between dispersed computer resources. FL brings the code to the data rather than the other way around. [139]

Researching federated learning algorithm strategies, such as how to combine models or updates effectively and how to be resilient to distribution shifts, is necessary for developing FL-based models. It is important to remember that with FL-based development, researchers are unable to see or visualize the complete collection of data that was utilized to train the model. Because of this, it is impossible to determine why the model performs poorly on a particular failure situation. [132]

A server that manages the learning process and several electronic devices collectively referred to as clients make up the federated learning framework. Local training datasets are kept locally on each client and are never uploaded to the server. By combining the outcomes of the local training clients, the goal is to train a global model. The final model is then given to clients again for additional training. There is a generic federated learning algorithm specified, but there is no structure for the local training procedure nor function for model aggregation. For these, different methods can be employed. [140] The generic federated learning algorithm goes as follows:

Input: N, C, T, E
Output: w_{TE}
  Initialize w_0
  for each round $\mathrm{t} \in \{0, \mathrm{E}, 2\mathrm{E}, \ldots, (\mathrm{T}-1)\mathrm{E}\}$ **do**
    $\mathrm{m} \leftarrow \max(\mathrm{C} \cdot \mathrm{N}, 1)$
    $I_t \leftarrow$ (random set of m clients)
    for each client $\mathrm{i} \in I_t$ **in parallel do**
      $w_t^i + \mathrm{E} \leftarrow \mathrm{CLIENT-UPDATE}(w_t)$
    end for
    $w_t + \mathrm{E} \leftarrow \mathrm{AGGREGATION}(w_t^1 + \mathrm{E}, \ldots, w_t^N + \mathrm{E})$
  end for
  return w_{TE}
[140]

In the algorithm above, A set I grouping N clients, the proportion of clients C selected at each round, the number of communication rounds T, and the number of local epochs E are the input parameters. The global learning system's centralized component sets these parameters. The model is defined by its weights. At the end of each epoch $\mathrm{t} \in \{0, \ldots, \mathrm{T}\,\mathrm{E}-1\}, w_{t+1}^i$ defines the weight of client $\mathrm{i} \in \mathrm{I}$. And, for each communication round $\mathrm{t} \in \{0, \mathrm{E}, \ldots, (\mathrm{T}-1)\mathrm{E}\}, w_t$ is the global model detained by the server and w_{TE} is the final weight.

There are I = {1,...,N}clients in the training set, each of whom has a local dataset. Before each communication round t ∈ {0,E,...,(T - 1)E}, the server randomly selects a set l_t of C · N clients, sending them the current state of the global algorithm before asking them to perform local computations based on the global state and their local dataset and sending back an update. At the conclusion, the server updates the model's weights by aggregating and after that, the process starts over.

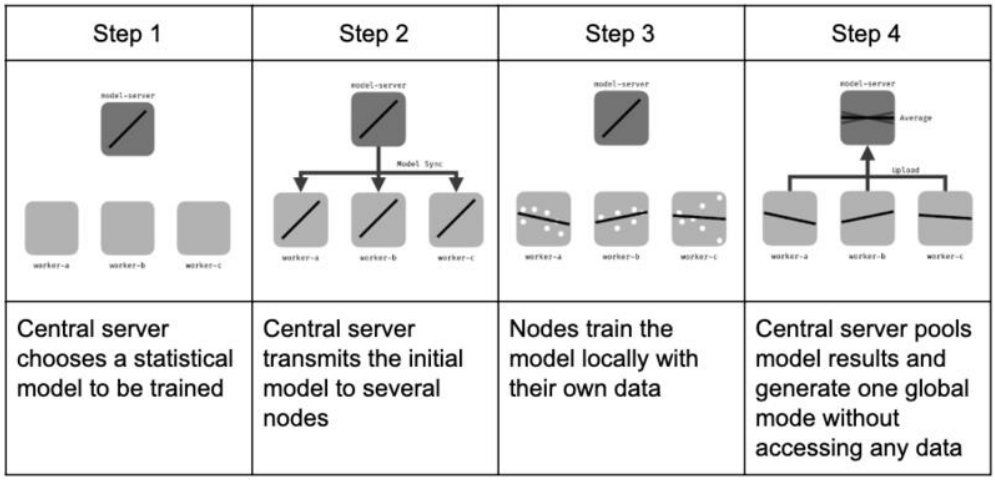

Figure 19. Federated learning process' four steps visualized. by Jeromemetronome via Wikimedia Commons, GNU Free Documentation license.

The four steps that make up the FL training procedure explained in more detail:

1. Setup the FL task. The FL task's training aim and the data requirements for training are decided by the server.
2. The FL job is then made available for clients to participate who match the requirements. The overall model and training parameters are chosen based on the clients participating in the training task's computing, communication, and data volume constraints. The server then makes the initialized global model and training needs available to the task's clients.
3. Carry out the FL job to train the model. The client trains the supplied global model using the local data, updating the model parameters in accordance with the training conditions, which are often minimized loss functions. The client uploads the revised local model to the server after the training is finished. The server waits for all clients to upload their local models before obtaining the updated global model by aggregating the local model's parameters into a weighted average.
4. Final step of FL job. The FL task is completed when the global model performance reaches the task objective. The modified global model is now being tested. The global model is provided back to the client for parameter updates if it doesn't achieve the task target while awaiting another round of model aggregation and testing by repeating step 2. [141]

For model aggregation, a variety of aggregating functions have been put forth. A straightforward coordinate-wise mean averaging of model weights was suggested by McMahan et al. in 2017. To ensure the closeness of local and global updates, Ek et al. modified this in 2018. In 2019, Yurochkin et al. developed an extension that considered the

network weights' invariance to permutation. The coordinate-wise mean averaging was expanded by Cho et al. in 2020 by adding a term that amplified the contribution of the most informative terms in comparison to the contribution of the least informative ones. [140]

It is crucial to talk about the various difficulties that federated learning faces. They primarily deal with security and training-related subjects. The communication overhead throughout numerous training iterations, the heterogeneity of the devices, and the variability of the data used for learning are some of the training-related issues. A malevolent user with only a black-box access to the model is one of the adversaries that pose security issues. Other adversaries include malicious clients on the local device. [138]

In FL, even though the sensitive information is stored on the device, it is still feasible for a competitor or a curious bystander to learn that a piece of information required to train local models is present. Some sort of cryptographic method is required to differentially secure the information from this assault. Due to the distributed nature of FL, it might be challenging to pinpoint system participants who are malicious. [138]

Federated learning has been used on EEG data on couple of recently published studies, but they mainly focus on EEG classification.

Federated learning has been used in EEG signal classification in an architecture that uses previously introduced Federated Transfer Learning (FTL). It works with the single-trial covariance matrix and extracts common discriminative information from multi-subject EEG data using domain adaptation techniques. In the absence of multi-subject data, the architecture provided 6% better accuracy compared to other state-of-the-art deep learning architectures. According to the study, distributed training of EEG classifiers from various heterogeneous data configurations can be successfully accomplished using the federated learning framework. [142]

Hierarchical Heterogeneous Horizontal Federated Learning (HHHFL) for EEG is an approach to train machine learning models over heterogeneous EEG data and preserving the data privacy of each party. The work deals with the problem that many federated learning algorithms now in use concentrate on homogeneous datasets, where many parties use the same feature space. [143]

To overcome the issues of insufficient data volume and complexity and to enable institutions with small datasets to collectively train machine learning models, federated learning has been applied to EEG signal-based emotion identification. The study's validation revealed that using the FL approach can increase model accuracy. [141]

3.1.2. Performance and error measures

No matter what type of machine learning method we are using, a comprehensive evaluation of ML models is required. This is a crucial step in ensuring that the produced ML model is viable for understanding a complicated phenomenon given a small amount of data points and that the same models are properly extended to new or future datasets. Traditionally, performance fitness and error metrics (PFEMs) have been used to determine whether ML models are adequate. These are logical, mathematical, and/or other structures that are used to gauge how closely actual observations match expectations or predictions. [131]

The performance and error metrics used in the machine learning of BSR are mean squared error (MSE), mean percentage error (MPE), error standard deviation (STD), and combined error. Combined error combines the first three by giving them different weights

according to their importance. When the hyperparameters are being optimized, the algorithm looks for the parameters resulting in the best combined error.

The mean squared error is a commonly used metric in machine learning and it is used to assess the accuracy or performance of regression models. It measures the average squared difference between the predicted values of a model and the corresponding true values. MSE is especially useful when we are evaluating models that are predicting continuous or numerical values. The squaring operation ensures that both positive and negative errors are contributing to the metric, emphasizing larger errors due to the squared term. The MSE formula goes as follows: [144]

$$MSE = \left(\frac{1}{n}\right) * \sum(y_i - \hat{y}_i)^2$$

Where n is the number of data points, y_i represents the predicted value for i:th data point and $\hat{y}_i$ represents the true value for the i:th data point.

Mean percentage error is another metric commonly used in forecasting and regression tasks for evaluation of the accuracy of predictive models. MPE measures the average percentage difference between the predicted values and the corresponding true values. MPE is useful in machine learning when we want to understand the average relative error of our model's predictions. MPE can have either positive or negative values. Positive values indicate an overestimation of the true values by the model and negative values indicate an underestimation. An absolute MPE can also be used for focusing on the magnitude of the error. The MPE formula goes as follows: [145]

$$MPE = \left(\frac{1}{n}\right) * \sum(y_i - \hat{y}_i)/\hat{y}_i * 100$$

Where n is the number of data points, y_i represents the predicted value for i:th data point and $\hat{y}_i$ represents the true value for the i:th data point.

Error standard deviation is the third metric and commonly used in regression or prediction models. It is used to quantify the spread or dispersion of errors and it measures the average amount of variation or deviation between the predicted values and the corresponding true values. It is a measure of how closely the predicted values align with the true values on average. The STD formula goes as follows:

$$STD = \sqrt{\left(\frac{1}{n}\right) * \sum(y_i - \hat{y}_i)^2}$$

Where n is the number of data points, y_i represents the predicted value for i:th data point and $\hat{y}_i$ represents the true value for the i:th data point.

There are many other metrics besides the ones employed in this study that might be applied. The performance of regression and classification problems are measured differently.

Classification is the process of grouping data into separate classes. It is a form of supervised learning in which computers are taught to divide observations into single or multiple classes. Some examples of classification algorithms are logistic regression, k-nearest neighbors, and support vector machines. In a confusion matrix, the effectiveness of categorization methods is frequently reported. This matrix sets the core framework required to comprehend accuracy metrics for a particular classifier. It contains statistics regarding actual and expected classifications. This matrix's rows represent real cases, while its columns

indicate anticipated instances. The confusion matrix is the go-to metric used but there are some other performance and error metrics used to evaluate classification models. Some examples of these are True Positive Rate (TPR), True Negative Rate (TNR), and Accuracy (ACC). [131]

The machine learning problem at hand in this study is a regression problem. The simplest form of common performance and error metrics for regression approaches, which forecast a target value using independent variables, comes from deducting a projected value from its corresponding real or observed value. Some other, commonly used metrics for regression include Mean Error (ME), Mean Normalized Bias (MNB), Mean Absolute Error (MAE), and Correlation coefficient R. [131]

4. MATERIALS AND METHODS

Data from the BrainICU study was utilized for the purpose of implementation of novel federated learning method for the BSR machine learning. The study where the utilized data comes from is observational, non-interventional, and it was initiated by the investigator. The role of Cerenion in the study is a collaborator and because of this role, Cerenion has the right to use the study data. Cerenion has not been the sponsor of the study. The dataset and preparation techniques are first discussed, and then a thorough explanation of the BSR machine learning implementation follows.

4.1. Dataset and Preprocessing

BrainICU data was collected in Oulu University Hospital during the years of 2015 and 2016 using the Bittium's NeurOne device. NeurOne was developed by a company called Mega Electronics, but it was bought by Bittium in 2016. The NeurONe system, also known as the NeurOne Tesla EEG system, was created to meet the demands of scientists and medical practitioners for the simultaneous high precision detection of neurophysiological signals from numerous channels. NeurOne can be used with transcranial magnetic simulators (TMS-EEG) with optional possibility to use it during magnetic resonance imaging (fMRI-EEG). Eight of the 32 EEG channels are dipolar channels. For the investigation, only the dipolar channels were used. [146]

The data has been previously used in a master's thesis and a study researching heart rate variability during propofol anesthesia in predicting neural recovery from cardiac arrest. [147] The data consists of EEG data from 25 cardiac arrest patients who were intubated and received propofol sedation and TTM (targeted temperature management). The level of anesthesia was changed during the measurement with additional propofol boluses ranging from standard sedation to deep anesthesia. Burst suppression pattern occurred in EEG in the stage of deep anesthesia.

The data consisted of 71 EEG signals which had information in the following channels: F3, F4, C3, C4, O1, O2, T3, T4 and additionally there was an ECG channel. In the preprocessing phase, all the channels but ECG were chosen for the analysis but in the calculation of the BSR, only the channels F3 and F4 are considered.

From the data, 20-minute-long snippets were extracted where the burst suppression pattern in different forms was present. There were also periods of slow wave activity where there were no bursts nor suppressions. MATLAB annotation tool was used for extracting the wanted snippets and different kinds of burst suppression phenomena were included. Altogether 45 20-minute-long snippets were chosen from the dataset. Those snippets were annotated with the Annotation Tool developed by Niemelä.

For annotation of the data, an Annotation Tool developed by Erika Niemelä was used. [148] She developed the tool for her master's thesis. The software development of the tool was carried out entirely in Python as it provides easy interfaces with other tools and libraries, being the most popular programming language for machine learning development. As a database system, PostgreSQL was used. The database has a Python interface provided by SQL Alchemy, which was used for ORM (object relational mapper) creation. For the setup, a popular deployment scheme, a combination of Flask, uWSGI, and NGINX was used.

The tool has a graphical interface which has been created with the Python GUI toolkit Tkinter and it enables manual annotation and analysis of EEG signals. It can be run on both Windows and Linux as it is platform-independent, having very few dependency issues in general.

In annotation, the 'suppression' annotation segment label was used for the analysis. A python script employing the REST API was created for getting the annotations of the dataset from the annotation tool in the form that the ML pipeline could read it. ML also requires header files for the annotations, which were manually scripted for each file.

9 folders, each of which contained 5 EEG files and accompanying annotations, were created from the 45 data snippets. In addition, 9 folders containing the data sequentially were generated for conventional machine learning. The first one contained the first five, while the final one contained all the data. These made running the machine learning codes convenient.

Python and Linux command-line tools were used to perform the coding of the project. For the creation of the BSR machine learning and federated learning coordination and testing, the machine learning tools and codes offered by Cerenion were used. Additionally, the preprocessing of the data is handled by the machine learning pipeline.

4.2. BSR machine learning

Burst-suppression Ratio was chosen for the study due to its algorithmic simplicity, but federated learning could be applied to all the other C-Trend parameters also. The main objective was to observe how close the performance of federated learning gets compared to the conventional one. The performance of federated learning was expected to get closer and closer to the conventional one. If we use all the data for model training, federated learning's performance should not be able to exceed the performance of the conventional one as we are only transferring parameters and the data is incomplete.

The burst suppression machine learning algorithm that the federated learning is applied to utilizes the NLEO (Nonlinear Energy Operator) feature to detect and classify burst suppression patterns in EEG signals. NLEO captures the nonlinear dynamics and energy changes in a time series, and it involves applying a nonlinear transformation to the signal to emphasize or extract certain features related to energy variations. When NLEO is used in the context of burst suppression detection, it can help in differentiating between burst and suppression states by capturing the nonlinear properties of the signal during these periods.

The algorithm's performance is measured with the four metrics mentioned earlier; MSE, MPE, STD and combined. The algorithm looks for the best hyperparameters by using grid search. When the algorithm looks for the best hyperparameters, the combined metric is being optimized. All the metrics are being saved for exploration and comparison. The hyperparameters of the algorithm are called the following (names changed): Param1, Param2, Param3, Param4, and Param5. As an input, the algorithm takes the range for these parameters, a step size, and the dataset with the annotations. As an output, it gives us the best parameters it finds from the range to optimize combined metric and the performance metrics.

The performance metrics have a certain test criterion and if the metrics fall below that, the model can be accepted. In the combined metric, the three other metrics are combined with the weights: MSE (1), MPE (10), and STD (20). The test criterions are the following:

- MSE: 200

- MPE: 20
- STD: 10
- Combined: 600

The data was used in the Federated Learning system simulation, where we simulated having clients where the edge learning happens and a server where the global model is. Clients in our case would be in different hospitals and the server could be in our premises, for example. In the client side in the hospital, they would have the local model and local data coming in measured from patients using an EEG device. Also, the computing resources would be in the hospital. We are assuming that the annotations regarding the suppression periods are made in the edge by a qualified medical professional through a graphical user interface.

At first, BSR machine learning was implemented in a conventional way for our data set. It was noted before that researchers are unable to see or visualize the complete collection of data that is being utilized to train the model, but in our case, we have the whole dataset and visualization, and comparison can be done. The starting point was to find optimal hyperparameter ranges. As the hyperparameter ranges depend on the specific machine learning algorithm, dataset, and problem at hand, it required some experimentation and iteration to find the optimal ranges for this task. The range can't be too large as exhaustive searches can be computationally expensive and time consuming. The default parameter ranges, taken from literature, are the following: Param1 (0.5 – 1.5), Param2 (0.6 – 1.5), Param3 (1.7 – 2.5), Param4 (0.5 – 2) and Param5 (0.7 – 1.5). Using the ranges this wide for the whole task would have been too time consuming and by experimenting, it was found that for this case, ranges a little outside those ranges worked better.

Tested with 10 pieces of data, the parameter range for determining the best hyperparameters was first established, and the best performance was obtained with the following values: Param1 (0.3 - 0.9), Param2 (0.4 - 0.8), Param3 (2.8 - 3.2), Param4 (0.1 - 0.5), and Param5 (0.3 - 0.9). The default step size was 0.1. These ranges performed successfully with the first 10 data snippets, which had a Combined error of only 254,65; but, after testing with the entire dataset, the error increased to 426,29, necessitating more experimentation. 426,29 meets the test condition, however it was anticipated that the result may be better because it was so good with just 10 pieces of data. It could be that the first 10 pieces of data were more homogeneous and after that, more variation started to exist. STD and MPE got around the same values with the whole dataset as with the first ten, but the MSE, which has a big weight in the Combined, got a significantly higher value.

After some experimenting with the whole dataset a Combined metric of 360,30 was acquired by using the following parameter ranges: Param1 (0.7 – 1,3), Param2 (0.1 - 0.5), Param3 (2.6 - 3.0), Param4 (0.2 - 0.6), and Param5 (1.1 - 1.7). For this range, 6125 different combinations were found and explored. With the ranges, the best parameters found all settled in the middle of the ranges except suppression length, which was 1,7, being in the upper end of the range. It wasn't set higher because the range was already higher than the default one. These ranges were then selected for analysis and conventional machine learning was performed.

After gaining the results from the conventional run, federated machine learning was implemented. It was performed following these steps:

1. First the global model is trained with the first five pieces of data with the same parameter ranges that were used for the conventional run.
2. Delta is defined as Delta = 0,05 and later used for the model aggregation.
3. Global model's optimized parameter values and Delta are sent to the client.

4. Client has the model locally and looks for the best parameters in the range [parameter value – delta, parameter value + delta]. The search is done with the notion that the parameter value must stay inside the hyperparameter range. The step size was set to 0,05 as with Delta we are also searching for smaller changes.
5. The client compares the found parameter values to the parameter values it received from the global model and marks a **change number** depending on whether they are smaller (0), larger (1), or equal (2).
6. An array of change numbers (for example: 00121) is sent back to the global model.
7. The global model updates or 'aggregates' its parameters one by one based on the change numbers with the following equation:

$$GlobalParameter_{change} = C\frac{Delta}{D} * 10$$

   Where C is either 0, -1 or 1 based on the change number and D is amount of data that received at that point. As we are using D, the model changes less the more data we have. If we had a larger dataset and more training rounds, it would be good to have a minimum for the global parameter change to allow it to adapt at later phases as well. This could be for example 0,005.
8. The process starts over; the global model sends the updated parameters values and the Delta to the client.

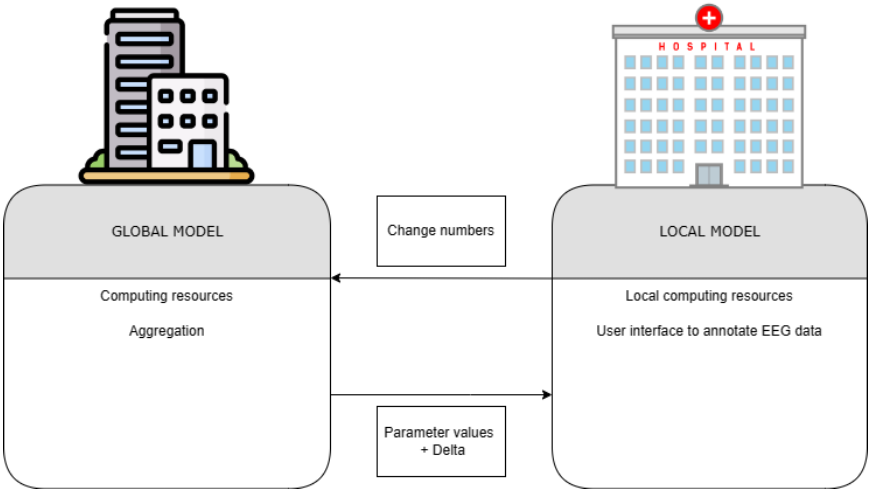

Figure 20. Federated Learning system architecture. In reality, there would several hospitals which would be communicating with the global model. Hospital icon by Alexey_Huslov via PixaBay, CC0 license. Office icon by Freepik via Flaticon, CC0 license. created with draw.io.

In this system, the parameters of the global model are shifted to a certain direction based on the data that the client receives. The only information that the global model receives is the change number pointing the direction of the change. And the global model only sends values of parameters and the Delta value. This information is something that can't trace the patient nor their personal information.

The aggregation method used is simple and it takes the amount of data into account when the model is being aggregated. If we had more data and several clients like in real situation we would, we could use Federated Averaging as an aggregation method. The

aggregation could be performed so that the global model always sends the parameter values to five clients at once and their results are taken an average of, and this is aggregated to the global model proportional to the previous iterations. Also, one client could perform several local model trainings on one iteration, and we could use weighting and give bigger weights to clients that received more data when aggregating the model.

All the four performance metrics of Federated and Conventional learning were then compared after every iteration. The results were plotted using Python and Matplotlib which is a visualization library for Python.

Descriptive analysis was chosen to understand and summarize the gained performance metrics. Firstly, the mean (representing the average value), standard deviation (indicating the dispersion of the data), median (representing the middle value) were calculated for each performance metric, separately for both the federated learning and conventional machine learning approaches. This allowed us to gain insights into the central tendency, variability, and spread of the data.

Additionally, visualizations including box plots and histograms were employed to provide representations of the data distribution and its spread. The box plots facilitated the comparison of medians, quartiles, and potential outliers between the two approaches. Histograms were constructed to understand the frequency distribution and shape of the data. Box plots and histograms were created using Python and Matplotlib.

5. RESULTS

The data that was used contained burst suppression patterns in its different forms that were caused by the anesthetic drug propofol. Thus, the data was seen suitable for BSR machine learning analysis. Overall, from 71 pieces of EEG data, 45 20-minule-long data snippets were found which included burst suppression pattern in one form or another, but also, periods without any suppressions nor bursts were included. The final parameter ranges that were used for all the rounds of conventional run and for the first round of the federated run were:

- Param1 (0.7 – 1,3)
- Param2 (0.1 - 0.5)
- Param3 (2.6 - 3.0)
- Param4 (0.2 - 0.6)
- Param5 (1.1 - 1.7)

Conventional

	1	2	3	4	5	6	7	8	9
p1	0.80	0.80	0.80	0.80	0.80	1.10	1.10	1.10	1.10
p2	0.40	0.40	0.30	0.30	0.30	0.30	0.30	0.30	0.30
p3	3.00	3.00	3.00	3.00	3.00	3.00	3.00	3.00	2.80
p4	0.30	0.30	0.50	0.50	0.50	0.50	0.50	0.50	0.50
p5	1.20	1.20	1.70	1.70	1.70	1.70	1.70	1.70	1.70
MSE	76.55	79.04	127.62	117.72	105.49	123.00	129.98	119.88	114.98
MPE	8.79	8.71	10.68	10.76	10.29	10.91	10.34	9.99	9.96
STD	6.10	5.81	7.19	7.27	6.91	7.47	7.76	7.46	7.30
C	286.44	282.40	378.13	370.69	346.69	381.45	388.55	369.06	360.60

Table 1. The numeral results of the conventional machine learning run with the annotated BrainICU dataset. The development of the parameters and the performance metrics over the training rounds can be seen here.

As seen in the results of conventional run, many of the parameters find their final optimized value early meaning that the model is not changing significantly when we get more data. There are some limitations arising already from this stage as it is setting the parameter ranges for the first iteration of the federated learning run also. As the model does not change significantly at the end when we have more data, the step size of the grid search in the conventional machine learning run may have been a bit too large. For example, by changing it from the default (0.1) to (0.05) we could already get slightly different results.

Global model

	1	2	3	4	5	6	7	8	9
p1	0.80	0.85	0.82	0.80	0.82	0.84	0.85	0.86	0.86
p2	0.40	0.45	0.42	0.40	0.40	0.42	0.43	0.43	0.44
p3	3.00	3.00	2.97	2.95	2.93	2.93	2.92	2.92	2.93
p4	0.30	0.35	0.38	0.40	0.38	0.38	0.37	0.37	0.36
p5	1.20	1.25	1.22	1.24	1.26	1.24	1.25	1.26	1.26
MSE	76.55	87.35	264.78	206.46	171.67	178.14	179.47	161.46	153.1
MPE	8.79	7.86	15.06	13.46	12.64	12.96	12.42	11.97	11.94
STD	6.10	5.94	8.79	8.45	7.70	8.13	8.30	7.91	7.65
C	286.44	284.79	591.30	510.08	452.02	470.31	469.80	439.31	425.6

↓ p1 p2 p3 p4 p5 + Delta

↑ Change numbers

Local model

	1	2	3	4	5	6	7	8	9
p1		0.85	0.80	0.77	0.85	0.87	0.89	0.90	0.86
p2		0.45	0.40	0.37	0.40	0.45	0.47	0.43	0.48
p3		3.00	2.90	2.95	2.90	2.93	2.88	2.92	2.97
p4		0.35	0.40	0.33	0.35	0.38	0.33	0.37	0.32
p5		1.25	1.30	1.27	1.29	1.21	1.29	1.30	1.26
MSE		85.01	524.85	71.63	28.11	130.45	143.41	40.02	56.22
MPE		7.62	20.82	10.88	7.48	12.24	10.57	6.12	5.66
STD		5.63	14.01	7.05	4.57	9.69	9.49	5.16	5.45
C		273.87	1013.3	321.48	194.28	446.75	438.92	204.37	221.7

Table 2. The numeral results of the federated machine learning run including the local and global model results with the annotated BrainICU dataset. The communication from the global model to the local model (marked with blue) and the communication from the local model to the global model (marked with yellow) can be seen. In the local model, the third round's performance metric values have been marked with red as those are not below the test values and thus, they would not pass the training. But as it is seen, its effect is not so significant on the global model as the global model's metric values are below the test values after that round.

All of the outcomes from the federated learning run are displayed in Table 2. The global model first trained itself using the first five pieces of data, and then it delivered the local model the discovered and optimized parameter values together with the Delta. The parameter values of the local model are found from the range that can vary them by a maximum of 0.05 to either be higher or lower than the one the global model sent. The parameter is always searched so that it cannot be outside of the parameter range if we are within its boundaries. And when the parameter is found, it is compared to the on that global model sent and a

change number is marked and sent back to the global model. Then the aggregation is performed.

The parameters of the local model are constantly changing, as can be observed from the findings, and the global model is also experiencing significant change. Something needs to be thought about in the red-highlighted area. We should test the models using both a centralized and a local validation criterion. Both of them must pass; otherwise, the older mode is kept, necessitating additional data up until a passing model is received that is sufficient. The local model number three would be disregarded in our situation, and we would wait for data that would pass validation.

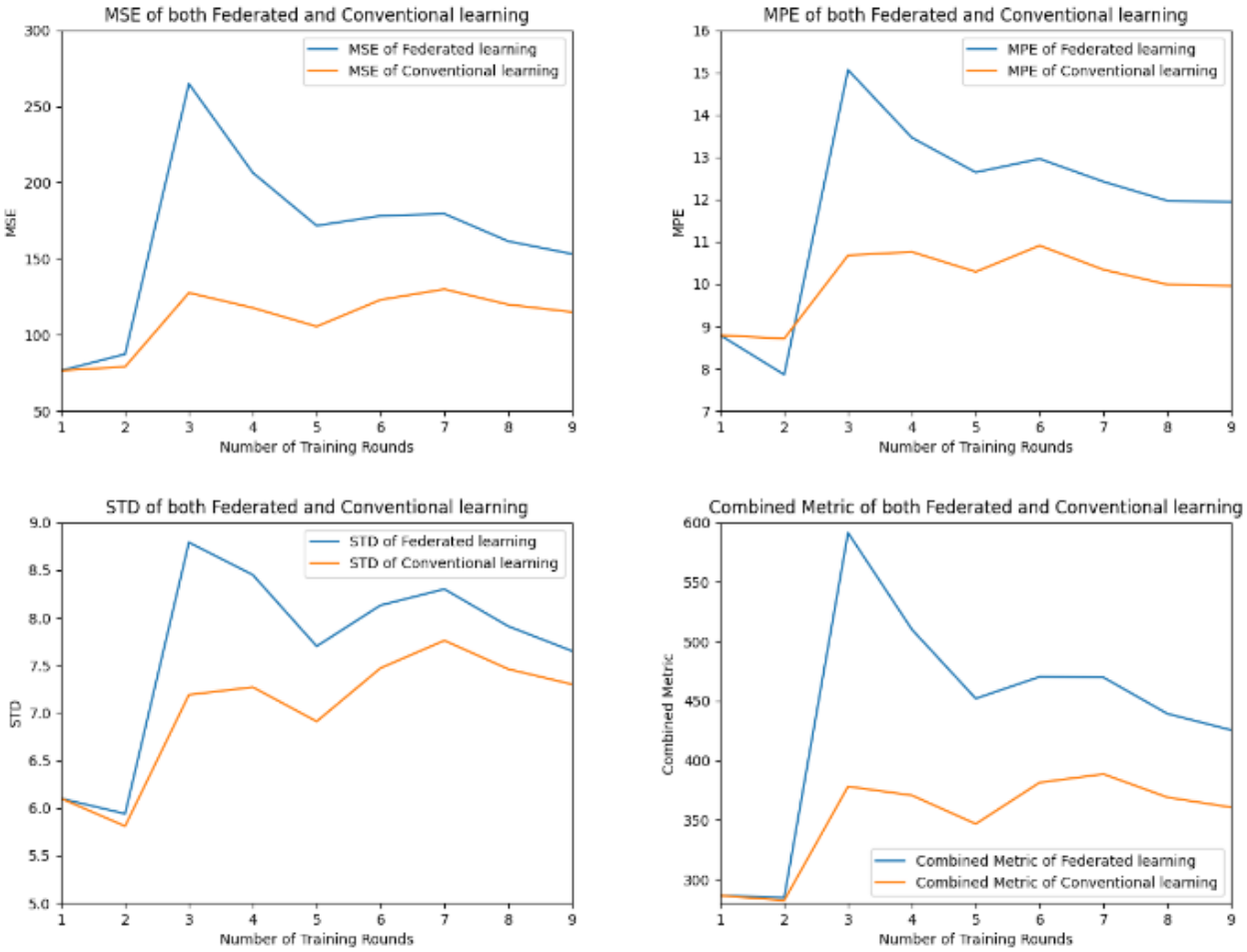

Figure 21. Comparison of how MSE, MPE, STD, and Combined metric of both methods develop over the training rounds. The starting point is the same as the first round is done with the same parameter ranges.

As can be observed from Figure 22, by the completion of the training, each of the four performance metrics for federated learning approaches ones of the conventional ones. The third round shows a significant change since the third dataset's data quality has a greater impact on the federated model. At the third cycle, both techniques show a considerable decline in all performance parameters, but the decline in federated is unmistakably larger. As we are still in the training phase, the data from round 3 may have a greater impact on the global model due to the aggregation approach. The data from round 3 appear to have a considerable impact on the federated performance. However, as the training goes on and we

receive more iterations, the federated parameters appear to be pointed in the right direction. If we had more iterations, it would be interesting to watch how the performances develop.

In the MPE, federated performs better in round 2, while round 3 shows a noticeable difference with higher values. Also, combine metric is almost the same for both approaches during the first two iterations.

	Mean	SD	Median
MSEf	164.33	53.86	171.67
MSEc	110.47	18.73	117.72
MPEf	11.90	2.12	12.42
MPEc	10.05	0.76	10.29
STDf	7.66	0.94	7.91
STDc	7.03	0.62	7.27
Combinedf	436.62	92.81	452.02
Combinedc	351.56	37.67	369.06

Table 3. Mean, Standard Deviation and Median of both approaches and all performance metrics. We can point out that MSE and Combined differ the most between federated and combined. But as MSE has a weight of 1 in the Combined while the others have larger weight, its effect is smoothed in the Combined metric.

Next, all the performance metrics are analyzed by looking at the box plots and histograms. The orange line inside the boxes in box plots represents the median value and the bottom edges of the boxes are 25^{th} percentiles and the top edges represents the 75^{th} percentiles. That means that the boxes incapsulate 50% of the data. Outliers are also possibly visible further away on both ends.

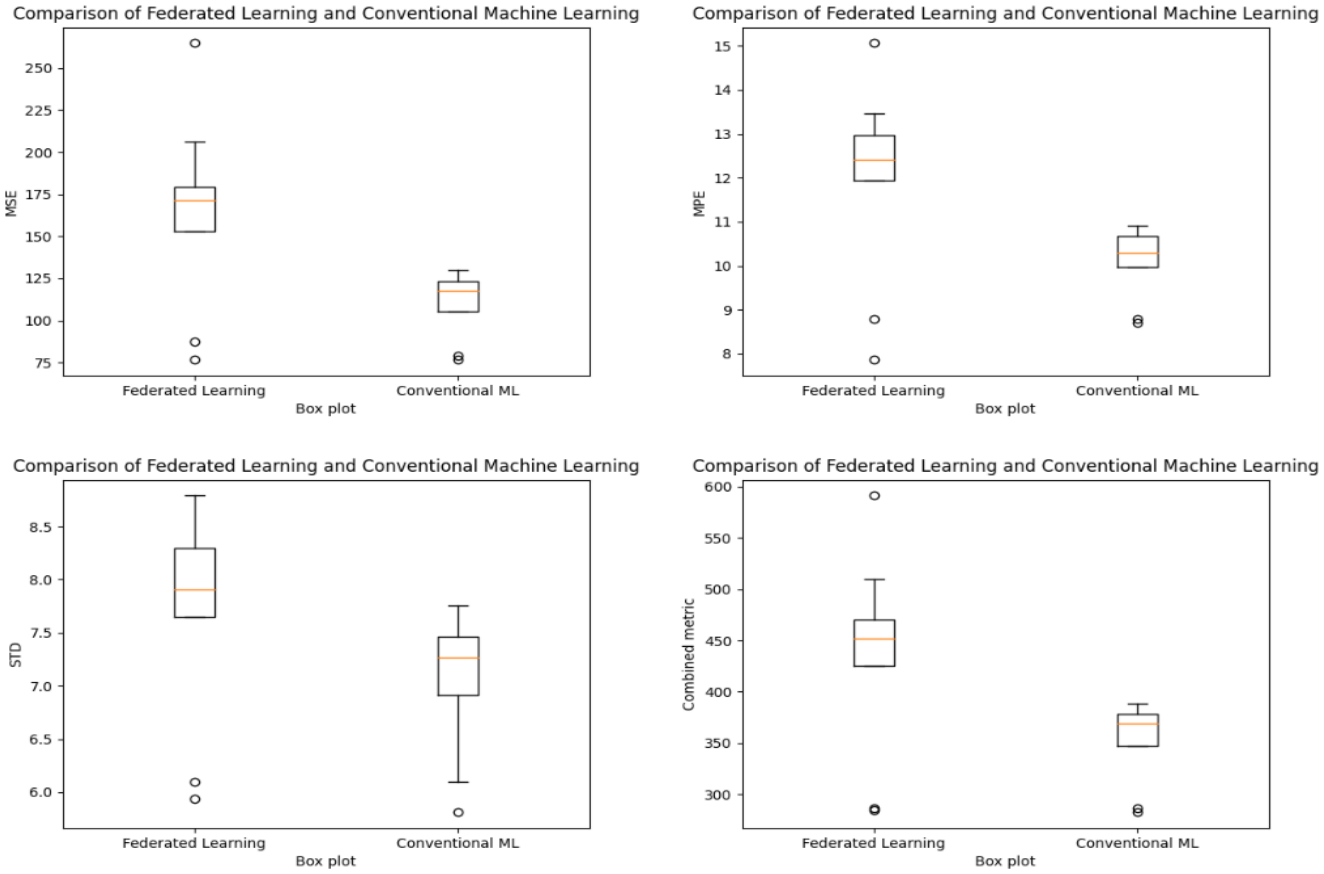

Figure 22. Box plots of all the performance metrics on both federated and conventional learning. Here we can see the medians, quartiles, and the outliers compared between the two approaches. The orange line is the median value, the upper and lower lines of the boxes are the 25th and 75th quartiles. Outliers are presented with the small dots.

As seen from Figure 23, the median value in federated and conventional are slightly different, federated having the larger value. Also, values of federated learning seem to be more spread out. There are also a couple more outliers in the results of federated learning and they tend to be on both sides, higher and lower than the median. In the conventional learning's results there are also outliers, but they always have significantly lower value than the median.

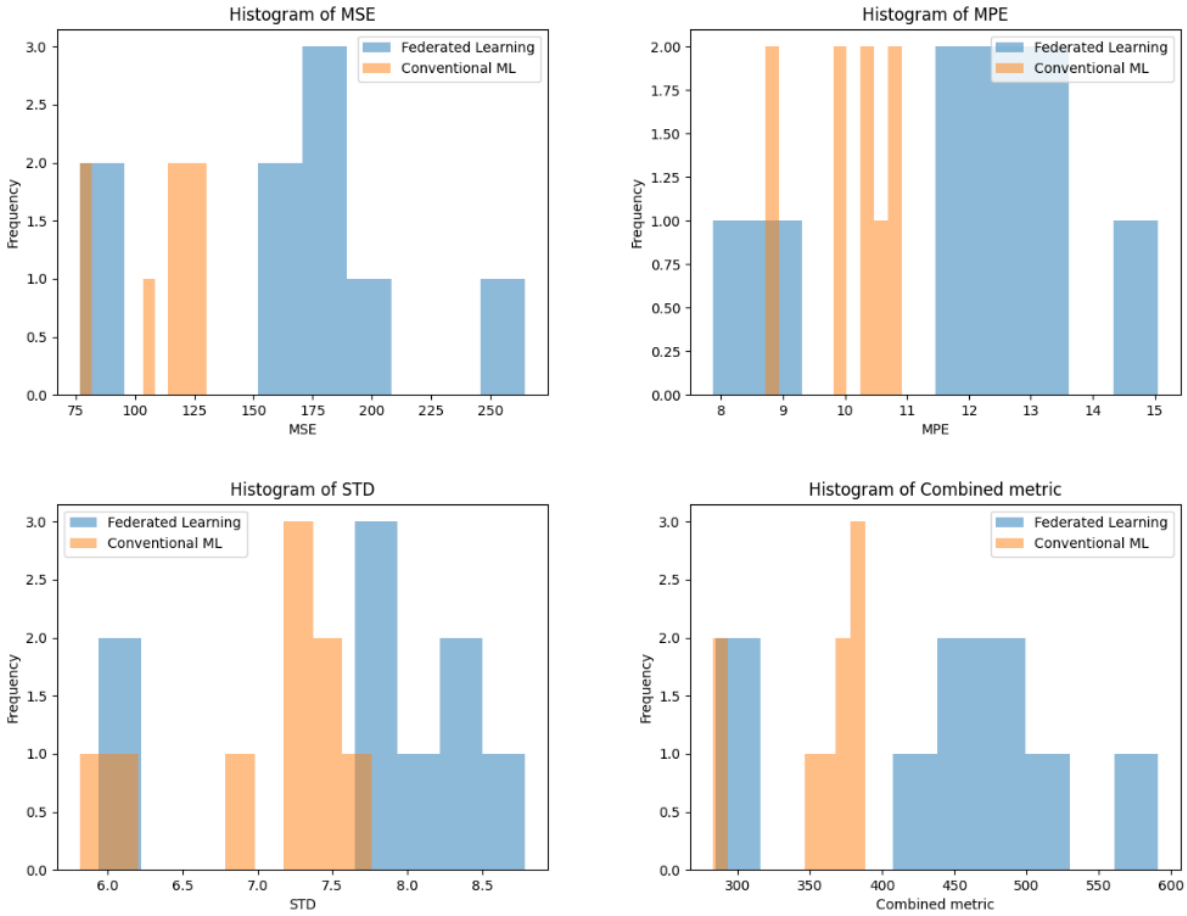

Figure 23. Histograms of all the performance metrics on both federated and conventional learning. With histograms, we can understand the frequency distribution and shape of the data. The x-axis shows the data intervals, and the y-axis shows the count of the data.

From the histogram (Figure 24) we can see how the data count is distributed and how the data is shaped. There is more space marked with blue as there is simply more data in federated as the performance metrics got higher values. In MSE, there is a clear peak in federated performance approximately between 175 and 190. Conventional does not show a clear peak but the values are distributed to a little lower values and on only around 50 different data points whereas federated has a range of almost 200. In all the histograms, federated learning's data is more widely distributed. In MPE, federated has the best performance value and in all the others, its lowest value is the same or very close to the lowest one of the conventional one.

It is important to note that we only have 18 data points for each histogram (9 for each approach) and that may be a bit too little for the histogram to work in the best way for the analysis.

6. DISCUSSION

The application of federated learning may significantly improve the process of calculating qEEG parameters. When we applied federated learning to the BSR calculation, we saw positive results, and it was shown that its performance does resemble that of the conventional one. The results of these two approaches vary somewhat, but as seen in the findings, towards the end of the training, the federated model had shifted its parameters in the right direction and appeared to be performing steadily closer to that of the conventional one. Additionally, the performance of federated learning meets the test criteria established across all iterations. The outcomes of federated learning should be expected to resemble conventional learning even more with a larger dataset. Most significantly, by using this strategy, we might be able to make use of data that would otherwise be kept private and, as a result, gradually develop models that perform better as we gain access to more data.

It is important to recognize the limits of this study and the use of federated learning for BSR. Using Erika Niemelä's annotation tool, the study needed a lot of human annotation work. The quality of the data varied widely, making it challenging to annotate the suppressions in certain data periods while they were simpler to see in others. The annotation tool can only mark specific time frames at once, and suppressions that carry over from one window to the next are halted when the window changes. As a result, certain annotations are shorter than the suppressions in reality. Because the study's investigator is neither a clinical specialist nor an experienced EEG signal analyst, there is also a chance for human error.

As previously said, employing a smaller step size may have improved the results from the conventional run because they restrict the entire implementation. However, it's important to know for the future and the results thus far are positive. When adopting federated learning with more data than we currently utilize, even if the amount of data was significant, setting a minimum for the global model update would be essential. This would be required to allow the model to develop even at later stages.

When implementing on a larger data collection, validation criteria should be defined both locally and centrally. This would guarantee that the raw data we use is adequate and that hospital annotations are carried out correctly. The data must satisfy both of those checks in order to be accepted; otherwise, it would be reasonable to wait for new data. The process of annotating the data should be consistent, and those who do it should be adequately trained. The annotation graphical user interface should be simple enough to use to make the process efficient.

Since the data from the local model in many iterations has identical qualities, we are using homogenous data to implement this study. Data samples were collected using the same instrument, under comparable circumstances, and with patients who shared the same profile, while disregarding minor variances. Additionally, the format, quality, and other characteristics of the data that the local model receives are virtually consistent. Future studies may concentrate on federated learning of quantitative electroencephalograms (qEEGs) on heterogeneous data, which lets us use data that has been captured with a number of devices, in a variety of formats, and to varied degrees of quality. This would be helpful because Cerenion uses a range of special EEG measurement tools. When dealing with heterogeneous data, data standardization, model compatibility, and resolving the differences in data attributes among devices would all be more challenging. The model would be challenging to aggregate generally, but these problems may be resolved.

Understanding and considering both the GDPR and the AI Act are crucial when applying federated learning to any of the C-Trend parameters. Despite the seeming incompatibility of these two regulations, they both place a strong emphasis on the

cryptosecurity features that would be the focus of the development as there would be data processing and transmission. The GDPR authorizes data processing activities as a proper basis for carrying out legally mandated post-market surveillance measures, as well as for ensuring or developing the safe operation of a medical device. For an AI product using federated learning, there will surely be significant technology demands related to both of these regulations, such as ensuring the accuracy and completeness of data and annotations, data administration, processing, protection, and transfer. Cryptosecurity has lately been in the focus of regulations concerning medical devices and thus, solutions this are needed in the future.

There are some ways to deploy federated learning that could help us comply with the AI Act's requirements. The data may be accessible at the edge, where only fine-tuning would be done, as it is necessary that the manufacturer is able to give the authorities the used data when requested. The provider's device approvals are subsequently always carried out using centralized data that can be fully transferred. Centralized data might be used to validate the models.

We also need to talk about aggregation and communication between the global model and the server. The suggested solution calls for the local model to only communicate with the global model by transmitting change numbers, and for the global model to only give parameter values and a delta value. Since this information cannot be used to track the patient or their patient data, as was already mentioned, it should make this method more acceptable in terms of data privacy and governance. This study's aggregation approach, which uses the equation $\text{GlobalParameter}_{\text{change}}$, accounts for the quantity of data the global model possesses at that time, making the change proportionate to the data. As we perform more iterations, this enables the model parameters to alter gradually less. As was already said, the change set needs to have a minimum value in order for the model to adapt in the future.

Data privacy regulations often require obtaining consent from individuals before collecting and processing their personal data. This is done in all the studies where conventional machine learning is used. But in the case of federated learning, the consent would not necessarily be needed in its common form as we are not collecting nor processing their personal data for the global model. The personal data, also including the raw EEG data, would stay inside the hospital. As a result, the central server never directly accesses or stores individual-level data, which ensures better data privacy. For local data, each client should be able to retain ownership of their data and have control over how it is used. This empowers patients to maintain control over their personal data and decide whether or not to participate in the collaborative training process.

A fundamental tenet of federated learning is privacy protection. During model updates and aggregation, it frequently employs techniques like encryption, differential privacy, and secure aggregation to safeguard the privacy of individual data. These techniques make it harder for the central server or any other party to extract sensitive information from the updates by introducing noise into the updates or by utilizing cryptographic techniques. Additional encryption was not deemed necessary in this method because we are simply communicating parameter values, deltas, and change numbers; however, various methods may be more thoroughly investigated in the future.

Federated learning enables compliance with data localization rules, which call for data to be stored and processed inside particular jurisdictions, by allowing data to stay on the original device or data source. Federated learning keeps track of model updates and aggregation procedures to improve auditing and make sure the model's actions comply with governance guidelines. In order to ensure that all participants follow the organization's data governance policies when training the model, data governance policies can be enforced at the

client level. This promotes data compliance and uniformity throughout the federated learning network.

The central server of federated learning collects model changes even though the real data is still decentralized. This centralized organization may manage the learning process, enforce particular governance guidelines, and guarantee that participants adhere to the set regulations. One big advantage of federated learning is that it allows for continuous updates to the model, meaning that organizations can quickly respond to changes in regulations or data governance requirements without compromising data privacy.

Overall, we want to strike a compromise between protecting data privacy and encouraging cooperation for better machine learning models by employing federated learning. We deploy privacy-preserving approaches, keep the raw data locally, and apply client-level governance regulations. All of this takes care of a lot of the issues with centralized data processing in conventional machine learning techniques, and the study also shows that it is possible to achieve performance that is nearly as excellent as that of conventional machine learning. By using this method, it is easier to make use of data from diverse sources without disclosing sensitive information, supporting responsible data governance, and improving the precision and generalization of machine learning models at the same time.

7. CONCLUSION

This thesis proposes the use of federated learning, a revolutionary machine learning technique, in the machine learning of BSR, one of the parameters of C-Trend Technology. The thesis's objective was to apply federated learning to BSR and evaluate its effectiveness in comparison to conventional machine learning. This thesis also covers the additional C-Trend parameters and potential federated learning integrations within their machine learning architecture. The thesis also looked at how federated learning might be used to address privacy issues that hinder machine learning from reaching its full potential in the medical industry. The objective was fulfilled; the study suggests one method utilizing federated learning that can be used as a machine learning solution for BSR algorithm and analyses its future directions including the aspects of AI Act and heterogeneous data.

The data that was utilized in the study was EEG data of cardiac arrest patients who were under propofol induced anesthesia. Thus, there is a literature review in the beginning of the study concerning the EEG from the point of view of history, brain origin, technology, and the signal. After that, EEG in diagnosis in the environments of ICUs and ORs was discussed and the concepts of anesthesia were talked upon. Lastly, different qualitative parameters of C-Trend Technology and background information of federated learning and privacy concerns were included.

The implementation effectively contrasted the performances of federated learning with conventional machine learning, and the outcomes were encouraging as the performances got close to one another. Additionally, minor variations were discovered in the MSE, MPE, STD, and combined metrics, which varied from one another in terms of performance. The most significant distinction between those two methods was seen in MSE. Federated learning appears to be a viable method for calculating BSR because its performance metric values consistently fall below the test criterion, and the model has the ability to shift its parameters in the right direction to produce a better performing model.

Limitations and potential future directions are covered in the discussion. Even if there are a lot of factors to take into account in the future and there will always be a need to adapt to constantly changing legislation, the study's answer is one feasible and relatively easy way to use federated learning. But before we put the method to use, surely, further research and testing are needed.

8. REFERENCES

[1] M. Murray, B. Franceschiello and A. Biasiucci, "Electroencephalography," *Curr Biol,* pp. 4;29(3):R80-R85, 2019.

[2] C. Nayak and A. Anilkumar, "EEG Normal Waveforms," *StatPearls,* p. 1, 25 Jul 2022.

[3] B. Burle, L. Spieser, C. Roger, L. Casini, T. Hasbroucq and F. Vidal, "Spatial and temporal resolutions of EEG: Is it really black and white? A scalp current density view.," *Int J Psychophysiol.,* pp. -, 12 May 2015.

[4] B. Fahy and D. Chau, "The technology of processed electroencephalogram monitoring devices for assessment of depth of anesthesia," *Anesthesia & Analgesia,* vol. 126, no. 1, pp. 111-117, 2018.

[5] J. Britton, L. Frey and J. Hopp, "Electroencephalography (EEG): An Introductory Text and Atlas or normal and abnormal findings in adults, children and infants," *Chicago: American Epilapsy Society,* vol. 6, no. -, pp. -, 2016.

[6] M. D, "Hans Berger: From psychic energy to the EEG," *Perspectives in biology and medicine,* vol. 44, no. 4, pp. 522-542, 2001.

[7] F. Gibbs, E. Gibbs and W. Lennox, "Effect on the electro-encephalogram of certain drugs which influence nervous activity," *Archieves of Internal Medicine,* vol. 60, no. 1, pp. 154-166, 1937.

[8] C. TF, "History and evolution of electroencephalographic instruments and techniques," *Journal of clinical neurophyciology,* vol. 10, no. 4, pp. 476-504, 1993.

[9] O. Ahmed and S. Cash, "Finding synchrony in the desynchronized EEG: the history and interpretation of gamma rhythms," *Frontiers in integrative neuroscience,* vol. 58, no. 7, pp. -, 2013.

[10] R. Ince, S. Adanir and F. Sevmez, "The inventor of electroencephalography (EEG): Hans Berger (1873-1941)," *Child's Nervous System,* vol. 37, no. 9, pp. 2723-2724, 2021.

[11] E. Niedermeyer and F. da Silva, Electroencephalography: basic principles, clinical applications, and related fields., -: Lippincott Williams & Wilkins, 2005.

[12] T. M, "Fundamentals of EEG measurement," *Measurement science review,* vol. 2, no. 2, pp. 1-11, 2002.

[13] S. FLD, "EEG: origin and measurement," *EEg-fMRI,* Vols. -, no. -, pp. 19-38, 2009.

[14] K. Maldonado and K. Alsayouri, "Physiology, Brain," *StatPearls,* pp. -, 27 Dec 2021.

[15] K. Jawabri and S. Sharma, "Physiology, cerebral cortex functions," *StatPearls,* pp. -, - - 2021.

[16] H. Hallez, B. Vanrumste, R. Grech, J. Muscat, W. De Clercq, A. Vergult, Y. D'Asseler, K. Camilleri, S. Fabri, S. Van Huffel and I. Lemahieu, "Review on solving the forward problem in EEG source analysis," *J Neuroeng Rehabil,* Vols. -, no. -, pp. 4-46, 2007.

[17] P. Ludwig, V. Reddy and M. Varacallo, "Neuroanatomy, Neurons," *StatPearls,* pp. -, 25 July 2022.

[18] L. Marcuse, M. Fields and J. Yeoun, Rowan's Primer of EEG E-Book, New York: Elsevier, 2015.

[19] E. Niedermeyer and F. da Silva, Electroencephalography: basic principles, clinical applications, and related fields, -: Lippincorr Williams & Wilkins, 2005.

[20] M. Cascella and S. Bandyopadhyay, "Lambda Waves," *StatPearls,* pp. -, 17 Feb 2022.

[21] S. Beniczky and D. Schomer, "Electroencephalography: basic biophysical and technological aspects important for clinical applications," *Epileptic disord.,* pp. 697-715, 1 Dec

2020.

[22] S. Debener, R. Emkes, M. De Vos and M. Bleichner, "Unobtrusive ambulatory EEG using a smartphone and flexible printed electrodes around the ear," PubMed Central, -, 2015.

[23] Bittium, "Bittium BrainStatus Device," Bittium, 17 Jul 2023. [Online]. Available: https://www.bittium.com/medical/bittium-brainstatus.

[24] M. Lopez-Gordo, D. Sanchez-Morillo and F. Pelayo Valle, "Dry EEG electrodes.," *Sensors,* pp. 12847-70, 18 Jul 2014.

[25] P. Y, "Various epileptic seizure detection techniques using biomedical signals: a review," *Brain Inform,* pp. -, 10 Jul 2018.

[26] G. Rojas, C. Alvarez, C. Montoya, M. De la Iglesia-Vaya, J. Cisternas and M. Galvez, "Study of resting-state functional connectivity networks using EEG electrodes position as seed," *Frontiers in neuroscience,* vol. 12, no. 235, pp. -, 2018.

[27] S. Feravich and C. Keller, "Overview of using T1/T2 and 10-10 subtemporal electrode chains for localizing EEG abnormalities," *The Neurodiagnostic Journal,* vol. 53, no. 1, pp. 27-45, 2013.

[28] J. Acharya and V. Acharya, "Overview of EEG Montages and Principles of Localization," *Journal of Clinical Neurophysiology,* pp. 325-329, - Sep 2019.

[29] E. Kutluay and G. Kalamangalam, "Montages for Noninvasive EEG recording," *Journal of Clinical Neurophysiology,* vol. 36, no. 5, p. 330, 2019.

[30] ACNS, "American Clinical Neurophysiology Society's Standardized Critical Care EEG Terminology," *Journal Clinical Neurophysiology,* vol. 38, no. -, pp. 1-29, 2021.

[31] K. W, "EEG alpha and theta oscillations reflect cognitive and memory performance: a review and analysis," *Brain research reviews,* vol. 29, no. 2-3, pp. 169-195, 1999.

[32] B. Hjorth, "An on-line transformation of EEG scalp potentials into orthogonal source derivations," *Electroencephalography and clinical neurophysiology,* vol. 39, no. 5, pp. 526-530, 1975.

[33] Z. Hajat, N. Ahmad and J. Andrzejowski, "The role and limitations of EEG-based depth of anesthesia monitoring in theatres and intensive care," *Anaesthesia,* vol. 72, no. -, pp. 38-47, 2017.

[34] M. Cascella, "Mechanisms underlying brain monitoring during anesthesia: limitations, possible improvements, and perspectives," *Korean journal of anesthesiology,* vol. 69, no. 2, pp. 113-120, 2016.

[35] K. DA, "What is quantitative EEG?," *Journal of Neurotherapy,* vol. 10, no. 4, pp. 37-52, 2007.

[36] J. Cooley, P. Lewis and P. Welch, "The fast Fourier transform and its applications," *IEEE Transactions on Education,* vol. 12, no. 1, pp. 27-34, 1969.

[37] A. Rayi and K. Mandalaneni, "Encephalopathic EEG patterns," *StatPearls,* pp. -, 26 jun 2022.

[38] S. Sanei and J. Chambers, EEG signal processing, John Wiley & Sons, 2013.

[39] A. Rodenbeck, R. Binder, P. Geisler, H. Danker-Hopfe, R. Lund, F. Raschke and H. Schulz, "A review of sleep EEG patterns. Part I: A compilation of amended rules for their visual recognition according to Rechtschaffen and Kales.," *Somnologie,* vol. 10, no. 4, pp. 159-175, 2006.

[40] J. Frohlich, D. Toker and M. Monti, "Consciousness among delta waves: a paradox?," *Brain,* vol. 144, no. 8, pp. 2257-2277, 2021.

[41] T. Harmony, "The functional significance of delta oscillations in cognitive processing," *Frontiers in Integrative neuroscience,* vol. 7, no. 83, 2013.

[42] M. Perlis, H. Merica, M. Smith and D. Giles, "Beta EEG activity and insomnia," *Sleep medicine reviews,* vol. 5, no. 5, pp. 365-376, 2001.

[43] M. Jose, K. Yelvington and W. Tatum, "Normal EEG variants," *Handbook of clinical neurology,* vol. 160, no. -, pp. 143-160, 2019.

[44] K. Wang, M. Steyn-Ross, D. Steyn-Ross, M. Wilson and J. Sleigh, "EEG slow-wave coherence changes in propofol-induced general anesthesia: experiment and theory," *Frontiers in systems neuroscience,* p. 215, 29 Oct 2014.

[45] T. Mestrovic, O. Ozegic and I. Bujas, "EEG cerebral dysrhythmia in non-epileptic individuals as an incentive for seeking online health consultation," *Journal of Postgraduate Medicine,* vol. 59, no. 2, p. 163, 2013.

[46] S. Ai-Rawas, R. Poothrikovil, K. Abdelbasit and R. Delamont, "The correlation between electroencephalography amplitude and interictal abnormalities: audit study," *Sultan Qaboos University Medical Journal,* vol. 14, no. 4, pp. -, 2014.

[47] E. Casula, L. Rocchi, R. Hannah and J. Rothwell, "Effects of pulse width, waveform and current direction in the cortex: A combined cTMS-EEG study," *Brain stimulation,* vol. 11, no. 5, pp. 1063-1070, 2018.

[48] A. Caricato, I. Melchionda and M. Antonelli, "Continuous Electroencephalography Monitoring in Adults in the Intensive Care Unit," *Critic Care,* pp. -, 20 Mar 2018.

[49] S. Sheng, K. Nalleballe and S. Yadala, "EEG benign variants," *StatPearls,* pp. -, 2 Sep 2022.

[50] J. D. e. al, "The application of EEG mu rhythm measures to neurophysiological research in stuttering," *Frontiers in human neuroscience,* vol. 13, no. 458, pp. -, 2020.

[51] L. Fernandez and A. Luthi, "Sleep Spindles: Mechanisms and Functions," *Physiological Reviews,* pp. -, 25 Feb 2020.

[52] L. Sewell, A. Abbas and N. Kane, "Introduction to interpretation of the EEG in intensive care," *BJA Educ,* pp. 74-82, 19 Mar 2019.

[53] V. Alvarez and A. Rossetti, "Cllinical use of EEG in the ICU: technical setting," *Journal of Clinical Neurophysiology,* vol. 32, no. 6, pp. -, 2015.

[54] L. Hu and Z. Zhang, EEG signal processing and feature extraction, -: Springer, 2019.

[55] X. Jiang, G. Bian and Z. Tian, "Removal of Artifacts from EEG Signals: A Review," *Sensors (Basel),* pp. -, 26 Feb 2019.

[56] I. Karpiel, Z. Kurasz, R. Kurasz and K. Duch, "The influence of filters on EEG-ERP testing: analysis of motor cortex in healthy subjects," *Sensors (Basel),* pp. -, 19 Nov 2021.

[57] H. Zeng, A. Song, R. Yan and H. Qin, "EOG artifact correction from EEG recording using stationary subspace analysis and empirical mode decomposition," *Sensors (Basel),* pp. -, 1 Nov 2013.

[58] C. e. a. Dai, "Removal of ECG artifacts from EEG using an effective recursive least square notch filter," *IEEE Access,* vol. 7, no. -, pp. 158872-158880, 2019.

[59] C. Saritha, V. Sukanya and Y. Murthy, "ECG signal analysis using wavelet transforms," *Bulg. J. Phys,* vol. 35, no. 1, pp. 68-77, 2008.

[60] X. Chen, X. Xu, A. Liu, S. Lee, X. Chen, X. Zhang and Z. Wang, "Removal of muscle artifacts from the EEG: a review and recommendations," *IEEE Sensors Journal,* vol. 19, no. 14, pp. 5353-5368, 2019.

[61] I. Rejer and P. Gorski, "Benefits of ICA in the case of a few channel EEG," Annu Int Conf IEEE Eng Med Biol Soc, -, 2015.

[62] A. Al-Fahoum and A. Al-Fraihat, "Methods of EEG signal features extraction using linear analysis in frequency and time-frequency domains," *ISRN Neurosciencce,* pp. -, 13

Feb 2014.

[63] Y. Sun, C. Wei, V. Cui, M. Xiu and A. Wu, "Electroencephalography: clinical applications during the perioperative period," *Frontiers in medicine,* pp. -, 09 Jun 2020.

[64] S. Romagnoli, F. Franchi and Z. Ricci, "Processed EEG monitoring for anesthesia and intensive care practice," *Minerva Anestesiologica,* pp. 1219-1230, - Nov 2019.

[65] J. Marshall, L. Bosco, N. Adhikari, B. Connolly, J. Diaz, T. Dorman, R. Fowler, G. Meyfroidt, S. Nakagawa, P. Pelosi, J. Vincent, K. Vollman and J. Zimmerman, "What is an intensive care unit? A report of the task force of the World Federation of Societies of Intensive and Critical Care Medicine," *J Critic Care,* pp. 270-276, 25 Jul 2016.

[66] Y. Kubota, H. Nakamoto, S. Egewa and T. Kawamata, "Continuous EEG monitoring in ICU," *J Intensive Care,* pp. -, 17 Jul 2018.

[67] S. Sharma, M. Nunes and A. Alkhachroum, "Adult Critical Care Electroencephalography Monitoring for Seizures: A narrative review," *Frontiers in Neurology,* pp. -, 15 July 2022.

[68] S. Jain and L. Iverson, "Glasgow Coma Scale," *StatPearls,* pp. -, 21 Jun 2022.

[69] W. E. F., "Clinical scales for comatose patients: the Glasgow Coma Scale in historical context and the new FOUR Score," *Reviews in neurological diseases,* vol. 3, no. 3, pp. -, 2006.

[70] M. e. a. Mak, "Measuring outcome after cardiac arrest: construct validity of Cerebral Performance Category," *Resuscitation,* vol. 100, no. -, pp. 6-10, 2016.

[71] J. Huff and N. Murr, "Seizure," *StatPearls,* pp. -, 8 May 2022.

[72] A. Chang and S. Shinnar, "Nonconvulsive status epilepticus," *Emerg Med Clin North Am,* vol. 29, no. 1, pp. 65-72, 2011.

[73] C. Rubinos and D. Godoy, "Electroencephalographic monitoring in the critically ill patient: What useful information can it contribute?," *Med Intensiva,* vol. 44, no. 5, pp. 301-309, 2020.

[74] K. Patel and J. Hipskind, "Cardiac Arrest," *StatPearls,* pp. -, 8 May 2022.

[75] J. Kortelainen, T. Ala-Kokko, M. Tiainen, D. Strbian, K. Rantanen, J. Laurila, J. Koskenkari, M. Kallio, J. Toppila, E. Väyrynen, M. Skrifvars and J. Hästbacka, "Early recovery of frontal EEG slow wave activity during propofol sedation predicts outcome after cardiac arrest," *Resuscitation,* pp. 170-176, 7 Jun 2021.

[76] E. Thenayan, M. Savard, M. Sharpe, L. Norton and B. Young, "Electroencephalogram for prognosis after cardiac arrest," *Journal of critical care,* vol. 25, no. 2, pp. 300-304, 2010.

[77] C. Hui, P. Tadi and L. Patti, "Ischemic Stroke," *StatPearls,* pp. -, 2 Jun 2022.

[78] A. Unnithan, J. M Das and P. Mehta, "Stroke," *StatPearls,* pp. -, 16 May 2022.

[79] B. Bachar and B. Manna, "Coronary Artery Bypass Graft," *StatPearls,* pp. -, 11 Aug 2021.

[80] M. DaCosta, P. Tadi and S. Surowiec, "Carotic Endarterectomy," *StatPearls,* pp. -, 29 Sep 2021.

[81] I. Constant and N. Sabourdin, "Monitoring depth of anesthesia: from consciousness to nociception. A window on subcortical brain activity," *Pediatric anesthesia,* pp. 73-82, 20 Nov 2014.

[82] D. Robinson and A. Toledo, "Historical development of modern anesthesia," *J Invest Surg,* vol. 25, no. 3, pp. 141-149, 2012.

[83] F. Boland, The first anesthetic: the story of Crawford Long, Georgia: University of Georgia

Press, 2009.

[84] K. Knuf and C. Maani, "Nitrous Oxide," *StatPearls,* pp. -, - Jan 2022.

[85] R. Miller and M. Pardo, Basics of anesthesia e-book, -: Elsevier Health Sciences, 2011.

[86] M. Alkire, A. Hudetz and G. Tononi, "Consciousness and anesthesia," *Science,* vol. 322, no. 5903, pp. 876-880, 2008.

[87] H. Shehata, Basic Science in Obstetrics and Gynaecology, Chapter Twelve - Drugs and therapy, -: Churchill Livingstone, 2010.

[88] A. Jerath, M. Parotto, M. Wasowicz and N. Ferguson, "Volatile anesthetics. Is a new player emerging in critical care sedation?," *American journal of respiratory and critical care medicine,* vol. 193, no. 11, pp. 1202-1212, 2016.

[89] S. Bryan and M. King, Assisted Ventilation of the Neonate, Chapter 26 Intraoperative management, -: Elsevier, 2003.

[90] N. Ferry, L. Hancock and S. Dhanjal, "Opioid anesthesia," *StatPearls,* pp. -, 10 Aug 2022.

[91] "American Society of Anesthesiologists," American Society of Anesthesiologists, 27 Jan 2023. [Online]. Available: https://www.asahq.org/madeforthismoment/anesthesia-101/types-of-anesthesia/general-anesthesia/.

[92] B. Siddiqui and P. Kim, "Anesthesia Stages," *StatPearls,* pp. -, 9 Mar 2022.

[93] J. Platholi and H. Hemmings, "Effects of general anesthetics on synaptic transmission and plasticity," *Current Neuropharmacology,* vol. 20, no. 1, pp. 27-54, 2022.

[94] M. Suzuki and M. Larkum, "General anesthesia decouples cortical pyramidal neurons," *CellPress,* pp. 666-676, 20 Feb 2020.

[95] "American Society of Anesthesiologists," American Society of Anesthesiologists, 27 Jan 2023. [Online]. Available: https://www.asahq.org/madeforthismoment/anesthesia-101/types-of-anesthesia/ivmonitored-sedation/.

[96] S. SA, "Procedural sedation analgesia," *Saudi journal of anesthesia,* vol. 4, no. 1, p. 11, 2010.

[97] D. Early, J. Lightdale, J. Vargo, R. Acosta, V. Chandrasekhara, K. Chathadi and J. DeWitt, "Guidelines for sedation and anesthesia in GI endoscopy," *Gastrointestinal endoscopy,* vol. 87, no. 2, pp. 327-337, 2018.

[98] B. Molaee-Ardekani, L. Senhadji, M. Shamsollahi, E. Wodey and B. Vosoughi-Vahdat, "Delta waves differently modulate high frequency components of EEG oscillations in various unconcsciousness levels," in *29th Annual International Conference of the IEEE Engineering in Medicine and Biology Society*, 2007.

[99] S. Hagihira, "Brain Mechanisms during Course of Anesthesia: what we know from EEG changes during induction and recovery," *Frontiers in Systems Neuroscience,* pp. -, 29 May 2017.

[100] V. Chidambaran, A. Costandi and A. D'Mello, "Propofol: a review of its role in pediatric anesthesia and sedation," *CNS Drugs,* vol. 29, no. 7, pp. 543-563, 2015.

[101] V. Bonhomme, C. Staquet, J. Montupil, A. Defresne, M. Kirsch, C. Martial, A. Vanhaudenhuyse, C. Chatelle, S. Larroque, F. Raimondo, A. Demertzi, O. Bodart, S. Laureys and O. Gosseries, "General ANesthesia: A probe to explore consciousness," *Frontiers in Systems Neuroscience,* pp. -, 14 Aug 2019.

[102] E. Sohn, "Decoding the neuroscience of consciousness," *Nature,* pp. -, 24 July 2019.

[103] T. Folino, E. Muco, A. Safadi and L. Parks, "Propofol," *StatPearls,* pp. -, - - 2022.

[104] Y. Adachi, K. Watanabe, H. Higuchi and T. Satoh, "The determinants of propofol induction of anesthesia dose," *Anesthesia & Analgesia,* vol. 92, no. 3, pp. 656-661, 2001.

[105] T. Schnider, C. Minto, T. Egan and M. Filipovic, "Relationship between propofol target concentrations, bispectral index, and patient covariates during anesthesia," *Anesthesia & Analgesia,* vol. 132, no. 2, pp. 735-742, 2021.

[106] J. Soukup, K. Schärff, K. Kubosch, C. Pohl, M. Bomplitz and J. Kompardt, "State of the art: sedation concepts with volatile anesthetics in critically ill patients," *Journal of critical care,* vol. 24, no. 4, pp. 535-544, 2009.

[107] S. Hemphill, L. McMenamin, M. Bellamy and P. Hopkins, "Propofol infusion syndrome: a structured literature review and analysis of published case reports," *Br J Anaesthesia,* vol. 122, no. 4, pp. 448-459, 2019.

[108] D. San-juan, K. Chiappa and A. Cole, "Propofol and the electroencephalogram," *Clinical Neurophysiology,* vol. 121, no. 7, pp. 998-1006, 2010.

[109] S. Shafer and D. Stanski, "Defining depth of anesthesia," *Modern Anesthetics,* Vols. -, no. -, pp. 409-423, 2008.

[110] P. e. al, "Electroencephalogram signatures of loss and recovery of consciousness from propofol," *PNAS,* vol. 110, no. 12, pp. -, 2013.

[111] S. Mathur, J. Patel, S. Goldstein and A. Jain, "Bispectral Index," *StatPearls,* pp. -, 24 Jul 2022.

[112] E. Ely, B. Truman, A. Shintani, J. Thomason, A. Wheeler, S. Gordon, J. Francis, T. Speroff, S. Gautam, R. Margolin and C. Sessler, "Monitoring sedation status over time in ICU patients: reliability and validity of the Richmont Agitation-Sedation Scale (RASS)," *Jama,* vol. 289, no. 22, pp. 2983-2991, 2003.

[113] B. TA, "Depth of anesthesia monitoring," *Anesthesiology Clinics of North America,* vol. 24, no. 4, pp. 793-822, 2006.

[114] J. Kortelainen, E. Väyrynen and T. Seppänen, "Depth of anesthesia during multidrug infusion: separating the effects of propofol and remifentanil using the spectral features of EEG," *IEEE Transactions on biomedical engineering,* vol. 58, no. 5, pp. 1216-1223, 2011.

[115] D. e. a. Sattin, "Analyzing the loss and the recovery of consciousness: Functional connectivity patterns and changes in heart rate variability during propofol-induced anesthesia," *Frontiers in systems neuroscience,* vol. 15, no. -, pp. -, 2021.

[116] M. Westover, M. Shafi, S. Ching, J. Chemali, P. Purdon, S. Cash and E. Brown, "Real-Time segmentation of burst suppression patterns in critical care EEG monitoring," *Journal of neuroscience methods,* vol. 219, no. 1, pp. 131-141, 2013.

[117] D. Rani and S. Harsoor, "Depth of general anesthesia monitors," *Indian J Anesth,* vol. 56, no. 5, pp. 437-441, 2012.

[118] H. Lee, H. Ryu, Y. Park, S. Yoon, S. Yang, H. Oh and C. Jung, "Data driven investigation of Bispectral Index algorithm," *Sci Rep,* vol. 9, no. 1, pp. -, 2019.

[119] M. Kreuzer, "EEG based monitoring of general anesthesia: taking the next steps," *Frontiers in Computational Neuroscience,* 22 June 2017.

[120] S. Singh, S. Bansal, G. Kumar, I. Gupta and J. Thakur, "Entropy as an indicator to measure depth of anesthesia for laryngeal mask airway insertion during sevoflurane and propofol anesthesia," *J Clin Diagn Res,* vol. 11, no. 7, pp. -, 2017.

[121] L. Livint Popa, H. Dragos, C. Pantelemon, O. Verisezan Rosu and S. Strilciuc, "The role of quantitative EEG in the diagnosis of neuropsychiatric disorders," *J Med Life,* vol. 13, no. 1, pp. 8-15, 2020.

[122] P. Watson, A. Shintani, R. Tyson, P. Pandharipande, B. Pun and E. Ely, "Presence of electroencephalogram burst suppression in sedated, critically ill patients is associated

with increased mortality," *Crit Care Med,* vol. 36, no. 12, pp. 3171-3177, 2008.

[123] N. Pawar and O. Barreto Chang, "Burst suppression during general anesthesia and postoperative outcomes: mini review," *Front Syst Neuroscience,* pp. -, 7 Jan 2022.

[124] W. Muhlhofer, R. Zak, T. Kamal, B. Rizvi, L. Sands, M. Yuan and J. Leung, "Burst-suppression ratio underestimates absolute duration of electroencephalogram suppression compared with visual analysis of intraoperative electroencephalogram," *BJA: British Journal of Anesthesia,* vol. 118, no. 5, pp. 755-761, 2017.

[125] H. Glass, C. Wusthoff and R. Shellhaas, "Amplitude-integrated electro-encephalography: the child neurologist's perspective," *J Child Neurol,* vol. 28, no. 10, pp. 1342-1350, 2013.

[126] N. Shah and C. Wusthoff, "How to use: amplitude-integrated EEG (aEEG)," *Arch Dis Child Educ Pract Ed,* vol. 100, no. 2, pp. 75-81, 2015.

[127] N. Bruns, S. Blumenthal, I. Meyer, S. Klose-Verschuur, U. Felderhoff-Muser and H. Muller, "Application of an amplitude-integrated EEG monitor (cerebral function monitor) to neonates," *J Vis Exp,* vol. 6, no. 127, pp. -, 2017.

[128] J. Leon-Carrion, J. Martin-Rodriguez, J. Damas-Lopez, Y. Barroso, J. Martin and M. Dominguez-Morales, "Delta-alpha ratio correlates with level of recovery after neurorehabilitation in patients with acquired brain injury," *Clin Neurophysiology,* vol. 120, no. 6, pp. 1039-1045, 2009.

[129] J. Claassen, L. Hirsch, K. Kreiter, E. Du, E. Connolly, R. Emerson and S. Mayer, "Quantitative continuous EEG for detecting delayed cerebral ischemia in patients with poor-grade subarachnoid hemorrhage," *Clinical neurophysiology,* vol. 115, no. 12, pp. 2699-2710, 2004.

[130] "Cerenion C-Trend," Cerenion Oy, 11 Jan 2023. [Online]. Available: https://www.cerenion.com/solutions.php.

[131] M. Naser and A. Alavi, "Insights into performance fitness and error metrics for machine learning," *arXiv preprint arXiv,* Vols. -, no. -, pp. -, 2020.

[132] N. Rieke, J. Hancox, W. Li, F. Milletari, H. Roth, S. Albarqouni, S. Bakas, M. Galtier, B. Landman, K. Maier-Hein, S. Ourselin, M. Sheller, R. Summers, A. Trask, D. Xu, M. Baust and M. Cardoso, "The future of digital health with federated learning," *npj Digital Medicine,* vol. 3, no. 119, pp. -, 2020.

[133] M. Crowson, D. Moukheider, A. Arevalo, B. Lam, S. Mantena, A. Rana and Et al, "A systematic review of federated learning applications for biomedical data," *PLOS Digit Health,* vol. 1, no. 5, pp. -, 2022.

[134] G. D. P. Regulation, " Regulation (eu) 2016/679 of the european parliament and of the," *Official Journal of the European,* vol. 59, no. 294, pp. 1-88, 2016.

[135] J. e. a. Konečný, "Federated optimization: Distributed machine learning for on-device intelligence," *arXiv preprint arXiv,* vol. 1610, no. 2527, 2016.

[136] B. Ikiz, "AI pandemic engine," Stanford University, 10 Aug 2020. [Online]. Available: https://hai.stanford.edu/news/pandemic-ai-engine-without-borders. [Accessed 5 July 2023].

[137] J. K. e. al, "Adaptive Aggregation For Federated Learning," *arXiv preprint arXiv,* vol. 2203, no. 12163, pp. -, 2022.

[138] P. Mammen, "Federated learning: opportunities and challenges," *arXiv preprint,* vol. 2101, no. 05428, pp. -, 2021.

[139] L. J. e. al., "From distributed machine learning to federated learning: A survey," *Knowledge*

and information systems, vol. 64, no. 4, pp. 885-917, 2022.

[140] e. a. Mansour AB, "Federated Learning Aggregation: New Robust Algorithms with Guarantees," *arXiv preprint arXiv,* vol. 2205, no. 10864, pp. -, 2022.

[141] C. Xu, H. Liu and W. Qi, "EEG Emotion Recognition Based on Federated Learning Framework," *Electronics,* vol. 11, no. 3316, pp. -, 2022.

[142] C. Ju, D. Gao, R. Mane, B. Tan, Y. Liu and C. Guan, "Federated Transfer Learning for EEG signal classification," in *42nd Annual International Conference of the IEEE Engineering in Medicine & Biology Society*, Montreal, 2020.

[143] e. a. Gao D, "HHHFL: Hierarchical Heterogeneous Horizontal," *airXiv preprint arXiv,* 2019.

[144] G. James, D. Witten, T. Hastie and R. Tibshirani, An introduction to statistical learning with applications, -: Springer, 2013.

[145] R. Hyndman and G. Athanasopoulos, Forecasting: Principles and Practice, -: OTexts, 2018.

[146] Bittium, "Bittium NeurOne Device," Bittium, 5 July 2023. [Online]. Available: https://www.bittium.com/medical/bittium-neurone.

[147] M. Huusko, Writer, *Heart rate variability during propofol anesthesia in predicting neural recovery from cardiac arrest.* [Performance]. Master's Thesis, 2018.

[148] E. Niemelä, "Tool for EEG data visualization, annotation and management," University of Oulu, Oulu, 2020.

[149] R. Chatterjee, A. Datta and D. Sanyal, "Ensemble learning approach to motor imagery EEG signal classification," in *Learning in Bio-Signal Analysis and Diagnostic Imaging*, -, 2019.

[150] "Nihon Kohden CerebAir device," Nihon Kohden, 10 Jan 2023. [Online]. Available: https://eu.nihonkohden.com/en/products/neurology/eegs/cerebair.html.

[151] A. Caricato, G. Della Marca and E. Ioannoni, "Continuous EEG monitoring by a new simplified wireless headset in intensive care unit," *BMC Anesthesiology,* pp. -, - - 2020.

[152] K. Miki, T. Morioka, A. Sakata, N. Noguchi, M. Mori, T. Yamada and Y. Natori, "Initial experience of a telemetry EEG amplifier (Headset) in the emergent diagnosis of nonconvulsive status epilepticus," *Interdisciplinary Neurosurgery,* vol. 18, no. 100486, pp. -, 2019.

[153] M. Meyer, S. Fuest, D. Krain, M. Juenemann, T. Braun, S. Thal and P. Schramm, "Evaluation of a new wireless technique for continuous electroencephalography monitoring in neurological intensive care patients," *Journal of Clinical Monitoring and Computing,* vol. 35, no. 4, pp. 765-770, 2021.

[154] A. Biondi, V. Santoro, P. Viana, P. Laiou, D. Pal, E. Bruno and M. Richardson, "Noninvasive mobile EEG as a tool for seizure monitoring and management: a systematic review," *Epilepsia,* vol. 63, no. 5, pp. 1041-1063, 2022.

[155] L. Larsen, M. Wegger, S. Le Greves, L. Emgaard and T. Hansen, "Emergence agitation in pediatric day case surgery: A randomized, single-blinded study comparing narcotrend and heart rate variability with standard monitoring," *European Journal of Anesthesiology,* vol. 39, no. 3, pp. 261-268, 2022.

[156] R. Anaya-Prado and D. Schadegg-Pena, "Crawford Williamson Long: The true pioneer of Surgical Anesthesia," *J Invest Surg,* vol. 28, no. 4, pp. 181-187, 2015.

[157] S. Murakami and Y. Okada, "Contributions of principal neocortical neurons to magnetoencephalography and electroencephalography signals," *J Physiology,* pp. 925-936, 15 Sep 2006.

[158] W. Florian, R. Florian and K. Alois, "Computation by Time," *Neural Processing Letters,* pp. -, 11 Aug 2016.